Mathematical Modelling of a Small Biomass Gasifier for Synthesis Gas Production

Atainu Ernest Mbikan

A thesis submitted in partial fulfilment of the requirements of the University of Northumbria at Newcastle for the award of Doctor of Philosophy

Research undertaken in the Mechanical and Construction Engineering Department of the Faculty of Engineering and Environment

March 2019

Abstract

The depletion of fossil fuels coupled with the growing demands of the world energy has ignited the interest for renewable energies including biomass for energy production. A reliable affordable and clean energy supply is of major importance to the environment and economy of the society. In this context, modern use of biomass is considered a promising clean energy alternative for the reduction of greenhouse gas emissions and energy dependency. The use of biomass as a renewable energy source for industrial application has increased over the last decade and is now considered as one of the most promising renewable sources. The direct combustion of biomass in small scales often results in incomplete and inconsistent burning process which could produce carbon monoxide, particulates and other pollutants. Therefore, biomass is required to be transformed into more easily handled fuel such as gases, liquids and charcoal using technologies such as pyrolysis, gasification, fermentation, digestion etc. Biomass gasification upon which this thesis focuses is one of the promising routes amongst the renewable energy options for future deployment. Gasification is a process of conversion of solid biomass into combustible gas, known as producer gas by partial oxidation.

This research work is carried out to investigate various methods employed for modelling biomass gasifiers, it also studies the chemistry of gasification and reviews various gasification models. In this work, a mathematical model is developed to simulate the behaviour of downdraft gasifiers operating under steady state and determine the synthesis gas composition. The model distinctly analyses the processes in each of the three zones of the gasifier; pyrolysis, oxidation and reduction zones. Air is used as the gasifying agent and is introduced into the pyrolysis and oxidation zones of the gasifier for both single and double air operations. These zones have been modelled based on thermodynamic equilibrium and kinetic modelling; the model equations are solved in MATLAB. Given the biomass properties, consumption, air input, moisture content and gasifier specifications, the MATLAB model is able to accurately predict the temperature and distribution of the molar concentrations of the synthesis gas constituents. The downdraft gasifier is also represented in Aspen HYSYS based on the same models to study the effect of both single and double air gasification operation. For known biomass properties, consumption, air input, moisture content and

gasifier operating conditions, the Aspen HYSYS model can accurately predict the distributions of the molar concentrations of the syngas constituents (CO, CO_2, H_2, CH_4, and N_2). The models were validated by comparing obtained theoretical results with experimental data published in the open literature. Parametric studies were carried out to study the effects of equivalence ratio, moisture content, temperature on the gas compositions and its energy content. The proposed equilibrium model displayed a variable ability for the prediction of various product yields with this being a function of the feedstock studied. It also demonstrated the ability to predict product gases from various biomasses using both single and double stage air input. In the case of gasification with double air stage supply, higher amounts of methane are obtained with specific tendencies of the gases reaching a peak at certain conditions. The kinetic model was partially successful in predicting results and comparable with experimentally published results for a range of conditions. There were discrepancies particularly with CH_4 formation and the operating temperatures predictions which were usually consistently lower than those actually measured experimentally. The use of the PFR, however, did show a greater potential for the use in further modelling.

Declaration

I declare that the work contained in this thesis has not been submitted for any other award and it is all my own work. I also confirm that this work fully acknowledges the ideas, opinions and contributions from the work of others.

Word count of main body of Thesis:

Name: Atainu Ernest Mbikan

Signature:

Date: March 2019

Acknowledgement

I wish to express my sincere appreciation and gratitude to my supervisor Prof. Khamid Mahkamov whose support and guidance have been immensely invaluable all through this study.

I will also like to thank Dr Dave Pritchard for his assistance. My thanks also go to my friends; Joshua Benamaisia, Ayodeji Sowale and others for all their various support.

Finally, I will like to give special thanks to my parents Chief Ernest Duke and Mrs Mabel Mbikan and to all my siblings Mr Eneile Mbikan, Engr.Cliff-Njah, Mrs Amanowaji Uloyok, Mr Munyeowaji Mbikan, Mr Mowon Mbikan, Mr Ufikairo Dickson, Mrs Owajima Atteng and Mrs Helen Edward for their constant care, prayers, financial and moral support throughout my study.

Table of Contents

List of Figures

List of Tables

Nomenclature

Symbols

Ai Frequency factor of reaction i, s^{-1}

Cp Heat capacity J kg^{-1} K^{-1}

Dp Average particle diameter in the bed, m

Ei Activation energy of reaction i, J

F_{rg} gasification relative fuel/air ratio

G Gibbs function of formation, J mol^{-1}

K Equilibrium constant

M Biomass moisture %

R_x Rate of formation of species x by chemical reactions in $mol.m^{-3}. s^{-1}$

T Temperature, K

V Superficial gas velocity, $m. s^{-1}$ or volume, m^3

a Molar flow rate of oxygen from the air, mol s^{-1}

bvC Molar flow rate of carbon from biomass, mol s^{-1}

bvH Molar flow rate of hydrogen from biomass, mol s^{-1}

bnvC Molar flow rate of non-volatile specie mol s^{-1}

bvO Molar flow rate of oxygen from biomass, mol s^{-1}

c_x Molar heat capacity of the gas $J.K^{-1}.mol^{-1}$

hf Enthalpy of formation, J mol^{-1}

n_x Molar density of species x in $mol.m^{-3}$

m^b Amount of oxygen per kmol of feedstock

ri Rate of reaction i, $mol.m^{-3.}\ s^{-1}$

w Molar flow rate of biomass moisture, $mol\ s^{-1}$

W Mass of moisture kg

y Mole fraction

z Depth, m

Greek symbols

ε Void fraction

μ Fluid viscosity, $kg\ m^{-1}\ s^{-1}$

ρ Mass density, $kg\ m^{-3}$

φ Equivalence ratio

ω_i Acentric factor

Subscripts

bnvC Molar flow rate of non-volatile species in biomass, $mol\ s^{-1}$

e Electric

i Reaction m Mole fraction of hydrogen in biomass

n Mole fraction of oxygen in biomass

p In the pyrolysis zone

o In the oxidation zone

th Thermal

x Chemical species

Supercripts

0 Ambient

a Air

Abbreviations

CRF Char reactivity factor

HHV Higher heating value

LHV Lower heating value

PFR Plug flow reactor

Chapter 1 Introduction

1.1 The Energy situation of the world

The demand for sources of energy to satisfy human energy consumption is on the sharp increase [1]. A considerable part of population in the world is still not serviced with energy at the minimum level even in this 21st century. This is true with developing countries like Pakistan, India, Bangladesh, Brazil, Chile, Costa Rica etc. This is also including countries in Africa like Zimbabwe, Zambia, Uganda etc. which have a large part of their population living in remote locations which makes it uneconomical to extend the centralised grid. Also, their economic structure is not sufficiently strong towards importing oil for generating power [2]. Furthermore, as concerns over the problems of global warming and climate change have increased, renewable energy is of growing importance in fulfilling the energy demands over the usage of fossil fuel. In contrast to the conventional sources of energy, which is more in limited number of countries, renewable energy resources exist over the wide geographical area. Deployment of renewable energy technologies can contribute significantly to energy independence of the region including both economic and environmental benefits [3]. Biomass is considered as the renewable energy source with the most potential to contribute to the energy needs for both the developed and developing societies [4].

Biomass gasification is a very mature technology, its discovery and development dates back to the 18th century. In 1789, a French engineer, Philippe Le Bon, studied the distilling of wood to produce gas. In 1785, another French author, Jean Pierre Minckelen reported using the first gas lights: these gases were produced from wood and coal. There was a renewed interest in wood gas by the 1900s, this time as a transport fuel. In 1901, a British inventor Thomas Hugh Parker built the first car to run on wood gas and during the 1920s, George Imbert developed the first wood gasifier suitable for a vehicle and from then the development of commercial wood vehicles began to increase especially in France [5]. A number of cars and trucks in Europe operated on coal or biomass gasified in on-board gasifiers. Within this period, many small gasifiers were developed mainly for transportation (see Figure 1).

Figure 1.1 Bus with an on-board gasifier during the Second World War][6]

The beginning of plentiful natural gas in the 1950s inhibited the further development of biomass and coal gasification while synthesis gas production from natural gas by steam reforming increased. However, between 1975 and post 2000 two significant occasions triggered the use of biomass gasification as an important source of energy. One was the 1973 oil embargo, when members of the Organization of Arab Petroleum Exporting Countries (OPEC) barred oil exportations to the United States, and other western countries which were at the time heavily dependent on oil from the Middle East. The second occasion was between the 1980s and post 2000 when the concerns for the depletion of fossil fuels and environmental impact, such as the effect of pollutants in the atmosphere and the threat to climate change, increased. These intensified the need for moving away from carbon-rich fossil fuels.

1.2 Biomass as a source of clean and renewable energy

Biomass refers to biological material containing energy stored in organic compounds such as crops, forestry and agricultural waste, industrial and domestic waste. When compared with that of fossil fuels, the energy density of biomass is lower [7]. One of the major problems associated with the utilization of biomass relates to its bulkiness and inconvenient form as it is a solid and can be distributed as a bulk material. Most forms of biomass have relatively low energy density within the range of 9±5MJ m^{-3} compared to that of 38 MJ m^{-3} (both on LHV basis). Handling, storing and

transportation of biomass in its raw form becomes more expensive in contrast to fossil fuels. Thus, to productively utilize biomass, it is necessary to improve its properties which enhances its handling, storing and transportation. Also similar kinds of biomass can have very different composition and appearance thus making it difficult to assure constant product specification [8]. Figure 1.2 shows the main parts of transformation.

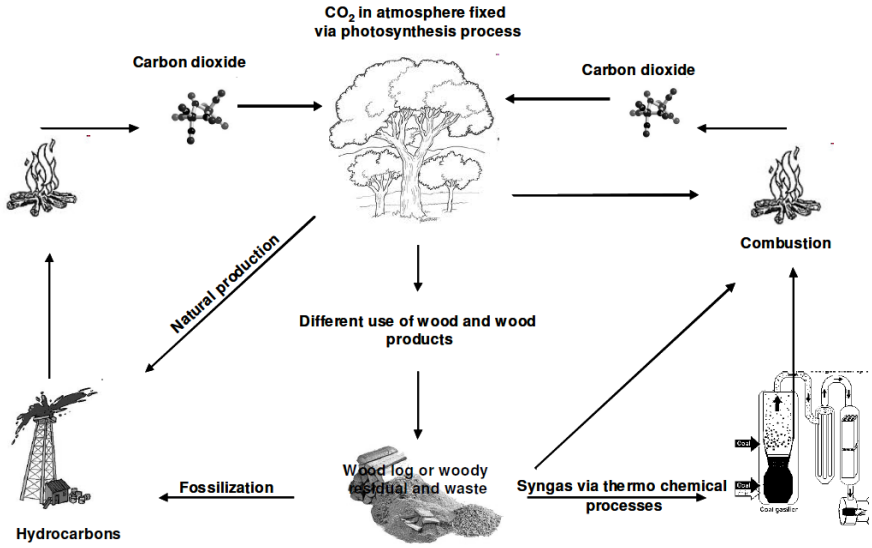

Figure 1.2 Main Parts of biomass transformation [9]

In general biomass can be used as food, fibre, fertilizer, timber products, chemicals etc. as well as energy. In terms of energy, biomass is usually used to mean plant-based material however, it can equally apply to both animal, vegetable derived materials and waste. Fossil fuels such as coal, oil and natural gas are also derived from biological materials, however they are materials that absorbed carbon dioxide (CO_2) from the atmosphere several million years ago. Therefore, the main difference between the biomass and fossil fuels as energy sources is the time scale of their formation [10].

The use of biomass as a fuel is considered to be carbon neutral because plants and trees remove carbon dioxide (CO_2) from the atmosphere and store it as they grow. As the energy in these biomasses is released as it burns in homes, in industrial processes, transport activities or energy generation, it returns this stored CO_2 to the atmosphere. At the same time as new plants grow it keeps the carbon cycle in balance as by recapturing the carbon dioxide. Hence when biomass is managed on a sustainable basis, biomass is considered the renewable energy source [11]. The sun is the primary source of energy supply to biomass as solar energy is used indirectly to grow plants

via photosynthesis. The photosynthesis captures 3000 EJ from the solar energy of about 3,850,000 EJ per year and produces more than 100 billion tons of dry biomass [12].

Solar Energy ⟶ Photosynthesis ⟶ Biomass (complex Polymers)

The energy of the sun is absorbed by the green pigment chlorophyll in the plant leaves and is stored within the plant in the form of chemical bond energy. Less than five percent of solar energy incident on a leaf is absorbed while the rest is reflected and transmitted. In the process, water and CO_2 molecules are broken down and a carbohydrate is formed with the release of pure oxygen. A simple chemical equation for photosynthesis can be written as follows:

Carbon dioxide + water + Energy → carbohydrate + Oxygen (1.1)

$$6CO_2 + 6H_2O + Light \rightarrow C_6H_{12}O_6 + 6O_2 \quad (1.2)$$

The stored energy is recycled through a series of chemical and physical conversions processes in the plant, soil, surrounding atmosphere and living matter. Thus when biomass is burnt, this reaction is reversed and energy is released [13]. Biomass energy is derived from the plant sources such as natural forests, industrial human or animal wastes, they can also be sourced from agricultural and forestry processes. The energy stored in the plants and animals and in the waste they produce is referred to as bioenergy. Biomass decomposes via natural process to its molecules with the release of heat. The combustion of biomass imitates the natural process [14]. Biomass is known to be the major source of energy for mankind. In 2010, biomass accounted for about 12.2% of global energy consumption, which makes up 73.1% of the world's renewable [15] and is the fourth source of energy following oil, coal and natural gas. In most developing countries, biomass plays a significant role in the energy sector, especially as the main source of energy for cooking in the domestic sector and thermal energy for many small and medium industries and commercial establishments.

1.3 Biomass Conversion Technology

To gain from the chemical energy contained in the biomass, this energy has to be transformed into more convenient energy forms like heat or electricity. Some processes involve an intermediate transformation from the solid fuel into another

energy carrier such as gas or liquid fuel [8] . There are in principle, mainly three types of conversion processes namely:

- Biochemical via microbial action
- Physical/chemical processing
- Thermochemical via heat treatment

1.3.1 Biochemical processes

With biochemical conversion, biomass molecules are broken down into smaller molecules by bacteria and enzymes [6]. This process is a lot slower than thermochemical conversion but does not require external energy. The three principal routes for biochemical conversion are

- Digestion (anaerobic and aerobic)
- Fermentation
- Enzymatic or acid hydrolysis [6]

Anaerobic digestion is the use of microorganisms in oxygen- free environments to break down organic material. Anaerobic digestion is widely used for the production of methane and carbon-rich biogas from crop residues, food scraps and manure (human and animal). It is also used in treatment of waste water and to reduce emissions from landfills. Anaerobic digestion process has several stages. Firstly, bacteria are used in hydrolysis to break down carbohydrates into forms digestible by other bacteria. The next set of bacteria converts the resulting sugars and amino acids into carbon dioxide, hydrogen, ammonia and organic acids. Finally, these products are acted upon by other bacteria and converted into methane and carbon dioxide. Optimal temperature ranges from 0 to 60 degrees C are used to characterise mixed bacterial cultures. At optimal functions, the bacteria could convert 90% of the biomass feedstock into biogas which contains up to 55% of methane and is a readily usable energy source. The by-products in form of solid remnants from the original biomass, which are leftovers, have potential uses such as fertilizers, animal bedding and low-grade building products like fibre board. The advantage of anaerobic digestion is that it naturally occurs to organic material and releases methane, a potent greenhouse gas, into the atmosphere. Capturing and combusting the methane makes use of the energy inherent in the gas and produces carbon dioxide which is a less potent greenhouse gas. The disadvantages

of anaerobic digestion are that the required microbes pose a health risk to people and animals. Also, the microbes are sensitive to changes in the feedstock such as anti-microbial compounds and changes in reactor conditions; they require constant circulation of the reactor fluid and a constant operating temperatures and pH [16].

Aerobic digestion or composting, on the other hand, is also a biochemical process except that it takes place in the presence of oxygen. It uses different types of microorganisms that access oxygen from the air producing carbon dioxide, heat and solid digestate.

In fermentation, part of the biomass is converted into sugar using acid or enzymes. The sugar is then converted in ethanol or other chemicals with the help of yeasts. The lignin is not converted and is left either for combustion or thermochemical conversion into chemicals. Unlike anaerobic digestion, the by-product of fermentation is liquid [6].

The overall process involves various stages. In the first stage, the crop material is crushed and mixed with water to form slurry. Heat and enzymes are then applied to break down the crushed material into a finer slurry. Other enzymes are added to convert starches into glucose sugar. The sugary slurry is then pumped into a fermentation chamber to which yeasts are added. After about two days the fermented liquid is distilled to separate the alcohol from the solid left-over materials. Lignocellulose which is the structural material of plant must first be broken down into sugars before being fermented into alcohol (ethanol). Molecules of cellulose, hemicellulose and lignin; the components of lignocellulose have strong chemical bonds and are difficult to separate. Mechanical pre-treatment and zymotics are essential to break down lignocellulose. Consequently, at present, conversion of lignocellulosic materials into ethanol is less cost effective than conversion of starch and sugar crops into ethanol. Improving the efficiency and reducing the cost of separating and converting cellulosic materials into fermentable sugars is one of the characteristics of a viable industry. Research and development efforts are focusing on the development of cost-effective biochemical hydrolysis and pre-treatment process to overcome this barrier. Hydrolysis is a chemical process in which molecules are split into parts with the addition of salt and water or weak acid [16]. Figure 1.3 shows the products and uses obtained from biochemical conversion

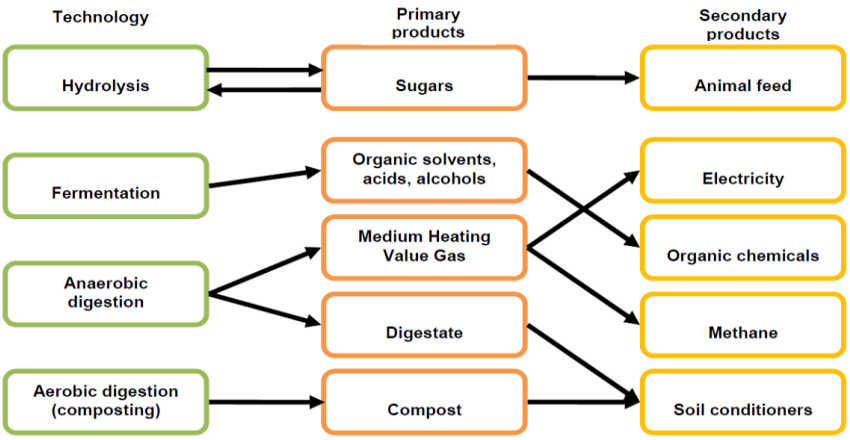

Figure 1.3 Biochemical conversion process [17]

1.3.2 Physical/chemical processes

This is mainly related to wood densification and drying. Wood densification is a process of using wood by-products such as sawdust, residues, slabs, chips and processing them into uniform sized particle so they can be compressed into a fuel product [18] The physio-chemical technology involves various processes to improve physical and chemical properties of solid waste. The part of the waste that is combustible is converted into high energy fuel pellets which could be used for steam generation. Firstly, the waste is dried in other to lower the moisture levels then the incombustible matter is separated mechanically before the waste is converted. The mostly used methods of densification based on shapes and sizes are logs, pellets and briquettes. Fuel pellets have several unique advantages over coal and wood as it is cleaner, free from incombustibles, uniform in size, cost effective, eco-friendly and contains lower ash and moisture contents [19]. Pellets are used more in commercial applications for industrial boilers where ease of handling and burning characteristics offer a competitive alternative. The main advantage of pellets is the higher energy density which significantly brings down the cost of transportation, storage and handling costs per energy unit. However, the drawback of pellet is about the global energy efficiency drop and the rise in cost resulting from investment and operation. The energy cost of producing pellets may rise by 30% as compared to wood chip as drying is a requirement.

Torrefaction

Torrefaction is a thermal pre-treatment step of biomass in an inert atmosphere and in a relatively low temperature range of about 200-300^{0}C for the purpose of producing a fuel with increased energy density [20]. Nitrogen is the mostly used carrier gas to provide a non- oxidizing environment for most laboratory tests. Torrefaction is sometimes described as mild pyrolysis since it is conducted at conditions similar to those of pyrolysis which takes place between 350 -650^{0}C. Torrefaction not only removes moisture and reduces organic volatile components in the biomass but also induces chemical reactions of the polymers found in the plant cell wall such as cellulose (a polymer glucosan), hemicellulose (also known as polyose) and lignin (a complex phenolic polymer) including organic extractives and inorganic extracts (ash). Thus, it affects the mechanical strength of the material and as a result, torrefied biomass has higher calorific value and carbon content in comparison to its parent biomass [21]. Biomass is characterized by its high moisture content, low calorific value with a tendency to absorb moisture. Other characteristics include its large volume or low bulk density which results in in low conversion efficiency including difficulties associated with its collection, grinding, storage and transportation. The evidences from research suggests that the properties of biomass improve to a good extent after undergoing torrefaction, the benefits include higher heating value, improved grindability and reactivity, hydrophobicity and more uniform properties of biomass. When biomass is torrefied, the pre-treatment can further be classified into light, mild and severe torrefaction processes corresponding to temperatures approximated to 200-235, 235-275 and 275-300^{0}C respectively [22]. When biomass undergoes light torrefaction, the moisture and low molecular weight volatiles within the biomass is released and hemicellulose which is the more active constituent in the biomass is degraded to an extent, however, the cellulose and lignin constituents are slightly or hardly affected. With mild torrefaction, hemicellulose decomposition and the liberation of volatiles are intensified while cellulose is consumed to an extent. With respect to severe torrefaction, hemicellulose is almost completely depleted while cellulose is oxidised to an extent. Lignin is the most difficult constituent to be thermally degraded [23].

1.3.3 Thermochemical gasification process

Gasification is a process of energy production via thermochemical route [24]. It is a partial thermal oxidation resulting in a high proportion of gaseous products (carbon dioxide, water, carbon monoxide, hydrogen and gaseous hydrocarbons), small quantity of char (solid products), ash and condensable compounds [tars and oils) [25]. The chemical energy contained in the solid fuel is converted into both chemical and thermal energy of the gas [26]. Gasification has been given a great deal of attention in the past few decades as a result of increasing demand for clean gaseous fuels as well as chemical feedstock. The mechanism of gasification has been studied comprehensively. Recent modelling efforts include the application of equilibrium model to predict the performance of commercial gasifiers (which are reactors in which gasification of solid fuel takes place giving out synthesis or producer gas) and several kinetic models for particular reactor types [27]. In the downdraft gasifier which is the reactor we are considering in this work; the carbonaceous material undergoes several processes. The reason for developing a downdraft gasifier is its specific advantages. The most important is its capability to produce low tar containing producer gas for engine applications. The principle stages of gasification process are drying, pyrolysis, oxidation and gasification.

Drying

The main purpose of the drying zone is the drying of the biomass (solid fuel). In this stage, considering the downdraft gasifier, the feed goes down the downdraft gasifier as a result of consumption of the feed in the reaction zone. Drying of the biomass takes place due to the heat transfer from the hotter zones beneath the drying [28] hence the moisture content of the biomass reduces. The physical moisture present in the wood evaporates and the rate at which it gives up moisture depends on the prevailing temperature in this zone. Typically, the moisture content of biomass is within the range of 5% to 35% and drying occurs at temperatures between 100 and 200^{o}C [25]. The water vapour descends and adds to the water vapour formed in the oxidation zone as represented Part of the water vapour reduced to hydrogen while the rest ends up as moisture in the gas [29].

Pyrolysis

Pyrolysis is the application of heat to raw materials in the absence of air. This is basically, the thermal decomposition of the biomass, in this process the volatile matter in the biomass is reduced as the large molecules such as cellulose, hemi-cellulose and lignin are broken down into carbon (char), various gases and liquids [29]. During pyrolysis the volatile matter in the biomass corresponds to the pyrolysis yield while the carbon and ash content estimates the char yield. The hydrocarbon gases can condense at a low temperature to generate liquid tars [25]. It is the starting step in the combustion and gasification processes where it is preceded by total or partial oxidation. The pyrolysis process may be represented by a generic reaction

$$C_nH_mO_p(Biomass) \rightarrow \sum_{gas} C_x H_y O_z + H_2O + C(char) \quad (1.3)$$

The lower process temperature and longer vapour residence time promote the production of charcoal. The high temperature and longer residence time favour the increase of the biomass conversion to gas while a lower temperature and short residence time promote the conversion of biomass to liquids [4].

Pyrolytic products can be used as fuels with or without upgrading and they can also be utilised as feedstock for chemical or material industries. Due to the nature of the process, yield of useful products is high compared to other processes. In general, pyrolytic products are more refined and therefore can be used with greater efficiency. Materials suitable for pyrolysis processing include coal, animal and human waste, cardboard, plastics, rubber, food scraps and biomass [30]. The products derived from pyrolysis depend on the physical and chemical characteristics of the biomass, the design of the pyrolyzer and operating parameters such as heating rate, pyrolysis temperature and residence time in the zone.

Pyrolytic Modes

There are three primary types of pyrolytic reaction usually distinguished by temperature and the processing or residence time of the biomass. These are slow, flash and fast pyrolysis.

Carbonization is a slow pyrolysis process. Conventional or slow pyrolysis is characterised by slow biomass heating rates, low temperatures, lengthy gas and solid

residence times. Depending on the system, heating rates are about 0.1 to 2°C per second and the temperatures are usually around 500°C. The vapour (gas-phase) products have ample opportunity to react with other products to form char. During the conventional pyrolysis the biomass is slowly devolatilised hence tar and char are the main products. Flash pyrolysis is characterised by moderate temperature around (400 to 600°C) and rapid heating rates (>2°C/s). Vapour residence times are usually less than two seconds, when compared to slow pyrolysis, considerably low tar is produced however, the oil and tar products are maximised. Entrained flow or fluidised bed reactors are considered the best reactors for Flash pyrolysis. Due to the rapid heating rates and short reaction time, this process requires smaller particle size for better yields compared to the other processes. Fast pyrolysis is a process in which very high heat flux are exerted to biomass particles leading to very high heating rates in the absence of oxygen [31]. Fast pyrolysis is a process in which organic materials are rapidly heated to 450 – 600°C in the absence of air. Under these conditions, organic vapours, pyrolysis gases and charcoal are produced. The vapours are condensed to bio-oil. The main difference between flash and fast pyrolysis (more accurately defined as thermolysis) is the heating rates and hence the residence times and products derived. Heating rates are between 105 – 200°C per second and the prevailing temperatures are usually higher than 550°C. As a result of the short residence time, products are high quality, ethylene- rich gases that could subsequently be used for the production of alcohols or gasoline. Notably, the production of char and tar is considerably less during this process [26].

Physical process of pyrolysis

The basic phenomena that takes place during pyrolysis are heat transfer from a heat source leading to an increase in temperature inside the fuel. Sequel to this, initiation of pyrolysis reactions occurs as a result of increased temperature. This leads to the release of volatiles and the formation of char. The released volatiles flow towards the ambient temperature resulting in heat transfer between the hot volatiles and cooler un-pyrolysed fuel. Some of the volatiles condense in the cooler parts of the fuel, as result, tars are formed. Due to these interactions, auto catalytic secondary pyrolysis reactions occur [32]. From a thermal viewpoint, the pyrolysis process can be divided into four stages and distinguished by their temperature, however, the boundaries between them are not sharp so there is always some overlap. At the initial stage with temperatures within

100-300°C, exothermic dehydration of biomass takes place releasing water along with low molecular weight gases such as CO and CO_2. The intermediate stage also known as the primary pyrolysis stage takes place within the range of 200 -600°C. Most of the vapour or precursor to bio-oil is produced at this stage. Large molecules of biomass particles decompose into char (primary char), condensable gases (vapours and precursors of the liquid yield) and non-condensable gases. In the final stage where temperatures are within 300-900^{o}C, secondary pyrolysis takes place given rise to secondary cracking of volatiles into char and condensable gases. If the condensable gases are quickly removed from the reaction site, condenses as tar or bio-oil in the downstream reactor [6].

Chemical process of pyrolysis

The chemical composition of the fuel strongly influences the chemistry of pyrolysis**.** The elemental composition of the fuel may be obtained from ultimate analysis. Also, a reasonable idea of the percentage of the major products of pyrolysis (char and volatiles) is obtained from the proximate analysis. The biomass wood or material is directly affected as the pyrolysis process begins. These effects include the colour, weight, size, flexibility, strength, flexibility and mechanical strength. Size and weight are reduced while flexibility and mechanical strength are lost. Around the temperatures of 350 °C, weight loss reaches about 80% and the remaining biomass is converted to char. Extended heating, to about 600^{o}C reduces char fraction to about 9% of the original biomass weight. The primary pyrolysis reactions are either dehydration or fragmentation reactions (see Figure 1.4). Subsequently, several reactions products are formed [33].

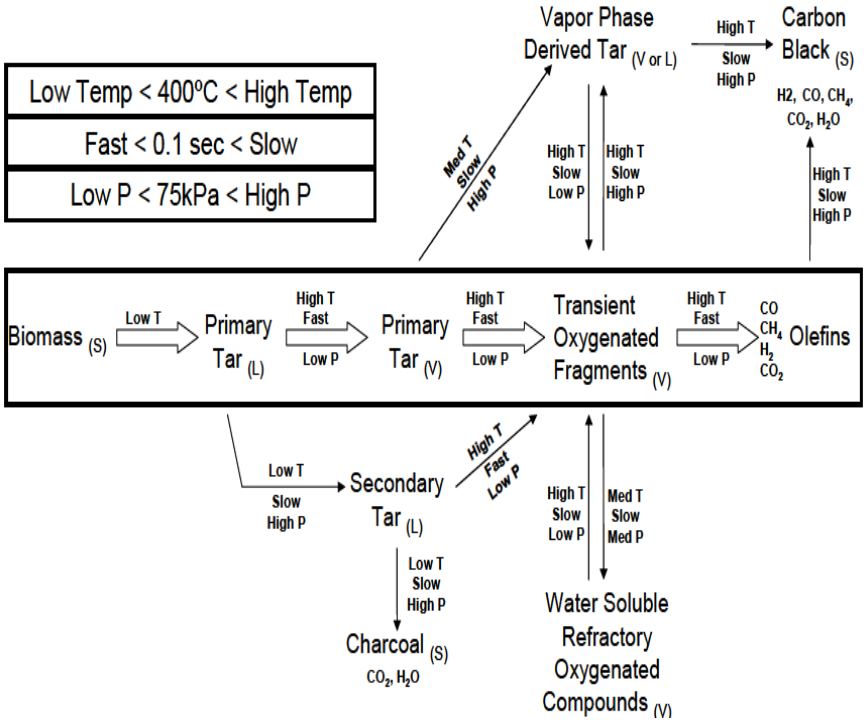

Figure 1.4 Reactions taking place in fast pyrolysis [33]

Biomass has three main components which are cellulose, hemicellulose and lignin. These constituents have different rates of degradation and preferred temperature ranges of decomposition. The decomposition of cellulose involves various complex multiple stages. The Broido-Shafizadeh model [4] has been proposed to explain it and can be applied qualitatively to most biomass. Figure 1.5 is a schematic of the Broido-Shafizadeh model showing the intermediate pre-reaction of the pyrolysis process shown as Reaction 1 followed by two competing reactions.

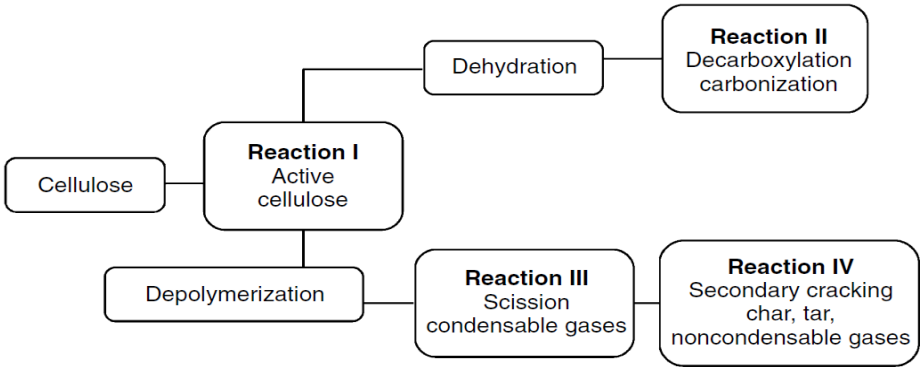

Figure 1.5 Modified Broido-Shafizadeh model of cellulose [6]

Reaction II involves the dehydration, decarboxylation and carbonization through an order of steps to produce char and non-condensable gases like water vapour, carbon monoxide and carbon dioxide. It is favoured at low temperatures of less than 300 °C. In reaction III, depolymerisation and scission takes place producing condensable gases and tar. It is favoured with faster heating rates and higher temperatures of over 300 °C, the condensable vapour can condense to form bio-oil or tar if left to escape the reactor quickly. If, however, it is held within the reactor in contact with the biomass it can undergo secondary reactions (reaction IV) cracking the vapour into secondary char, tar and gases. Cellulose is a polymer consisting of linear chains of B (1, 4) d-glucopyanose units with an average molecular weight of 100,000. Cellulose components normally constitutes about 45-50% of the dry wood. The study carried out by Shafizadeh on the pyrolysis of cellulose with respect to temperature shows that at temperatures less than 300 °C, a reduction in the degree of polymerization takes dominates, above this temperature, there is formation of char, gaseous products and tar which mainly comprises of laevoglucosan that vaporises and decomposes with increased temperature.

Hemicellulose is a mixture of polysaccharides mainly composed of glucose, mannose, galactose and galacturonic acid residues. Hemicellulose produces more gas and less tar and char compared to cellulose it constitutes about 20-40% of the dry wood. However, it produces equal amounts of aqueous products of pyroligneous acid. According to Soltes and Elder [34], Hemicellulose is thermally most sensitive and decomposes within the temperature range of 200 °C – 260 °C. This decomposition may occur in two steps; the decomposition of the polymer into soluble fragments and/or the subsequent conversion into monomer units that further decompose into volatile products.

Lignin is a random polymer of substituted phenyl propane units that can be converted to aromatics. Lignin is amorphous in nature and is considered the binder for agglomeration of fibrous components. Lignin constitutes between 17-30% of the biomass component and decomposes when subjected to temperatures around 280 ^{o}C - 500 ^{o}C. Char yield is more in the products of lignin pyrolysis as it constitutes about 55%, pyroligneous acid consists of 20% and tar residue is about 15%.

Oxidation or Combustion

The oxidation zone lies in the section where air/oxygen is supplied. This is a reaction between the volatile products of pyrolysis and oxygen in the air. The oxidation part of the biomass is necessary to obtain thermal energy required for the endothermic processes to maintain the operative temperature at the required level [35]. The oxidation is carried out in stoichiometric amount of oxygen in order to oxidize part of the fuel. It results in a rapid rise in temperature up to 1100 °C and 1500 °C; the reactions are as shown below:

$$C + O_2 \rightarrow CO_2 \qquad \Delta H = -394KJ/mol \tag{1.4}$$

$$C + 1/2O_2 \rightarrow CO \quad \Delta H = -111KJ/mol \tag{1.5}$$

$$H_2 + 1/2O_2 \rightarrow H_2O \ \Delta H = \text{ -242KJ/mol} \tag{1.6}$$

The heat generated is used to drive the drying and pyrolysis of the fuel and the gasification reactions. Apart from generating heat, the oxidation zones also function to oxidize almost all pyrolysis products coming from the pyrolysis zone. The oxidation reactions of the volatiles are very rapid, and the oxygen is consumed before it can diffuse to the surface of the char so combustion of the solid char does not occur. The oxidation of condensable organic fraction to form lower molecular weight fraction is important in reducing the amount of tar produced by the gasifier. The products of this step are CO_2, CO, H_2, H_2O, hydrocarbon gases, residual tars and chars which then descends into the gasification zone [28].

Reduction

The step includes all the products of the preceding stages of pyrolysis and oxidation; the gaseous mixture leaving the combustion zone mainly containing carbon-dioxide, water vapour, inert nitrogen and some lower molecular weight hydrocarbons such as methane, ethylene and ethane etc., passes over the hot charcoal in the reduction zone resulting in the formation of the final synthesis gas. In this process, sensible heat of the gases and charcoal is converted into chemical energy of the producer gas due to char reacting with these hot gases from the zones above. As a result, some reduction reactions occur, and the gases are reduced to form greater proportion of H_2 and CO as shown below.

Boudouard Reaction

$$C + CO_2 \leftrightarrow 2CO \quad \Delta H = 172.4 kJ/mol \tag{1.7}$$

The principal reaction in the reduction is that of carbon dioxide and hot carbon to produce carbon monoxide. This is an endothermic process and it is referred to as 'Boudouard' reaction (Eq. (1.7)).

Water gas reaction

$$C + H_2O \leftrightarrow CO + H_2 \quad \Delta H = 131.3 kJ/mol \tag{1.8}$$

The reaction between water vapour and carbon resulting in the formation of hydrogen and carbon monoxide (Eq. (1.8)) is called water gas reaction. It is an endothermic reaction that takes place between 600^{o}C and 950^{o}C. Since reactions (1.7) and (1.8) are endothermic, gas streams lose heat and temperature in the reduction zone consequentially drops. If there is excess water present in the reduction zone, a reaction known as water shift reaction can occur.

Water-gas shift reaction

$$CO + H_2O \leftrightarrow CO_2 + H_2 \quad \Delta H = -41.1 kJ/mol \tag{1.9}$$

Reaction (1.9) is an exothermic reaction and it is undesirable as it reduces the caloric value of the gas. Therefore, the excess moisture in the fuel needs to be avoided. Some of the hydrogen produced in the reduction zone remains free while a portion can combine with carbon to form small amounts (3 to 5%) of methane as shown in Equation (1.10).

Methane Reaction

$$C + 2H_2 \leftrightarrow CH_4 \quad \Delta H = -74.8 KJ/mol \tag{1.10}$$

Reforming reaction

$$CO + 3H_2 \leftrightarrow CH_4 + H_2O \quad \Delta H - 165.1\ KJ/mol \tag{1.11}$$

The gaseous mixture exiting the biomass gasifier mainly consists of hydrogen, carbon dioxide, nitrogen and water vapour. It may also contain some amount of hydrocarbons such as CH_4, C_2H_2, and C_6H_6, the amount of each of these gases may depend on the

configuration of the gasifier. Producer gas is also loaded with dust, tar and water vapour.

The main reactions indicate that heat is required during the reduction process. Hence, the temperature of the gas goes down during this stage. If gasification goes to completion, all the carbon is burned or reduced to carbon monoxide and some other mineral matter that is vaporised leaving ash and char (unburned carbon) [36]. Figure 1.6 shows the products obtained from thermochemical conversion process and its uses.

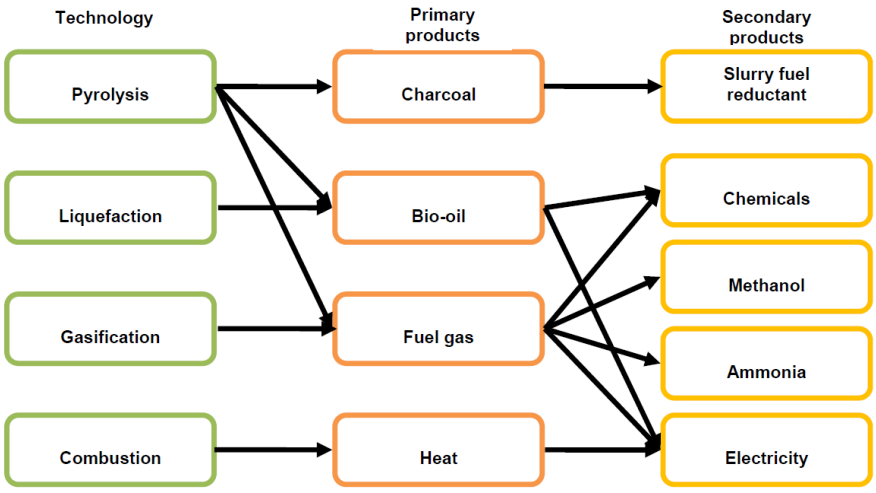

Figure 1.6 Thermochemical conversion process [17]

1.4 Application of Biomass Gasification

Biomass gasification has many potential applications, including:

- Thermal application
- Power generation
- Combined Heat and Power (CHP) application
- Chemical production

1.4.1 Thermal application

Most gasifiers used in commercial applications today are for the production of heat because of their simplicity, especially in the agriculture sector. The main advantages of gasifiers for heating applications are the ability to produce higher temperatures than conventional burning systems, better control over heating systems, enhancement of

boiler and total efficiency, lower emissions etc. Most conventional oil-fired thermal installation can be run by producer gas.

The use of biomass as an alternative fuel plays an essential role in the Indian economy contributing nearly 28% to India's Total Primary Energy Supply (TPES). Considering the rise in the prices of diesel and petrol, biomass has attracted significant attention in the micro, small and medium enterprises (MSMEs) sector. There are many energy intensive industries which use commercial fuels such as biomass, coal, oil and gas fuels. Figure 1.7 shows the application of TERI's biomass gasifier technology for the thermal application by an entrepreneur. The technology has been applied in a food processing unit in Chennapatana. The arrangement of the unit before the installation of the gasifier consists of two roasters. The first operates at a temperature of 120^{o}C to remove moisture while the second functions to roast grains at 250^{o}C. More wood is added to maintain the temperature in the unit. The unit operates for 12 hours and utilises an average of 3.5 tonnes of wood. The result is that 60% saving is achieved on fuel compared to furnace oil and high quality of product is also achieved due to maintaining the temperature.

Figure 1.7 Biomass Gasifier Technology for food processing [33]

1.4.2 Power generation

The producer gases from the gasification of biomass can be used to generate heat and electricity and can possibly be used for the synthesis of liquid fuels, chemicals or H_2. The main technologies that employ the use producer gases to generate power include co-firing; steam turbines; gas turbines; Stirling engines; internal combustion engines; combined cycle systems. Co-firing and combined cycle system and the integrated gasification combined cycle (IGCC) system which uses steam turbine for power generation are explained in the sections below.

Co-firing

In co-firing, the producer gases from biomass gasification are burned together with coal to avoid ash mixing, this is done by the direct application of the product gas in a coal power plant. Co-firing has the advantage of allowing the use of coal ash as a construction material, the costs are low and this application has an existing market. The issue with co-firing is the impact of biomass ash on quality of the boiler, fly and bottom ash. The technical risk is minimal as the gas is utilised hot which removes the tar products. Fuel gas produced by biomass gasification like coal can be co-fired with natural gas either directly in turbines, duct burners or as re-burning fuel.

1.4.3 Combined heat and power (CHP)

In combined heat and power (CHP) plants, the products gas is fired on gas engine. The producer gas even from air blown gasifier can be used after cleaning the system to power stationary engines such as diesel engines on dual fuel mode or sterling engines. For engine applications, the producer gas should have a heating value of approximately 5 -6MJ/m^3 [37]. Typically, the energy output is one third electricity and two thirds heat. The main challenge in the implementation of integrated biomass gasification CHP plants is the removal of tar from the product gas. There are a few technological successful biomass gasification plants; the plant in Güssing Austria as shown in Figure 1.8. The Pilot CHP plant based on a 75 kW Stirling engine is considered as a major breakthrough with regards to utilising of Stirling engines for small scale CHP plants using natural wood fuels.

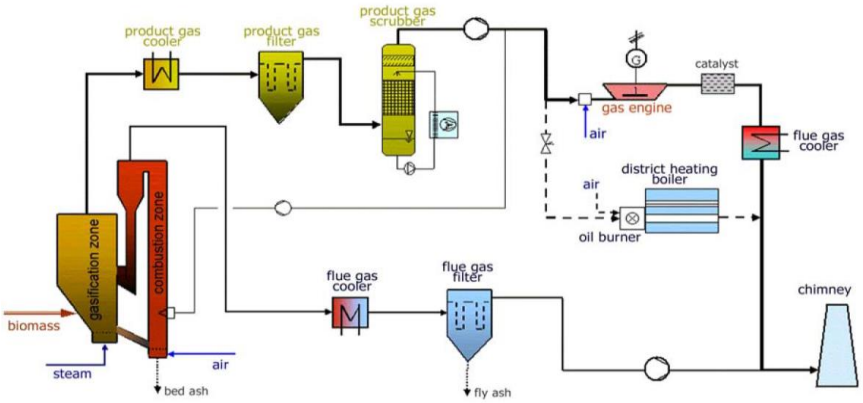

Figure 1.8 Process flow sheet of the Gussing Plant [38]

The combined heat and power plant has a fuel capacity of 8 MW, an electrical output of about 2 MW_e and heat output of 4.5 MW_{th} with an electrical efficiency of about 25%. Wood chip with content of about 20-30% of water content is used as fuel. The plant consists of a gas engine with an electrical generator, a fast circulating fluidised bed (FICFB) steam gasifiers and a heat utilising system. The calorific value of the producer gas is between 12-14 MJ/Nm^3 with compositions; H_2 35-45%, CO 20-30%, N_2 3-5%, CH_4 8-12%, CO_2 15-25% and tar content after the cleaning of the gas of < 20 mg/Nm^3 [38]. However, some of the problems that need addressing regarding further development and optimisation of the technology are those concerning the overall electric efficiency i.e. reduction in heat losses and reduction in ash deposition on the Stirling engine heater by an efficient automatic cleaning system.

Internal combustion engines

The internal combustion engine has had a colossal technological impact on the world over the last century. The main purpose of ICE is to convert chemical fuel energy into mechanical or useable shaft power. These engines are usually reciprocating piston engines with various processes occurring inside the cylinders according to the movement of the piston. The mode of conversion is carried out using either compression ignition (CI) engines or spark ignition (SI). In SI engines, the fuel is injected in the air flow during the intake stage, the mixture is almost adiabatically compressed and subsequently ignited by a spark produced by a plug, and it then expands producing useful work. This process is depicted as in the four-stroke configuration engine: intake, compression, combustion and power stroke, and exhaust. The name

stems from the fact that the whole work is realised by means of four strokes each corresponding to a thermodynamic process. With the similar configuration of CI engines, the processes also include intake, compression, combustion/expansion and discharge. With this operating concept, only air is compressed, the fuel is injected at high temperature into the cylinder and the air-fuel mixture selfignites due to the high temperature. In ICEs, the use of alternative gaseous fuels is one of the effective ways of reducing engine emissions because it produces little or no oxides of sulphur (SO_X) and relatively small amounts of (NO_X) during the combustion, which is the main constituent of acid rain, and significantly less CO_2 [39]. Whether spark or compression ignited, synthesis gas could serve to power large stationary engines such as those presently operated using natural gas. The main advantage achieved from the use of synthesis gas over the use of conventional liquid, petroleum-based fuels is the reduction of environmental impact. [40]. Usually, Diesel engines are converted the SI mode to operate on gaseous fuels since methane (CH_4) and carbon monoxide (CO) are known for their high anti-knock properties and will not selfignite at the end of the compression stroke.

Integrated gasification combined cycle (IGCC)

The integrated gasification combined cycle (IGCC) system is a power generation technology that allows the use of solid and liquid fuels in a power plant that has the environmental benefits as natural gas fuelled plant and the thermal performance of a combined cycle. The solid or liquid fuel is gasified with air or oxygen and the resulting gas which is syngas is cooled and clean off of its particulate matter and any sulphur species then subsequently fired in a gas turbine. As the emission-forming constituents is removed by pressure from the gas, IGCC plants have the potential to meet stringent air emission standards. Also, the hot exhaust gas emitting from the gas turbine is sent through to a heat recovery steam generator (HRSG) where it produces steam that drives a steam turbine. Therefore, energy in form of power is produced from both steam and gas turbines. Figure 1.9 shows a block diagram of an IGCC plant.

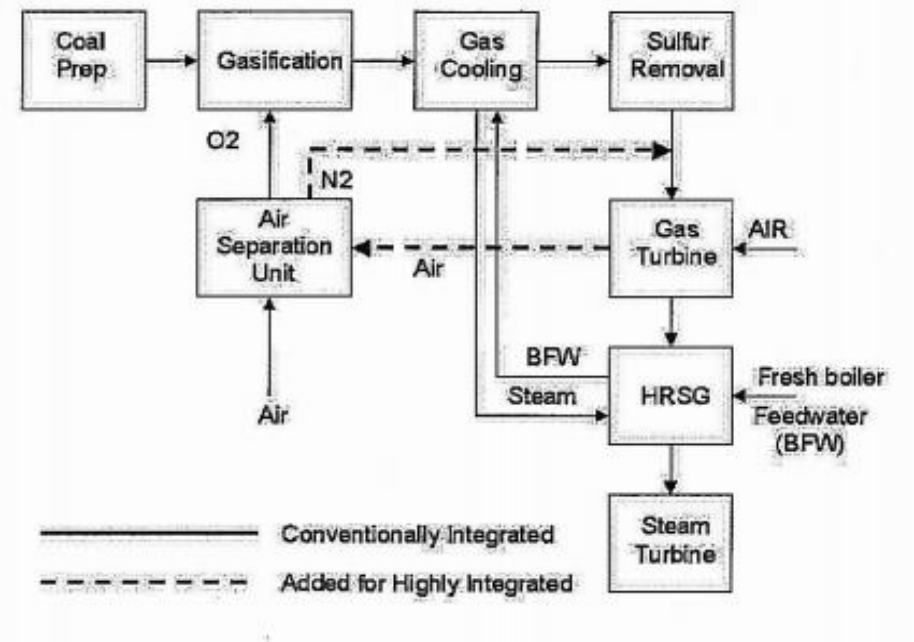

Figure 1.9 Flow diagram of an IGCC plant [34]

An effective and practicable option of biomass utilization for the production of energy is gasification integrated with a combined cycle. Biomass gasification integrated with gas turbine based combined cycle (BIGCC) is an efficient biomass energy conversion technology. BIGCC can also be applied to organic residue from all sources. This technology has the potential of reaching high efficiencies based on clean and renewable fuels. The plant uses low grade fuels but with reasonable efficiencies based on heating values. BIGCC systems are based on an advanced technology; it is a gasifier used in place of the traditional combustor that has both gasifier and gas turbine. The gas and steam turbines operate together as a combined cycle. BIGCC systems are very clean and more efficient than traditional fuel fired systems. In these systems, biomass is converted into gaseous fuel which when cleaned is comparable to natural gas. The hot gas is further cleaned with the use of an advanced cleaning process before it is burned in the gas turbine to generate electricity [41].

Stirling engines

Stirling engine processes heat into mechanical energy without explosive combustion process. The heat is supplied to the working medium via the heating of the external wall of the heater and therefore it is possible to power the engines practically from any source. Thus, the external heat could come from sources such as coal, wood, biomass or derivatives of oil. Stirling engines are usually made up of two cold and warm pistons

as well as a regenerative heat exchange and heat exchangers between the working medium and external heat sources [42]. A biomass-fired Stirling plant is an installation which converts biomass in solid, liquid or gaseous form into carbon neutral power and heat. In general, Stirling engines have reasonable efficiencies but at a very high cost and these engines have a fuel-flexibility as well as better control or emissions.

1.5 Aim and objectives of this research

The aim of the study is to develop an accurate mathematical modelling method of operation of a biomass gasifier for synthesis gas production. The downdraft gasifier is chosen for this study due to its easy fabrication and operation and also due to low tar content in the producer gas. They are also very suitable for small-scale applications. To achieve this, this work is split to achieve more specific objectives:

- Investigate and review various methods employed for modelling a biomass gasifier;
- Study the chemistry of gasification (thermodynamics and kinetics of the gasification reactions);
- Investigate and define process parameters as it affects the performance and operation of the downdraft gasifier;
- Modelling of the gasification process in downdraft gasifier in order to provide information on how process variables affect gasification to allow prediction of optimum performance.

1.6 Methodology of research

Biomass gasification as a thermochemical conversion of solid biomass to gaseous fuel have been carried out by various researchers since the Second World War II. Various reactor configuration has been developed in producing gases with low tar content. The process parameters and the operating conditions that determine the performance of the gasification include physical properties of the fuel sample such as the density, size and shape, the design of reactor, temperature, equivalence ratio, type of oxidant, moisture content, etc. It is important to understand how these operating conditions and parameters affect the maximising the conversion of energy from the solid fuel to the gaseous fuel. Important to note also, that the problem of tar in the exit gas can be

reduced if the pyrolysis products are exposed to elevated temperatures and longer residence times for cracking. Downdraft gasifier which is a common type of gasifier is chosen for this study as it is a solution to the problem of tar in the exit gas. The main advantage of using downdraft gasifier is the possibility of producing low tar output gas suitable for IC engine applications. Biomass feed stocks were chosen based on the availability of experimental data and these feed stocks include woodchip, rubber wood, wood pellets, eucalyptus wood and palm oil fronds. Gasification offers a way to convert various low-value lignocellulosic biomass to syngas for combined heat and power generation, production of H_2 and synthesis of liquid fuels. Co-firing of syngas in existing pulverised coal and natural gas combustors have been successfully commercialised. However, there is need for more research to improve syngas quality for commercial uses in a high energy efficient heat and power generator such as gas turbines and production of liquid fuels.

With the above background, a literature survey is carried out to investigate various methods employed for modelling a biomass gasifier, several types of gasifiers and reviews on gasification models. A mathematical model based on equilibrium and kinetic modelling is developed to simulate the behaviour of a downdraft gasifier divided into three zones. The simulation tools used are MATLAB and Aspen HYSYS due to their efficiency in modelling engineering systems. Based on the same models, the downdraft gasifier is represented in Aspen HYSYS for both single and double air stream operations for the production of synthesis gases. The predicted results from the model are compared with the published experimental data. A parametric study is then carried out to study the effect of varying the operating conditions on the predicted synthesis gas composition and its energy content.

1.7 Original Contribution to Knowledge

Accurate mathematical models are essential for process optimization purposes in finding optimal design parameters and operating conditions which can lead to better process performance**.** The fixed bed downdraft biomass gasifier has been chosen for this study as it has the advantage of producing low tar.

Original contribution to knowledge consists in the development of the method of numerical simulation of a downdraft gasifier operation, which is based on

thermodynamic and kinetic models applied to a downdraft fixed bed. The model presented in this work is made up from three constituent sub-models which attempt to simulate each of the zones namely pyrolysis, oxidation and reduction zones. These are then combined to form a complete model using both single and double air feed to the gasifier.

Initially for the single air operation, a mathematical model was developed from the generic biomass gasification equations and mass and energy balances applied across the zones. The resulting modelling equations were solved using codes written in MATLAB. The processes were subsequently simulated using Aspen HYSYS employing Gibbs and Plug Flow Tubular Reactors (PFR) arranged in the flow sheet to represent pyrolysis, oxidation and reduction zones of the gasifier. In one approach to simulation the three zones were all assumed to reach thermodynamic equilibrium and each zone was simulated using a Gibbs Reactor. In another approach an assumption was made that the third zone, the Reduction Zone, could be simulated using a chemical rate approach. This required chemical equations to be presented that could theoretically represent the formation and disappearance of species in the Reduction Zone. In HYSYS this zone was represented by a PFR. Whilst this operation requires the presentation of chemical kinetic data it also integrates over a stated tubular reactor to produce a unique solution according to the conditions calculated by the previous zone, the oxidation zone represented by a Gibbs Reactor. Using such an approach for this type of problem; simulation of a biomass gasifier is unique. This approach also gives the possibility of dynamic modelling of the operation as allowed in HYSYS and this could be a possibility in future work particularly in relation to the prediction of methane formation and disappearance in the biomass gasifier.

Use of the Gibs Reactors and the PFR allows the variation of moisture levels in the system and the flowsheet set up in HYSYS allows the creation of a double air stream using an appropriate mixer operation where the second air stream can be introduced prior to the oxidation stage. The use of the PFR is obviously limited by the quality of the kinetic data available and the reactions used to represent the reduction operation but the use of the PFR widens the flexibility of the simulation in representing this third stage. The overall simulation of the stream, exiting the reduction section, for both single and double air operation produces results close to the experimental ones.

1.8 Thesis Structure

This thesis is divided into 7 chapters. The first chapter reviews the biomass general characteristics, actual use and potential of biomass resources. Different biomass conversion processes are explained with the focus on biomass gasification process. With regard to biomass gasification, different steps and reactions are described. Finally, this chapter presents the justification for the work, aim and objectives of the thesis together with the original contributions made.

Chapter 2 reviews different types of gasifiers and approaches to model biomass gasification process: thermodynamic equilibrium models, kinetic models and ANN models and Aspen Plus models.

Chapter 3 describes the process of biomass gasification assuming pyrolysis, oxidation and reduction zones as presented in HYSYS and solved in MATLAB, the assumptions and model developments were presented here.

Chapter 4 describes the theory behind the simulation of biomass gasification in a downdraft gasifier using Aspen HYSYS and MATLAB in detail. Process description, components, physical properties and block specification are described in this chapter

Chapter 5 describes the simulations carried out for validating the models developed in this study for the various feeds utilized. Wood chips, wood pellets, rubber wood, palm oil fronds and eucalyptus woods have been used as biomass in a downdraft gasifier.

Chapter 6 presents the results obtained for the gasification of various biomass feedstock such as wood chips, wood pellets, rubber wood, Eucalyptus wood and oil palm fronds. These model results were compared with experimental data from literature.

Chapter 7 is the conclusions and recommendations section. It summarises all that have done in this work and goals achieved. It also proposes some recommendations for future research.

Chapter 2 Literature Review

2.1 Characteristics of Gasifier fuels

Since biomass fuels differ in their physical, chemical and morphological properties, different gasification technologies, methods and gasifiers are required. Thus a fuel can be characterised using several parameters [43]. Each type of gasifier will operate satisfactorily with respect to stability, gas quality, efficiency and pressure losses within certain ranges of characterised fuel properties such as;

- Energy Content
- Moisture content
- Volatile matter
- Dust content
- Tar content
- Ash and slagging features

2.1.1 Energy Content

The most important characteristics for any biomass to be considered as an energy source depend on the actual amount of energy that can be derived from its transformation and use. In order to calculate this, one needs to understand and appreciate the three distinct measures of the energy content of a fuel.

- Primary energy content – This represents the total energy of the resource in its untransformed state.
- Delivery energy- This characterises the amount of energy reaching the consumer. In the case of wood fuel used as firewood for instance, the delivered energy is the same as the primary energy. However, if the wood fuel is used as charcoal then the delivery energy in the charcoal is a fraction of the primary energy.
- Useful energy- This is the actual energy used by the end user after losses due to conversion inefficiencies have been accounted for.

The energy content of biomass and other fuels is measured by its calorific value. There are two measures for calorific value which are gross calorific value and net calorific value. The gross calorific also known as the higher heating value (HHV) is determined at constant volume for liquids fuel and for gaseous fuels at constant pressure. If the water formed and liberated during the combustion is in the liquid phase, then the corresponding calorific value is called gross calorific value. The net calorific value also known as the lower heating value corresponds to the process when the water formed during the combustion remains as steam. Here the lowType equation here.er heating value (LHV) of the gas is reported as a pointer to the quality of the gas. The lower heating value of the gas is dependent on the percentage quantities of CO, H_2 and CH4 in the producer gas and is thus calculated from the following equation [44]:

$$LHV_g = y_{CO} LHV_{CO} + y_{H_2} LHV_{H_2} + y_{CH_4} LHV_{CH_4} \quad (2.1)$$

where;

Y is volume fraction of combustible gas component

LHV is Lower heating value of the combustible gas component.

$LHV_{CO} = 13.1 MJ/Nm^3$

$LHV_{H_2} = 11.2 MJ/Nm^3$

$LHV_{CH_4} = 37.1 MJ/Nm^3$

One of the basic steps of performance modelling and simulation on thermal systems begins with determining the HHV from the elemental composition of the fuel. Examples of such calculations are shown in Table 2.1 Channiwala [45] presents a unified correlation derived using 225 data points for computation of HHV from elemental analysis of fuels. These variety of fuels range from gaseous, liquid, coals, biomass material, char to residue derived- fuels. Also, fuels having a wide range of elemental composition such as C- 0.00-92.5%, H-0.43- 25.15%, O- 0.00- 50%, N-0.00- 5.60%, S-0.00-94.08% and Ash-0.00-71.4% have been used to validate this correlation.

Table 2.1 Correlation for estimation of HHV

	Author	Correlation	Assumptions and basis
1	Strache and Lant [46]	$HHV^* = 0.3406C + 1.4324H^* - 0.1532O^* + 0.1047S^* (MJ/Kg)$	Modified version of Dulong with accuracy of 2% over a range of coals
2	Jenkins [47]	$HHV = 0.4791C + 0.6676H + 0.0589O - 1.2077S - 8.42\ MJ/Kg(a)$ $HHV = -0.763 + 0.301C + 0.525H + 0.064O\ (MJ/Kg)(b)$	Derivation based on 19 and then 57 data points of biomass material respectively. Correlation is about 7%
3	Niessen [48]	$HHV^* = 0.2322C^* + 0.7655^* - 0.072O^* - 0.0419N^* + 0.0698S^* + 0.0262Cl^* + 0.1814P^* + (MJ/Kg)$	Derived for waste water sludge, showed prediction fell short by 6%

These correlations of HHV are converted to MJ/Kg and expressed on dry bases and C, H, O, N, S and P represent carbon, hydrogen, oxygen, nitrogen, sulphur, chlorine and phosphorous content of the material. The correlations have been divided into two parts. In the part (a), the correlations are based on the combustion reactions of conversion of C, H and S to CO_2 , H_2O and SO_2 respectively with various assumptions in relation to the association of oxygen with hydrogen or carbon. In parts (b), correlation is based on the assumption that the HHV of fuel is proportional to the amount of oxygen/air required for complete combustion and the constant of proportionality is represented either as a function of oxygen or hydrogen content in the fuel [49].

2.1.2 Moisture Content

Moisture in high amounts is a major characteristic of biomass. Biomass absorbs moisture from the ground via the root and pushes into the sapwood, the moisture eventually travels to the leaves via the capillary passages. The reaction of photosynthesis in the leaves use some of it while the rest of the moisture is released

into the atmosphere. For this reason, the leaves contain more moisture than the plant trunk. The amount of moisture content of some biomass can be as high as 90% , however, high amounts of moisture in the biomass are not desirable as the moisture drains much of the deliverable energy from the gasification plant. This is because the energy used in evaporation is not recovered. The moisture in the biomass can exist in either free or external and inherent or equilibrium form. Free moisture resides outside the cell walls and it is above the equilibrium moisture content. Inherent moisture is absorbed within the cell walls, when the cell walls are completely saturated, the biomass is said to have reached its saturation point or equilibrium moisture. Moisture content can be determined by the test protocol given in ASTM standards D-871-82 for wood.

Moisture Basis

Biomass moisture is often expressed on dry basis. If wet biomass becomes dry after drying then, its dry basis is expressed as

$$M_{dry} = \frac{W_{wet} - W_{dry}}{W_{dry}} \quad (2.2)$$

For wet biomass, this can give a percentage higher than 100%, therefore it is important to specify the basis of the moisture.

The wet basis of moisture is expressed as

$$M_{wet} = \frac{W_{wet} - W_{dry}}{W_{wet}} \quad (2.3)$$

The relationship between the wet (W_{wet}) and dry (W_{dry}) basis can be expressed as

$$M_{dry} = \frac{W_{wet}}{1 - W_{wet}} \quad (2.4)$$

In the work carried out by Atnaw et al [50], they studied the variation of oxidation zone temperature with time from start of batch operation for gasification of fuel with moisture content at 22% and 29%. The results showed that the oxidation temperature in the case of the higher moisture content was consistently low during the entire process duration, with roughly half the average value recorded for lower moisture content. In the both cases, the oxidation temperature showed a sharp rise during the first 10 minutes of start-up. The oxidation temperature steadily increased with operation time for the

case of lower moisture content fuel, while it remained relatively stable at an average of 600 ^{o}C for that of higher moisture content fuel. They also investigated the influence of moisture content on the composition of syngas throughout the gasification period. The results show the variation of CO content from the start of the gasification operation of oil palm frond (OPF) for 22% and 29% moisture content. With the 22% moisture content of fuel, CO content increases during the initial phase of the gasification but decreases at about the 75th minute of operation, while the CO content of the OPF with 29% moisture content of fuel was consistently lower than that of the lower moisture content. During the 75th minutes an average of 25% CO content was obtained with moisture content of 22% and 11.4% CO was obtained with 29% moisture content of fuel. They also varied the calorific value of syngas with operation time for gasification of OPF with moisture contents 22 and 29%. The results show a consistent low calorific value concentration of CO obtained for the gasification of fuel with higher moisture content. This is due to the lower concentration of CO obtained from the experimental run using high moisture content of OPF.

In the study of the effects of different parameters on performance and emission of fired stoves carried out by Bhattacharya[51], they investigated the effect of moisture content in fuel on stove performance. Wood pellets with moisture contents of 5.9%, 9.4%, 18.2% and 22.1% were used for the test. The results show that the burning rate, cooking power and emission factors all decreased with the increase of MC.

Ratnadhariya et al [52] presents the influence of moisture content on the gas composition, temperature level and gasifier performance parameters at each zone with constant equivalence ratio of 0.3. In the pyrolysis zone, the gas composition as a function of moisture content shows that all concentrations except H_2O decreased with increasing moisture content. In the oxidation zone, all concentrations are decreasing with increasing moisture content with an exception to H_2O. Also, the influence of moisture content on the final gas composition reveals that concentrations such as H_2, CO and CH_4 are decreasing with increasing moisture. The reason is due to much availability of moles of moisture in the system. The influence of moisture on the temperature in each zone reveals that there is a decreasing trend. This is because higher moisture content consumes more amount of heat as a latent and sensible heat [52].

For some fuels, there is little choice in the moisture content as this is determined by the type of fuel, its origin and treatment. It is appropriate to use fuel with low moisture content because a considerable amount of heat is used for the evaporation before the gasification. For example, for fuel at 250 ^{o}C and raw gas temperature from the gasifier at 3000 ^{o}C, 2875 KJ/Kg heat must be supplied to heat and evaporate the moisture [53]. Besides limiting the gasifier heat budget, high moisture content also exerts load on cooling and filtering equipment raising the pressure drop across these units due to condensing liquids. Thus, in other to reduce the moisture content, some pre-treatment of the fuel is required. Normally, moisture content should be less than 20%.

2.1.3 Dust content

All gasifier fuels produce a certain amount of dust. If the dust drives with the producer gas and used in IC engines, the dust can clog the internal combustion engine and hence has to be removed. The gasifier design should be such that it should not produce more than 2-6 g/m^3 of dust.

2.1.4 Tar content

Tar is an unconverted volatile matter and constitutes one of the most unpleasant components of the contents of the producer gas. It tends to condense and deposits on various engine passages causing sticking and operational problems. The process that results in tar formation takes place in the pyrolysis zone.

The physical properties of tar are affected by temperature of the hot zone, heating rate and other materials in the fuel. There are about 200 chemical constituents that have been identified in tar. Not great deal of research work has been carried out on burning of tar inside the gasifier to produce a tar free gas. However, efforts are geared towards removing tar from the gas stream using suitable cleaning systems. Generally, a properly designed gasifier should have tar content less than 1 g/m^3.

2.2 **Gasification process parameters that affect the quality of the producer gas**

The characteristics of reactor design and the pattern of flow has a strong influence on the quality of syngas fuel generated in the gasification process. The major variable parameters used for to maintain an acceptable quality of gas are equivalence ratio and the superficial velocity.

2.2.1 Equivalence Ratio

ER is a measure of the amount of external oxygen (or air) supplied to the gasifier. ER is obtained by dividing the actual oxygen (or air) to biomass molar ratio [54]. A good number of researchers have addressed various gasification schemes. Zainal et al [55] defines equivalence ratio to incorporate the effect of rate of air flow, wood supply and duration of run in a bid to lower the number of parameters on which the biomass gasifier depends. In their work, the equivalence ratio for each run is calculated as

$$\text{Equivalence ratio } \emptyset = \frac{(Flow\ rate\ of\ air\ supply)*(Duration\ of\ the\ run)}{(Mass\ input\ of\ wood)*(^{A}/_{F}\ for\ \emptyset=1)} \qquad (2.5)$$

($^{A}/_{F}$) for Ø =1 is 5.22 m^3 of air /kg of wood. The equivalence ratio for their gasifier is found to be within the range of 0.268-0.43.

In order to investigate the influence of ER in a downdraft gasifier, Zainal et al, carried out an experiment using furniture wood and wood chips under various operating conditions. He observes that there is an increasing and then decreasing trend with CO and CH_4. The variation of the calorific value with equivalence ratio showed a peak value indicating there is an optimum equivalence ratio, the best performance of the downdraft gasifier yields a peak at an ER value of 0.38.

In the study of operating and performance gasification process parameters carried out by Sharkofow [56], ER represents the ratio between the amount of air/oxygen in the oxidant or gasification agent and the theoretical amount of air/oxygen required for complete combustion of the biomass feedstock according to the stoichiometry. They found that with higher ER, more CO_2 can be produced while the amount of CO in the synthesis gas is reduced. Reduction in the amount of carbon monoxide associated with ER is attributed to the fact that with a higher ER value more oxygen is introduced and more CO is converted to CO_2. With a lower ER value, less H_2 and CH_4 are produced. Low ER values approaching zero are usually encountered in the pyrolysis step whereas higher ER values approaching or greater than 1 are encountered in the combustion stage. A pyrolysis is carried out in the absence of oxygen, its ER is zero. In combustion, values of ER approach or exceed 1, this is in an effort to provide sufficient air/oxygen by which complete oxidation can take place. For partial oxidation reactions, i.e. gasification reactions, ER is usually between 0.25 and 0.5.

In the three zone equilibrium and kinetic free modelling of biomass gasifier study carried out by Ratnadhariya et al. [52]. They investigated the influence of ER on gas compositions in the pyrolysis, oxidation and reduction zones. In the pyrolysis zone, no effect of ER was observed as the model did not consider reaction rates and equilibrium in this zone instead the products in this zone are obtained through mass and energy balances including assumptions. In the oxidation zone, N_2 increases with increasing ER which is understandable while CH_4, C_2H_2, and H_2O are decreasing due to the fact that generations of these compositions depend on the elemental content of the biomass which is constant for a given biomass material therefore the relative compositions will decrease with increasing air intake and consequently ER. CO and CO_2 are seen to be increasing with increase of ER due to more oxidation of char. It is noticed that the rate of increase in CO is more than that of CO_2, this is attributed to the fact that the partial oxidation of char dominates in an oxygen deficient environment and reactive char. In the reduction zone, CO increases while CO_2 decreases with increasing ER, which is as result of more CO being oxidized at a higher ER [52].

Prokrash et al [57] in their work on modelling of a downdraft gasifier with finite rate kinetics in the reduction zone investigated the effect of ER on the composition of gases. In their work, equivalence ratio is defined as the ratio of stoichiometric to air-fuel ratios; in the gasifier, sub-stoichiometric air is supplied, and the equivalence ratio is above unity. The range of equivalence ratio over which a gasifier may operate is limited by the quality of the producer gases generated and the stable operation of it. The result of varying the ER on the composition and heating value of gases shows that increasing the equivalence ratio (that is decrease in the actual supply of air) increases the H_2 and CH_4 content in the producer gas. However, the CO fraction in the gas decreases and CO_2 increases [57] their observation contradicts the apparent fact that operating the gasifier in a richer atmosphere should produce more CO and less CO_2. Melgar et al [58] investigated the influence of varying ER on the gas compositions and reports similar findings to the present case, they attributed the results to the fact that equilibrium of water shift reaction in the model inclines to the production of CO_2 and H_2 when the fuel contains high moisture.

Narvaez [59] observed an increase in gas yield with an increase in ER from 0.20 to 0.45 and a decrease in the lower heating value (LHV) of the gas with decreasing fractions of H_2, CO, CH_4 including C_2H_2 and tar [59]. The increase in gas yield with

increase in ER infers that an increased air flow increases the rate of conversion. Some of the contradictions on the effects of ER on the contents of H_2, CO and CH_4 percent is rational because the percentage compositions of individual gases depend on both the overall gas yield and the individual gas yield. When the increase in the overall gas yield is more pronounced than the increase in the individual gas yield, then the percentage composition of individual gas decreases even if the individual gas yield may have increased. In the study of thermochemical biomass gasification performed on a bench-scale fluidised bed gasified with steam and air as fluidising and oxidizing agents, Kumar observed increases in gas yields, carbon conversion and energy efficiencies with increase in ER from 0.07 to 0.25 [60]. While some authors observed increases in gas yields with increase in equivalence ratio, some other authors observed a decrease in H_2 and CO yields with increase in ER.

2.2.2 Superficial Velocity

A superficial velocity, SV is defined as the ratio of the syngas production rate at normal conditions and the narrowest cross-sectional area of the gasifier. The SV of a gasifier is the most vital measure of the behaviour of the gasifier and controls most of the aspects of its operation such as gas production rate, char production, fuel consumption rate, gas energy content and tar production. It is not dependent on gasifier size and so permits comparison of gasifiers of very different dimensions. It affects the heat transfer around each particle during flaming pyrolysis of the volatiles and on combustion of the tars as well as the degree of gasification of the charcoal. This is because it controls the rate at which air and then gas passes through the gasifier [61]. Variations in the amount and composition of tar/gas with SV ranging from 0.3 to 0.7 m/s have been investigated in a downdraft biomass gasifier with air as the oxidant. Yamazaki et al experimental investigation shows that the lowest tar yields was achieved at SV around 0.4 m/s and the highest at 0.7 m/s. High tar yields at high SV are due to short residence time and channelling. Also, the result showed a noticeable change in the composition of gas with SV ranging from 0.3 to 0.4 m/s. In the range of 0.4 to 0.6 m/s gas composition is suitable for IC engines [62].

2.3 Gasifier Types

Various types of gasifiers have been developed and these gasifiers have different hydrodynamics particularly in terms of how the solid fuel and the gasification agent

such as air, oxygen and or steam are contacted and operating conditions such as temperature and pressure; authors [63]. [7, 64] agree that even though there has been a long experience of biomass gasification, reliable and large scale operations continue to be suffering from several problems. Those issues depending on the type of gasifier are according to [63] related to

- Scale of operations and availability of biomass
- Size distribution of raw biomass
- Operability of the gasifier with fuels containing large amounts of ash especially if the fraction of alkali, chlorine and sulphur is high
- Formation of condensable high hydrocarbons
- cleaning and upgrading of the gas for dedicated down-stream application

There are various types of gasification technology developed for converting biomass feed stocks. Most of these have been developed and commercialised for the production of heat and power from syngas rather than liquid fuel production. The main types are described in the Figure 2.1 below with the main differences being:

- The manner in which the biomass is fed into the gasifier and how it moves around within the gasifier;
- The kind of oxidant used- air dilutes the syngas due to the presence of nitrogen which subsequently increases the cost of the downstream processing. Oxygen however avoids but is very expensive to use;
- The temperature ranges at which the gasifier is operated;
- The method in which the heat for the gasifier is provided – whether the heat is provided by partially combusting some of the biomass in the gasifier or from an external source such as circulation of an inert material or steam;
- The level of pressure, the gasifier operates upon- pressurised gasification provides higher throughputs with larger maximum capacities which promotes hydrogen production and subsequently leads to cheaper downstream clean-up equipment. Moreover, since no additional compression is required, the temperature of the syngas can be kept high for downstream operations and liquid fuel catalysis. However, at pressures between 25-30 bar, cost quickly increase since gasifiers require more robust engineering and the needed feeding mechanisms involve complex pressurising steps [65];

2.3.1 Classification of biomass gasifiers

There are various technologies engaged for the gasification of solid fuels. The basic classification of these processes is carried out by considering the reactor principles that are applied [66] such as

- Fixed bed
  - Updraft gasifier
  - Downdraft gasifier
- Fluidized bed
  - Bubbling Fluidized bed
  - Circulating fluidized bed
  - Dual fluidized bed
- Entrained flow systems

Warnecke [67] characterised the gasifiers by classifying them into four categories based on the type of transport of fluids or solid that goes through the reactor;

- Mechanical-moved feed stock
- Quasi-non-moving or self-moving feedstock
- Special reactors
- Fluidically-moved feedstock

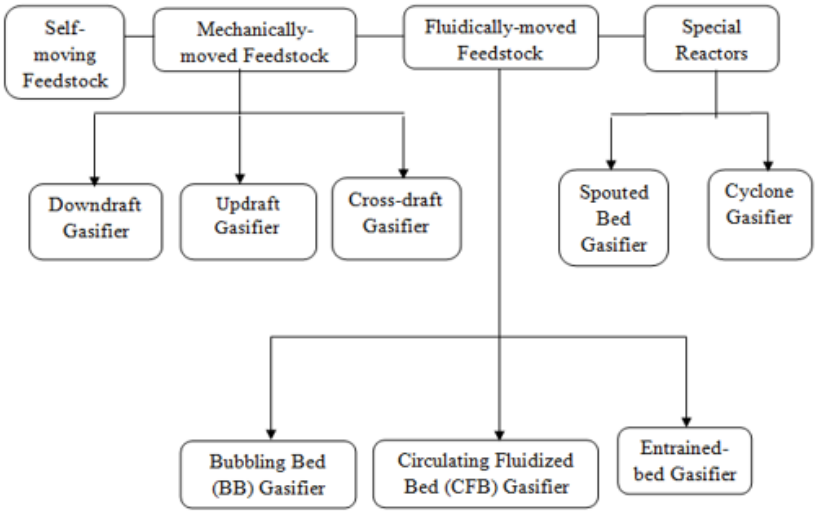

Figure 2.1 Classification of gasifier [36]

Fixed Bed gasifiers

Fixed bed gasifiers are of two main categories; updraft and downdraft gasifiers. The bed rests on the grate and in most cases, the fuel is fed at the top of the reactor while the product gas leaves the reactor at the bottom in the case of the downdraft gasifier and at the top in the case of the updraft gasifier. The fuel in the bed moves down due to gravity at the same rate at which the fuel is consumed. The residence time in the fuel is long while the gas velocity is low [68].

Updraft gasifier

The updraft gasifier is one of the oldest and simplest types of gasifiers as shown in Figure 2.2. With the updraft gasifier, the gasifying agent and the producer gas flow through the reactor in the opposite direction. The air, oxygen or steam intake is at the bottom around the grate while the reactor is fed from above. The sensitive heat of produced gas is used to dry the fuel and to start pyrolysis. The tars and volatiles produced during this process are carried into the gas stream.

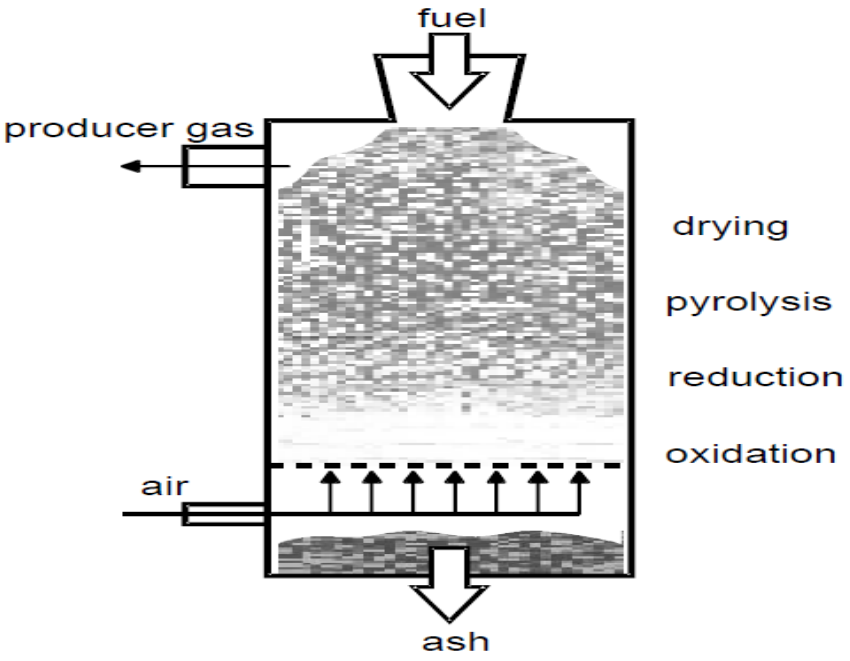

Figure 2.2 Updraft Gasifier [61]

The major advantages of these types of gasifiers are their simplicity, high charcoal burn-out and internal heat exchange; this allows for low gas exit temperatures, high equipment efficiency as well as the possibility of operation with various types of feedstock. Some of the major drawbacks result from the possibility of ‘’channelling’’

in the equipment which can cause the escape of oxygen and consequent explosion and in turn require the need for installation of moving grate [43].

Downdraft or Co-current gasifier

The downdraft gasifier is common type of fixed gasifier where the air and fuel flow concurrently. The oxidant can enter either at the top with the fuel in the case of the open core design or more often at an intermediate level to better control location of the high temperature oxidation zone, see Figure 2.3. The drying and pyrolysis zones lies above the oxidation and is supplied with the necessary process heat via thermal conduction in the bulk filling [66]. Downdraft gasifiers are the widely used reactors for small scale biomass and carbon conversion for power generation using Reciprocating Internal Combustion Engines (RICEs) [69, 70].

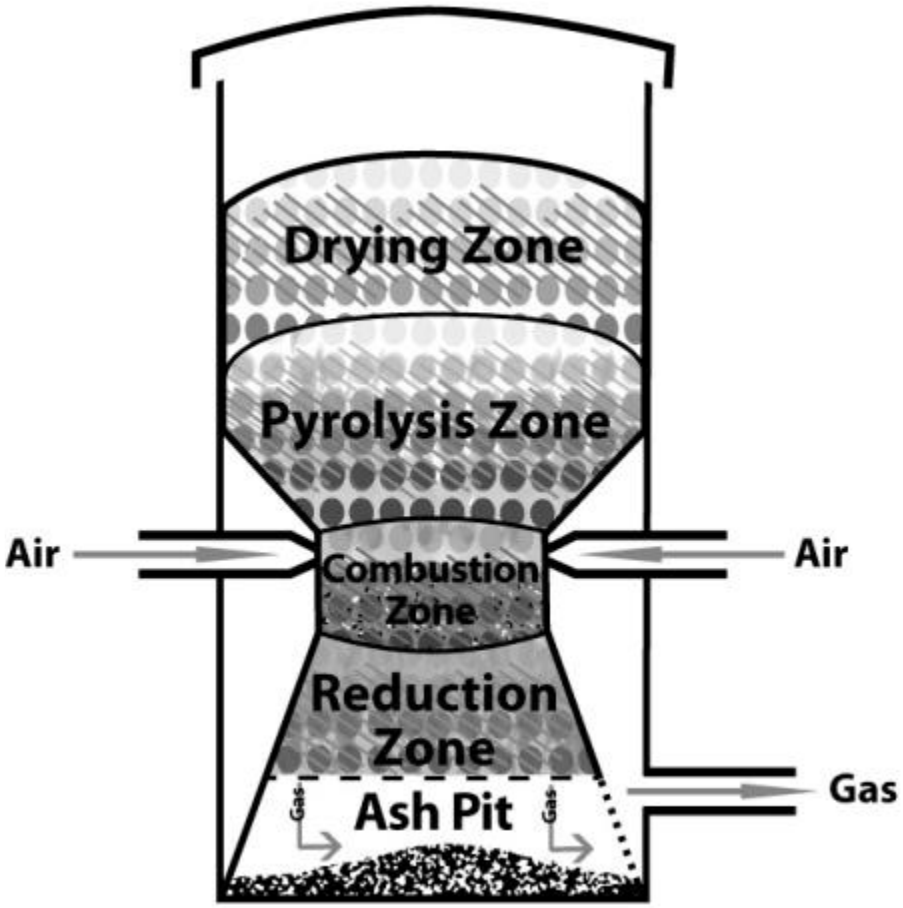

Figure 2.3 Schematic diagram of downdraft gasifier [71]

The product gases usually exit near the bottom of the reactor near the ash grate; this results in products originating from the pyrolysis zone to have to pass through the oxidation zone which is normally depicted as a treatment zone for tarry compounds. The construction and principle of the downdraft gasifiers makes them sensitive to the quality of fuel used; particular attention must be paid to the water content of the fuel. The steam given off in the drying zone must be removed through bulk filling; the vapour must be heated up in the temperatures in the oxidation zone. Some of the advantages are higher conversion efficiencies with low tar and particulate content in producer gas. The concentration of tar and particulates is considerably lower as compared with other reactors due to gas passing through a high temperature in the combustion zone causing the cracking of the tar formed during the gasification process. According to Bhattacharya [72] high char conversion and the lower ash carry over as gas passes through the charcoal bed allowing its filtration, catalysis and quick response to load changing. The drawbacks are that difficult to obtain a homogenous distribution of air in the reactors with large diameters; as the diameter of the reactor increases, so is the likelihood for increase in low temperature zones this is why the scale up capability in downdraft gasifiers is limited. Its inability to operate on a number of unprocessed fuels particularly fluffy and low density materials give rise to flow problems and excessive pressure drop. Moreover, solid fuels must be palletized, briquetted before use and face problems with high ash content fuels (slagging). Not suitable for small particle size of fuels [73].

The Imbert downdraft gasifiers are suitable for handling biomass fuel of uniform sizes and shapes as they flow through the constriction heart and also with ash and moisture content less than 5% and 20% respectively. Gases and solids flow through a descending packed bed supported across a throat. In throated gasifiers, gasification occurs over four zones namely pyrolysis, drying, oxidation and reduction zones. The biomass fuels enter through the hopper flows down and get dried and pyrolysed before being partially combusted by the gasifying media entering at the nozzles. The throat aids cracking as it allows for maximum mixing of gases in the temperature region which aids tar cracking. Underneath the throat the combustion gases and tar pass through the hot char and are reduced to CO and H_2 [74]. The gasifier has lower overall efficiency since a high amount of heat content is carried over by the hot gas. The biomass particle size limits the capacity of the Imbert downdraft gasifiers to 500KW

and operating mode of the gasifier ultimately influences the composition of the syngas [61]. The relative position of the zones in a throated downdraft gasifier and the main reactions which occur in these zones are shown in Figure 2.4.

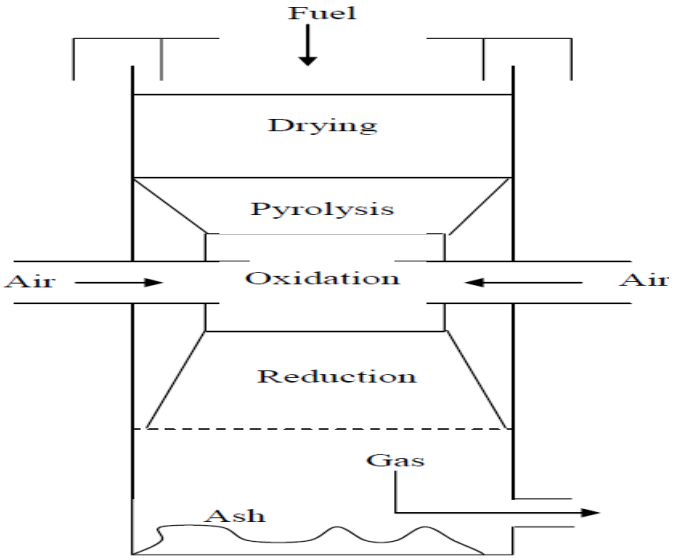

Figure 2.4 Imbert Gasifier [61]

Fluidised bed Gasifier

The fluidized bed gasifier operates with a combination of bed materials and biomass. The gasification agent flows in through the bottom of the nozzle and fluidises the bed materials. This can be inert as with quartz sand or catalytically active for the conversion of organic contaminants in the crude gas through possible after reactions in the gas phase [75]. Depending on the inflow speed of the gasification medium, the difference between a bubbling and circulating fluidized bed can be differentiated. Figures 2.5 and 2.6 show schematic views of the basic systems for gas solid fluidized bed reactors [39] and circulating Fluidised-Bed, respectively.

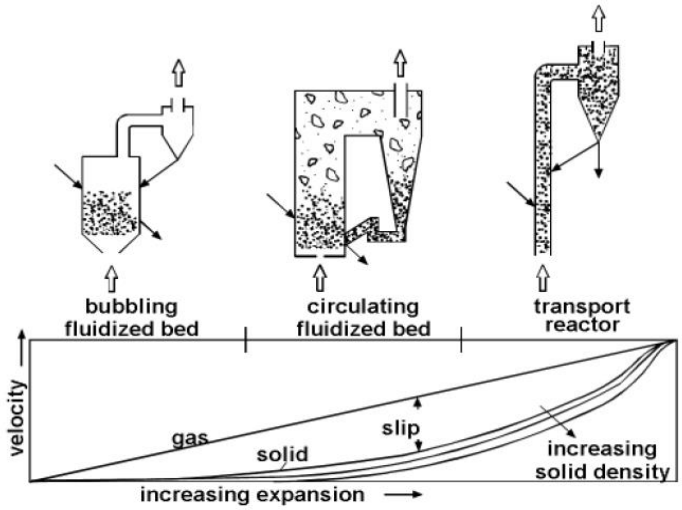

Figure 2.5 Basic systems for gas/solid fluidised-bed reactors [68]

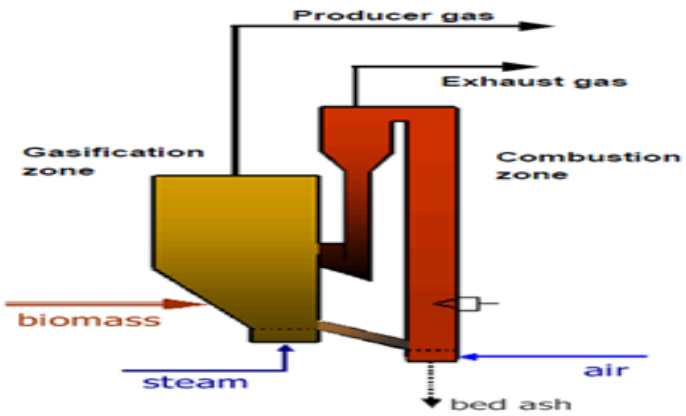

Figure 2.6 Circulating Fluidised-Bed [41]

Circulating Fluidised Bed

With circulating bed design, the bed material liberated from the combustion zone is precipitated out of the gas stream via a cyclone and then recirculated into the reaction chamber. The velocity of the oxidising agent is so high that the fuel particles and bed materials are entrained and leave the reactor together with the product gas. The bed materials contribute to a more even distribution of the temperature and stable operation. Some of the advantages of this design is that it is suitable for rapid reactions, high heat transport rates are likely due to high heat capacity of bed materials and high conversion rates are possible with low tar and unconverted carbon. Size of the fuel particle determines minimum transport velocity; high velocities may cause equipment

erosion [33]. Some of the disavatages to this technology include the higher loading of organic contaminants, tars and particles. For this design the temperature level has to be chosen as high as possible [76].

Bubbling Fluidised Bed

Bubbling bed is another type of FB gasifier which consists of a vessel with a grate at the bottom through which air is introduced. At the top of the grate is the moving bed of fine- grained material where in the biomass feed is introduced. The gasifying medium's velocity is controlled in a way that it is just greater than the minimum fluidisation velocity of the bed material. The temperature of the bed is regulated around 700-900^{o}C and this is maintained by controlling the air to biomass ratio. The product gas exits from the top of the gasifier while the ash is removed from the bottom or from the product with the use of cyclones [77]. Some of the advantages of this type of gasifiers are that they yield uniform syngas, accept a wide range of particle sizes and provide high rates of heat transfer between the inert material, fuel and gas. High conversion is possible with low tar and unconverted carbon. One of the disadvantage is that bubbles may result in the gas bypass through the bed [36]

Entrained flow Gasifier

There are three types of gasifiers, fixed or moving bed, fluidised bed and entrained flow with some variations within each of these designs [78]. The entrained flow gasifier has been developed for coal gasification, however, the need for a finely feed material (0.1 - 0.4 mm) presents problems for fibrous materials such as wood; this makes entrained flow gasifier design not suitable for most biomass material. However, in the work on numerical simulation of coal gasification by Grabner et al [79] the entrained-flow gasifier with a liquid ash removal system is an alternative for large scale systems (>400MW_{th}). The reason being that, the gas produced is almost free of tar with nearly complete conversion of carbon due to the high temperature employed. Also, the low melting point of biomass makes slagging operation possible at reduced temperature keeping the oxidant demand low when compared with entrained flow gasification of coal. Figure 2.7 presents a schematic diagram of entrained flow gasifier.

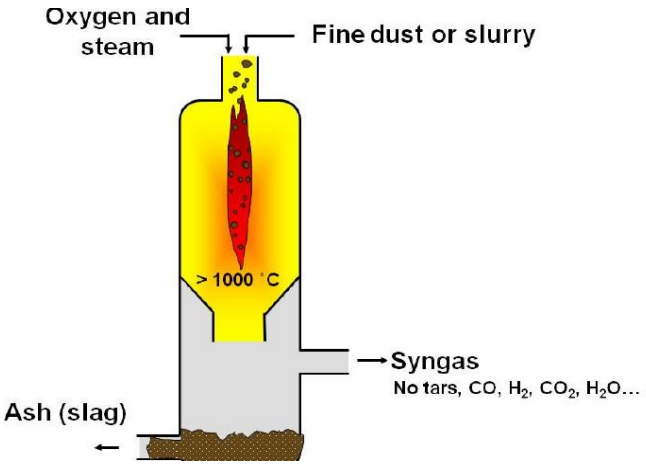

Figure 2.7 Schematic diagram of entrained flow gasifier [71]

2.4 Biomass gasification models

The optimal conversion of the chemical energy inherent in the biomass or solid fuel into the desired gas is determined by proper configuration, sizing, and choice of gasifier operating conditions. In commercial plants, optimum operating conditions are often derived through trials on unit or by experiments on pilot plants. Although experiments are expensive, they can give more reliable design data than modelling and simulation. However, the major limitation is that a change in one of the variables of the original processes changes, the optimum operating condition chosen for that specific experimental condition is no longer valid [80]. Also, optimum parameters obtained experimentally can be size specific that is, the optimum operating condition for one size of gasifier is not necessarily valid for any other size.

The efficient operation of a biomass gasifier depends on many complex chemical reactions such as fast pyrolysis, partial oxidation of pyrolysis products, gasification of the resulting tar and lower hydrocarbons and the water gas shift reaction. The major goals of these models are to study the thermochemical processes during the gasification of the biomass and to evaluate the influence of the input variables such as moisture content, air/fuel ratio, producer gas composition and the calorific value of the producer gas. While there are some studies have been concentrated only on final composition of chemical equilibrium, others have taken into account the different processes along the gasifier differentiating at least two zones [25]. Mathematical models which are used for hydrogen production can be classified into thermodynamic equilibrium models, kinetic equilibrium model and neural network models [81]. Some models employ the

use of process simulator Aspen plus [25] combining thermodynamic and kinetic rate models.

2.4.1 Aspen Plus/HYSYS Models

In trying to avoid complex processes, some authors have proposed simple models such as Aspen Plus simulator that integrates the principal gasification reactions and physical characteristics of the reactors. Aspen plus is a chemical process optimization software developed at Massachusetts Institute of Technology [82]. It is a problem-oriented input program which employs the use of unit operations, blocks such as pumps, reactors etc. The process simulation calculator uses in-built physical property data bank. The program solves the process scheme sequentially by calculating the outlet stream properties using the inlet stream properties for each block. This package has been used to model coal and biomass power generation systems.

To model a gasifier, using Aspen Plus, the total process must be broken down into many sub-processes; a model may include several zones such as drying, pyrolysis, oxidation and gasification zones. Each zone can be represented by separators or reactors. The mass and energy transfer across these zones can be incorporated in such a way that all unit operations combination represent the entire biomass gasifier [83].

Many authors have developed gasification models using Aspen Plus for coal and biomass. Ramzan et al [84] proposed a steady state model for hybrid biomass gasifier employing the use of Aspen plus in the comparative performance analysis of food waste, municipal solid waste and poultry waste. The gasification process has been modelled in three stages. In the first stage, moisture content of the solid fuel is reduced before feeding to the reactor. In the second stage, biomass is decomposed into volatile components and char. The yield distribution for this stage has been specified using FORTRAN statement in calculator block. Partial oxidation and gasification reactions has been modelled in the third stage by minimising Gibbs free energy.

Mitt et al. [85] proposed an equilibrium gasification model of a fluidised bed tyre gasification plant with air and steam using Aspen Plus. The authors validated their results with the gasification pilot plant at Technical University of Catalonia (UPC). The model was divided into three stages; drying, devolatization-pyrolysis and gasification-combustion. The first step of the modelling processing is heating and

drying of the particles. To model the drying stage, a ''RSTOIC'' module was used to model this instantaneous drying. Because of high content of the volatiles in the tyre, the authors considered the devolatization step of its conversion. The ''RYIELD'' block is used to model the pyrolysis/devolatization section of the model. The devolatization process produces volatiles, gases, tars and char. It was assumed that the total yield of volatiles equals the volatile content of the parent fuel which is determined by the ultimate analysis. The combustion and gasification have been modelled by the ''RGIBBS'' reactor. Stream from the ''RYIELD'' block and the preheated oxygen and steam were directed into ''RGIBBS'' module which can predict the equilibrium composition of the producer gas from the ''RYIELD'' at a specified temperature and pressure. The hydrodynamics of the gasifier was not considered; an overall equilibrium method was employed. The tars, oils and higher hydrocarbons were considered non-equilibrium products to reduce the difficulty of the model. Thus, CH_4 was the only hydrocarbon considered in the calculation, while other results were normalised make them free from tars while the sulphur was assumed to be converted to H_2S. The model could predict the flow rate, composition and temperature of the feed material and composition of the producer gas under varied conditions.

Kong *et al.* [86] proposed a three-stage equilibrium model for coal gasification in the Texaco type coal gasifiers using Aspen Plus model to calculate the carbon conversion, and gasification temperature and composition of product gas. Pyrolysis and combustion, char gas reaction stage and gas phase reaction stage forms the Aspen Plus model. Some of the water produced in the pyrolysis and combustion stage is assumed to be carried into second stage and reacts with the unburned carbon. Carbon conversion is then estimated in the second stage by steam participation ratio expressed as a function of temperature. The producer gas compositions were calculated from gas phase reactions in the third stage. They concluded that by separating the gasification process into three stages: pyrolysis and combustion, solid-gas reactions, gas phase's reactions, the proposed model gives the carbon conversion, product gas compositions and gasification temperature. The model can predict the carbon conversions by employing conventional equilibrium model with Aspen Plus simulator.

Barrio et al [87] proposed a model based on reaction kinetics and reactor hydrodynamics for biomass gasification in an atmospheric fluidized bed gasifier using Aspen Plus simulator. They used four Aspen Plus reactor models and external

FORTRAN subroutines for the hydrodynamics and kinetics nested to simulate the gasification process. The decomposition of the feed was modelled using the Aspen Plus yield reactor''RYIELD''. The step proceeded by converting biomass into its constituent components; carbon, hydrogen, oxygen, nitrogen, sulphur and ash by specifying the yield distribution from the biomass ultimate analysis. The separating column is used to separate the volatiles from the solid to perform the volatiles reaction. The''RGIBBS'' was used to model the combustion section while the ''RCSTR'' performed char gasification using reaction kinetics. Upon validation of the model with experiment values, the effect of reactor temperature, steam to biomass ratio, equivalence ratio and biomass particle size were investigated. The gasification process improved with higher temperature; it increased the carbon conversion efficiency and hydrogen. With increasing temperature, carbon monoxide and methane showed decreasing trends. Increasing the steam-to-biomass ratio increases hydrogen and carbon monoxide production and decreases CO_2 and carbon efficiency. The composition of the producer gas is not affected by the average particle size ranging from 0.25-0.75 mm.

Mansaray et al [88] developed two thermodynamic models to simulate a dual-distributor-type fluidized bed rice husk gasifier; a one compartmental model in which the hydrodynamic difficulty of the of the fluidized bed was neglected and an overall equilibrium applied, the two -compartmental model where the hydrodynamic conditions were considered. The model can predict the higher heating value, reaction temperature, gas composition, carbon conversion under varied conditions. The reactions considered in the development of this models are pyrolysis, partial oxidation and gasification. Predictions of the core exit temperature and annulus as well as the mole fractions of the combustible gas components, producer gas high heating value showed reasonable agreement with the experimental data.

Mathieu et al [89] developed a thermodynamic model of wood gasification in a fluidized bed using Aspen Plus. The model was based on minimization of the Gibbs free energy and the process was uncoupled in pyrolysis, combustion, Buourdard reaction and gasification. The authors carried out a sensitivity analysis and concluded that there is a critical air temperature above which preheating is no longer efficient role under a certain value; the operating pressure has only a slight positive effect on process efficiency.

Kuo et al [90] proposed an Aspen plus model to evaluate the gasification potentials of raw bamboo, torrefied bamboo at 250 ^{o}C and 300 ^{o}C in a downdraft fixed bed gasifier using thermodynamic analysis. Biomass and ash properties are not available in the standard Aspen Plus database thus, the stream referred to as MCINCPSD class was used. The Peng-Robinson equation of state employed to evaluate the physical properties. The enthalpies of non-conventional components of ash and biomass have been calculated by the stream referred to as HCOALGEN model which includes some empirical relationships for heat of formation, heat capacity and heat of combustion. The stream called DCOALIGT was used to model the density of the biomass. The authors used the Gibbs energy minimization method in the RGIBBS gasification reactor to predict the equilibrium composition of the producer gas. The simulation results of the output compositions from the water-gas shift reactions at various operating conditions like reaction temperatures and steam/CO ratios were compared with the experimental data in literature.

Paviet *et al* [91] developed a thermochemical equilibrium model using ASPEN Plus for downdraft and staged gasifiers. The author suggested the proposed model is easy to develop; and predicted with accuracy the composition of the flaming pyrolysis gas and the producer gas. The reaction temperature is the parameter that controls the whole gasification process and influences directly the final producer gas. The models developed in this work can be used as input parameters in the design of a gasifier. Gas concentrations given by the flaming pyrolysis model can be used as input parameters to the char gasification model. Concentrations given by the producer gas model used as input data to the combustion model of a SI engine to design and predict the overall performance of a gasification zone.

Ratnaip et al [92] carried out a simulation studies on biomass gasification reactor for fuel in gas turbine systems. The study was carried out to arrive at the power output under limiting conditions as well as perform changes in the fuel gas system for the augmentation. The study was carried out on the simulation software Aspen HYSYS and the findings show that, the available fuel gas obtained from the biomass can be optimally used for the power generation in the gas turbine. The simulation study shows that maximum possible power is generated with 55630 Nm^3/hr of fuel gas flow

bypassing the heater skid which saves energy on heating the gas which saves 900 kWh electric power.

2.4.2 Kinetic Rate Models

Thermochemical equilibrium does not occur in reality in gasification process and can only be approximated in the high temperature zones of the downdraft gasifier. Researchers have delved into this area of study to try and overcome the limitations of equilibrium model [93]. Kinetic models accounts for the kinetic reactions and the mechanics among the phases in the biomass gasifier [25, 94]. These kinds of models can be used for estimating the composition of producer gas with varying operating conditions which is in turn essential for evaluating, designing and improving gasifiers [95]. In order to evaluate the transfer of fluids to and from the reaction sites, the hydrodynamics of the gasifier is often incorporated into the kinetics modelling.

Wang and Kinoshita [96] developed a kinetic model for biomass gasification based on the mechanism of surface reactions. The rate constants are determined from minimising the differences between experimental and theoretical results assuming various residence times and temperatures. When the kinetic model was validated by comparing experimental data with the theoretical results for different equivalent ratios, the simulations agree well with the experimental data.

Giltrap et al [26] developed a steady state kinetic model for predicting the product gas composition and the temperature in the downdraft biomass gasifier using the values of kinetic rate expressions proposed by Wang and Kinoshita. The model was developed for the reduction zone of the downdraft gasifier. It assumes that all oxygen in the air is combusted to CO_2 and pyrolysis products are completely cracked. Solid carbon (char) is considered to be present in the reduction zone. The reaction rates are considered Arrhenius-type temperature dependence. The values for the activation energies in the rate equation were adopted from the work of Wang and Kinoshita. It is assumed that the (CRF) i.e. char reactivity factor which represents the reactivity of the char is incorporated in the model. A set of seven ordinary differential equations obtained by applying mass and energy balance including two more empirical equations for pressure drop and velocity variation. These equations were solved by using the ODE function in MATLAB. The model prediction of the gas composition reasonably agreed with the experimental data sources of Chee [97] and Senelwa [98] except that CH_4

concentration in the producer gas was over- predicted, this was as a result of the assumption that CH_4 produced by pyrolysis is rapidly combusted with the oxygen at the air inlets and this reduced the amount of CH_4 predicted but the prediction is still higher than the concentrations found experimentally.

The model developed by Giltrap was modified by Babu et al [99]. In this model, char reactivity factor, (CRF) along the reduction zone of the biomass gasifier was incorporated. The CRF value was increased both linearly and exponentially along the length of the reduction bed in the model. The model was implemented using the finite difference method in order to predict the temperature and composition profiles in the reduction zone of the gasifier varying CRF ranging from 1 – 10,000, both linearly and exponentially. The different values of CRF (1, 10, 100, and 1000) were used which were kept constant throughout the reduction zone. Based on the results, the authors of the model concluded that the value of the CRF which constitutes the reactivity of the char must be varied along the reduction zone of the downdraft biomass gasifier. When the simulated results were compared with the experimental data of Jayah et al, they were in good agreement and even better with the mathematical model of Jayah et al when the exponentially varying CRF was considered [25, 99].

Tinaut et al [55] developed a one-dimensional stationary steady state model of biomass gasification. The model was developed by incorporating mass and energy conservation equations along the bed and includes heat transfer via radiation from the solid particles. The model considers the processes taking place in the gasification reaction such as biomass devolatization moisture evaporation; heterogeneous and homogeneous reactions. The homogenous reactions are those such as water gas shift reaction and reforming reactions of methane and the heterogeneous reactions are such as char with hydrogen, water vapor carbon dioxide and oxygen. The equations developed by Di Blasi [100] were used to calculate the terms in the conservation equation such as convection between solid and gaseous phases and between each of the phases and the wall. The equations proposed by Ergun are used to account for the pressure losses. These model equations are solved iteratively considering the temperature as the variable. The model is used as a tool to study the influence of process parameters such as air flow velocity, biomass particle mean diameter, composition and temperature of the gasifying agent. The model was validated with biomasses of various sizes.

In the study by Di Blasi [101] a mathematical model for gasification of wood pellet in an open core downdraft gasifier with double air inlet was developed. The processes modeled include finite rate wood kinetics of pyrolysis, primary tar cracking, gasification of steam, gasification of stem, carbon dioxide and hydrogen, solid and gas-phase heat transfer with the reactor walls etc. The fractions of gas, primary tar and char produced are included in the general one step global reaction considered for wood devolatization. The solution of the model equations was divided into three sections; the first step is the chemical reaction processes, followed by the heat exchange between the walls of the reactor and the phases and the transport phenomena. First order implicit Euler method was employed to solve the ordinary differentia equations for each step in the first two stages while transport equations were solved in the third stage using a semi-implicit procedure. Parametric studies were carried out on the influences and position of the secondary air the temperatures profile and conversion of tar and char for a pilot scale reactor developed by Barrio and colleagues. Apart from the slightly higher prediction of methane, the composition of the producer gas shows a good agreement with the experimental data.

Scotts et al [102] developed a molecular level kinetic model for biomass gasification. The model development proceeded in two groups; the composition of the feedstock and the construction of the reaction network. The composition model was further divided into three sub models for cellulose, hemicellulose and lignin and the Flory-Stockmayer statistics to represent the distribution of the size of the polymer. The model was formulated using ultimate analysis from literature for fractions of lignin, cellulose and hemicellulose; the reaction network for the model comprises of pyrolysis and gasification in which the monomers derived from cellulose and hemicellulose in other to reduce the molecular size. The performance of the kinetic model was validated with experimental data of six different biomasses which showed reasonable agreement.

Saravankumar et al [103] developed a computational model to evaluate the performance characteristics of an updraft fixed bed gasifier using long stick wood as the fuel using long stick as the fuel source. This model showed that the incoming air was consumed in the charcoal combustion region and maintaining a specific air /fuel ratio could lead to a poor degree of the gasifier performance. Higher combustion temperature was found to aid gasification time but could waste energy via the exhaust gases carried out. The authors observed that air to fuel ratio could be a more suitable

measure when moisture was present in the lower portion of the bed regulate the formation of gasification products.

Gordillio et al [104] proposed a numerical model of solar downdraft gasifier using high carbon content feedstock; biomass char with steam based on systems kinetics with char reactivity factor (CRF) varying exponentially. The model aims to calculate the dynamic and steady state profiles as well as predicting the concentration and temperature profiles of the gas and solid phase based on mass and heat balances. The study proposes the downdraft set up could be a solution to improve the performance of the packed bed and the fluidized bed gasifiers with concentrated solar radiation in the upper part of the reactor. The gas produced was found to be high quality syngas the hydrogen and carbon monoxide as the main components; the concentrations of CO_2 was low since there was no combustion carried out. The system efficiency was found to be about 55% for small steam velocities. With increasing steam velocity, the energy conversion efficiency showed a decreasing trend. The model showed a good agreement with the experimental data.

Inyat et al [105] report the result of a parametric study performed using steam gasification process modelling for hydrogen enriched gas production. The model incorporates the reaction kinetics calculation of the steam gasification with in-situ CO_2 capture as well as mass and energy balances. Parametric studies based on temperatures and steam/biomass ratio have been used to analyse the hydrogen concentration in the product gas. Hydrogen efficiency to decrease with increasing steam/biomass ratio as more energy was required for additional steam usage. It was observed that the temperature had a more profound effect on hydrogen yield as compared to steam to biomass ratio.

Accurately predicting the syngas and tar compositions poses a challenge. Smith et al [106] proposed a chemical reaction kinetics model based on comprehensive gasification kinetics to simulate downdraft biomass gasification. The kinetic model is validated by direct comparison to experimental results of two downdraft gasifiers available in the literature and is found to be more accurate than the widely used Gibbs energy-minimizing model. The kinetic model is then applied to investigate the effects of equivalence ratio (ER), gasification temperature, bio-mass moisture content, and biomass composition on syngas and tar production. Accurate water-gas shift and CO shift reaction kinetics are found critical to achieve good agreement with experimental

results. In the kinetic model, a series of chemical reactions with kinetics were employed to calculate the syngas compositions. To model the downdraft gasifier using Aspen Plus, the process is modelled in three steps including RSTOIC model which was used to simulate the drying process and controlled by a FORTRAN block. The second stage used the RYIELD block to simulate the biomass decomposition into its elements (C, H, O, S, and N) by specifying the yield distribution. In the third stage, air was injected considering the gasifier as a tubular reactor.

2.4.3 Thermodynamic Equilibrium Models

The idea of chemical equilibrium is based on the second law of thermodynamics applied to reacting systems [54]. At the chemical equilibrium, the species of a reacting system are at a stable composition as the system does not experience a net change in concentration over time [94]. Equilibrium models are suitable simulation tools for processes whose duration are in most cases quite long with regard to the reaction timescale [81]. The thermodynamic equilibrium calculations are suitable for studying the influence of fuel and process parameters. By employing the governing equations describing the behaviour of such state, one can formulate an equilibrium model.

Equilibrium models can be created using two general approaches, stoichiometric and non-stoichiometric. Stoichiometric models are based on the equilibrium constants where specific chemical reactions used in the calculation are defined; it follows that appropriate chemical reactions are selected and information regarding the equilibrium constants are required [107]. The disadvantage of this method lies in the fact that a set of non- linear algebraic equations are solved for the mole numbers of each specie and this mostly difficult if the system is large [108]. Generally, the non- stoichiometric model can be applied for simulating various gasifier configurations as they are not dependent on the gasifier design and not limited to a specified range of operating conditions [95]. This modelling approach, usually referred as Gibbs free energy minimization approach, is based on the Gibbs free energy of reaction species. To minimise the Gibbs free energy, constrained optimization methods are generally used and this requires complex mathematical theories.

Altafini et al [109], chemical equilibrium via minimising the Gibbs free energy is used to model coal gasification. The authors investigated the influence of the ultimate

analysis, the gasifying agents and fuel ratio on the equilibrium temperature to find the producer gas composition plus the overall and conversion efficiency.

The thermodynamic equilibrium model is a tool used to calculate the maximum yield which can be reached for a desired product in a reacting system. Practically, it is not possible to achieve chemical or thermodynamic equilibrium within the gasifier. However, the model offers the designer with a sensible prediction of the maximum feasible yield of the products desired [110]. In the study carried out by Chern et al, they developed an equilibrium to evaluate the degree of approximation in predicting the performance of a downdraft gasifier with air as the gasifying agent and wood as the fuel with varying operating parameters such as exit temperature, gas composition and char yield. The experimental results were validated with experimental data. The gasification process was represented by a stoichiometric reaction and using the both elemental and energy balance equations solved simultaneously in relation to the mole fractions. The model predicts the temperature of char yield and gas compositions at the exit of gasifier. The trends predicted were in agreement with experimental data [111].

In order to predict the gasification process in a downdraft gasifier, Zainal et al [55] used stoichiometric equilibrium method to model the gasification process in a downdraft gasifier different biomass materials [112]. The model assumes that all reactions are in thermodynamic equilibrium and that all the pyrolysis product burn completely in the in the reduction zone of the gasifier. The chemical formula of the wood does not contain sulphur and nitrogen and the global gasification reaction does not yield any solid carbon. The model uses two equilibrium constant relationships, three elemental balances (C, H and O) including mass and energy balance to solve six unknown molar fractions (H_2, CO, H_2O, CH_4 and CO_2). However, the amount of oxygen in that model was eliminated by defining it in terms of components in the producer gas but was not shown when they compared their model with their experimental data, this is what makes this model different. These sets of equations were combined into a set of three equations involving one linear and two nonlinear equations and solved using the Newton Raphson method. The equilibrium model predicts the calorific value and composition of the producer gases of paddy husk, paper and municipal waste in a downdraft waste gasifier. The predicted value compares well the experimental values available in the literature for wood.

Jarungthammachote and Dutta [113] modified the equilibrium model proposed by Zainal et al by incorporating the nitrogen in the biomass formula and multiplying the equilibrium constant of the water-gas-shift reaction and the methane reaction with a coefficient of 11.28 and 0.91 respectively in order to improve the model. These coefficients have been derived from averaging the ratio of CH_4 obtained by comparing between the model and the results of other researchers' experimental data. Upon modification of the model, H_2 significantly reduced while CH_4 remarkably increased and showed a better comparison to the experimental value. The predicted results of the modified model show reasonable agreement to the experimental value. The modified model was applied in simulating the gasification of Thailand MSW and to study the effect of moisture content on temperature and producer gas composition is shown in Table 2.2.

Table 2.2 Comparison of predicted result of Jarungthammachote and Dutta [113]with the experimental data from Jayah et al [114].

Gas composition	The present model		Experimental data		RMS error	
%mol dry basis	MC 16%	MC 14%	MC 16%	MC 14%	MC 16%	MC 14%
H_2	18.04	18.03	17	12.5		
CO	17.86	18.51	18.4	18.9		
CH_4	0.11	0.11	1.3	1.2	0.882	3.917
CO_2	11.84	11.43	10.6	8.5		
N_2	52.15	51.92	52.7	59.1		
m^b	0.4647	0.4591	0.3361	0.3927		

Jarungthammachote and Dutta [115] employed the non-stoichiometric equilibrium model to three types of gasifiers: a circular split spouted bed, a spout fluid bed and a central jet spouted bed. In each of the experiments with the central jet and the circular spouted bed experiment, they were carried out with charcoal as feedstock and a constant equivalence ratio of 0.25. For the spout-fluid bed, coconut shell was used as the feedstock with equivalent ratios of 0.3 and 0.35. The simulation results from the model showed a significant deviation from the experimental data especially for CO_2 and CO. The main reason for this deviation has been attributed to carbon conversion hence, the need for a modified model to study the effect of carbon conversion.

The data from the experiments showed that carbon conversion percentage for the central jet spouted bed was in the range 55.5-65.1% and for the circular split spouted bed, it is in the range 56.8-65.3%. For the spouted fluid bed, a value of 60% was assumed. The simulation results from the modified model improved and were closer to the experimental data confirming the carbon conversion as one of the important factors for developing an equilibrium model. The heating value is another important parameter as it is used to estimate the energy that could be derived from using the producer gas. However, the modified model predicted heating values that were generally higher than those from the experimental due to over predicted CO in the producer gas especially for the central jet spouted bed gasification process.

Vaezi et al [116] developed an equilibrium model to predict the performance of a biomass gasifier. The model seeks to find how of a particular biomass can be suited for certain applications. The study incorporated 55 various biomass materials published for which a wide range oxygen content and the C/H ratio was used. They have employed a generalised format to plot the results which can allow the possibility of selecting biomass material based on the desired conditions. These conditions include the calorific value, volume of the syngas obtained, maximum efficiency, temperature etc. Upon investigating the influence of varying C/H ratio together with O_2, the results show that increasing C/H ratio increases the heating value (HHV) of the producer synthesis gas. It also reveals that the there is much higher influence of C/H ratio on HHV than that of O_2. The model slightly under predicts the experiments. This is attributed to the characteristic of equilibrium models because the equilibrium constant of hydrogasification reaction tends to zero at higher temperatures prevailing in the reduction zone. As a result, the predicted CH_4 amount in the final gas is small. However, in a real gasifier, the devolatization of fuel gives high amounts of CH_4 and higher hydrocarbons which do not react completely to equilibrium. The developed model agrees with those of the experiment.

Ratnadhariya and Channiwala [117] developed a three zone equilibrium and kinetic free model of biomass gasifier. Drying and pyrolysis zones combine to form the first zone while the second and third zones are oxidation and reduction respectively. The model constitutes reaction stoichiometry, mass and energy balances including some empirical relationships for each zone. In the drying and pyrolysis zone, species such as CO, CO_2, C, CH_4, C_2H_2, H_2 and H_2O. Also, several assumptions were made based

on the association of oxygen, carbon and hydrogen. It has been observed that some assumptions made in this model lacks justification as there no reactions of CH_4 and C_2H_2 in the oxidation and reduction zones and also there are no thermodynamic constant relationships.

The equilibrium model developed by Melgar et al [58] considers the mass fractions of sulphur, carbon, hydrogen, oxygen and nitrogen (CHONS) in the biomass. The model equations include the atomic balances of the C, H, O, N and S, the energy balance and two equilibrium constant relationships. The model considers water dissociation for the production of hydrogen. The non- linear equations were solved with the Newton-Raphson method. To achieve stability of the calculation process, a partial step of (δ/5) was applied correct the evaluation of each iteration. The model can be applied to predict the producer gas composition, gasifying efficiency and heating value. The reported model is validated with the experimental work of Jayah et al, see Table 2.3. Parameter F_{rg} in Table 2.3 is the gasification relative fuel/air ratio.

Table 2.3 Comparison between experiment al and model compositions for the producer gas of rubber wood with 14.7% moisture content.

Producer gas composition (vol%)	Model [95]	Experiment [95]	Model [99]	Experiment [99]
CO	18.3	19.1	19.2	19.3
H_2	16.4	15.5	16.6	17.6
CO_2	11.1	11.4	11	11.1
CH_4	1.1	1.1	0.2	0.4
N_2	53.2	52.9	53	51.6
Frg	2.3	2.39	2.3	2.4

Sharma [118] presented a model for the downdraft gasifier, the reduction zone has been modelled using finite rate of reactions succeeding the chemical kinetics. Thermodynamic equilibrium modelling is used to model the pyrolysis and oxidation zones. He proposed the global gasification reaction based on mixed model including char formation. The author incorporated the three-heterogeneous reaction including the methane reformatting reaction but did not consider the char combustion and

methane formation in the pyrolysis and oxidation zone. Four atomic balances (C, H, O and N) energy balance equations including four equilibrium constants constitutes the model. The model predicts the unreacted char at various thermodynamic condition. The presented model has been validated with experimental data available in literature.

Antolini et al [119] developed an in-house thermodynamic equilibrium model to predict the gas composition and char output from gasification of pelletized biomass using air and CO_2. The study was aimed at investigating the effect of CO_2 feed in biomass gasification as a viable way to directly exploit exhaust gas from the engine of combined heat and power systems to convert CO_2 to CO through Boudouard reaction, and in doing so increase the carbon conversion and reduce char yield. The reactor is a reverse downdraft gasifier mounted on a digital weighing balance. This approach is based on the enthalpy of the reactants. The model results showed a good agreement with the experimental results, especially in terms of predicted char yield.

2.4.4 Computational Fluid Dynamics (CFD) Models

Computational fluid dynamics plays an important role in the modelling of fixed bed downdraft and fluidised bed gasifiers. CFD models numerically solve the mass, momentum of species, hydro-dynamics, and energy flow and turbulence equations over a distinct region. CFD models are found to be highly accurate in predicting gas yield, temperature and the reactor if the reactor hydrodynamics is known. CFD modelling of biomass gasification involves the combining of dense particulates flow and specific chemistry [120]. The two aspects are very challenging in CFD; for instance, the composition of biomass can pose some complexity due to its dependence on geographical location, feedstock and age period of the year. These models have been used to study characteristics of diverse types of biomass gasifiers.

Janajreh et al [121] studied the conversion of efficiency in a small scale, air blown downdraft gasification system operated with wood as the fuel. CFD was used to model the Lagrangian particle couple evolution after investigating the temperature field inside the gasifier. The numerical simulation was conducted on a high-resolution mesh accounting for the solid and gaseous phases using the k-epsilon turbulence and reacting flow CFD model. The downdraft gasifier was modelled using the finite volume code coupled with a conjugate heat transfer with the bulk metal separators and the insulators.

The results of the temperature distribution and the evolvement of the species were validated by comparing with the experimental data of the ideal equilibrium and zero-dimensional case. The result of CFD computed cold gas efficiency (CGE) was found to be under predicted by 19 points less than that calculated for the ideal case. The authors observed that equilibrium modelling could not capture the physio-chemical processes inside the downdraft gasifier due to the complexity of the flow in the downdraft gasifier. On the other hand, the discrete phase method (DPM) in ANSYS was employed to model the devolatization effect of 0.1 mm particle diameter to account for the particle size of the wood. The corresponding CFD and experimental temperature profiles showed that the assumptions made were realistic.

Rogel et al [122] proposed a ''1-D +2-D''numerical model to simulate the gasification of pure pine wood pellets in a stratified downdraft gasifier. The model considers reactions for drying, primary pyrolysis of biomass, secondary tar cracking, combustion, gasification and particle shrinkage. The particle model is based on intraparticle mass and energy balances and is written in spherical coordinates for one dimensional unsteady system. However, the gas phase model includes mass, energy and momentum balances for two-dimensional unsteady system in cylindrical polar coordinates. A commercially available CFD code PHOENICS was used to solve the model numerically. The pressure drop inside the reactor is assumed constant and its model is based on modified Ergun equation. Fine rate equations were used for all the reactions and the transport equations were solved numerically. The model predictions were shown to be in reasonable agreement with the experimental data with respect to the gas temperature profiles, biomass temperature profile and biomass particle shrinkage and syngas composition.

Jakobs et al. [41] proposed a CFD model of a high pressure entrained flow gasifier. Finite volume solver was used to solve mass, momentum and energy balance equations and considering several species. The atomization quality of twin fluid nozzles with respect to gas velocity and reactor pressure was analysed. The proposed and characterized atomizers were used in the atmospheric entrained flow gasifier, to detect the influence of spray quality on gasification process. Sauter Mean Diameter (SMD) of the produced spray was found to have a profoundly affected by the gas velocity and reactor pressure. With an increase in the reactor pressure, the drop diameter was found to increase while increasing gas velocity decreased the SMD. The impact of the SMD

on gasification process was observed from organic carbon and methane concentration measurements as well as from the radial temperature profiles at various positions along the reactor centreline. The CFD model of high pressure entrained flow gasification of biomass based slurries showed a very significant influence of the drop size distribution on gasification quality.

Gao et al [123] proposed a CFD model of a cyclone gasifier based on the use of CFD package FLUENT. The model incorporates pyrolysis of sawdust, combustion of volatiles and char. The model can predict the outlet gas composition and the temperature in the gasifier. The influence of equivalence ratio was studied and validated with experimental data. The carbon conversion for the cyclone gasifier was found to be 77 and 94.2% and the cold gas efficiency varied between 53.6 and 63% when the equivalence ratio was varied from 0.23 to 0.35. The maximum lower heating value (LHV) of 5.7 MJ/Nm3 was achieved when the equivalence ratio (λ) was between 0.23-0.26. The predicted gas temperature and producer gas compositions were observed to follow the same trend as the experimental data, however, the CO and CO_2 concentrations were under predicted.

2.4.5 Artificial Neural Networks Model (ANNs)

Artificial Neural networks is a type of computational model in which a dense distribution of simple processing element is supplied to give a presentation of complex process which includes non- linear and discrete systems. The model consists of interconnected groups of artificial neurons and then processes the information via computation (Babu *et al.* 2009). ANN is a standard modelling tool which consists of multiple layers of perception paradigm (MLP) [124]). These layers consists of an input layer, a hidden layer and an output layer of neurons. The hidden and output layer neurons process their inputs by multiplying each input by a corresponding weight, summing the product, and then processing the sum using a nonlinear transfer function to produce a result [125]. The neurons in the input layer conveys the signals to the hidden and output layers. ANN is usually employed in signal processing, function approximation, simulation and for identifying patterns.

Brown et al [126] proposed an equilibrium model for the design of biomass gasifiers. From the ultimate analysis properties, fuels and chars were defined while tar was defined as a subset of known molecular species and their distribution was determined

by equilibrium calculations. The reaction temperature difference for a complete set of stoichiometric equations was used to explain the non-equilibrium behaviour of the tar and char formation. A non-linear regression including an artificial neural network evaluated the relationship between the changes in temperature and fuel consumption and operational variables. This approach applied with a fluidise bed reactor data, seems to improve the accuracy of the equilibrium calculations and reduces the number of required data by stopping the Neural Network from identifying atomic and heat balances. Sreejith et al. [44] proposed a feed-forward artificial neural network (ANN) model for the predicting the gasification temperature and product gas composition. They proposed a Redlich–Kwong real gas equilibrium correction model including tar and unconverted char to predict the product gas composition, heating value and thermodynamic efficiencies. A reasonable accuracy of ANN prediction with experimental results was reported based on the computed statistical parameters of comparison such as coefficient of correlation, root mean square error (RMSE), average percentage error and covariance. The equilibrium model corrected was developed by introducing correction factors for real gas equilibrium constants and these showed satisfactory agreement with the experimental values. Maximum concentration of hydrogen achieved experimentally was 29.1% at the equivalence ratio of 0.277 and steam to biomass ratio (SBR) of 2.53. The corresponding predicted values were 28.2% for ANN model and 31.6% for corrected equilibrium model. The equilibrium model corrected for wood sawdust was validated with air–steam gasification experimental results of other biomass materials and was found to be 95.1% accurate on average. It was revealed from the study that the ANN model (RMSE is 2.64) was a better predictor for the product gas composition than the corrected real gas equilibrium model (RMSE is 5.96).

Puig-Arnavat [25] developed two ANN models; one for circulating fluidized bed gasifiers (CFB) and the other for bubbling fluidized bed gasifiers (BFB). Both models were used to determine the producer gas composition (CO, CO_2, H_2 and CH_4) and gas yield. The effect of ash, moisture, carbon, oxygen and hydrogen content of dry biomass, equivalence ratio and gasification temperature were studied for CFB and BFB whereas the effect of steam to dry biomass ratio (kg/kg) was studied for BFB only. The two ANN models developed for CFB and BFB gasifiers showed the possibility that ANN may offer some contribution to research in the area of biomass gasification

modelling. The results obtained by the two ANN's showed high agreement with published experimental data used: very good correlations in almost all cases and small RMSE.

Considering engineering design and process optimization of biomass gasifier for the production of synthesis gas, an extensive investigation of the plant behaviour depending on various operating parameters is required. Whilst performing experiments on large scales may pose problems due to associated safety risks and high costs, developing a mathematical model can also give a good representation of the complex chemical and physical phenomena taking place in the gasifier as this allows fewer and better experiments to be performed with minimal costs. Also, a simulation model allows prediction of the progress of these complex occurrences as it is needed for optimizing the gasifier design and its operating conditions. In view of this, this work consists in the development of the method of numerical simulation of a downdraft gasifier operation, which is based on thermodynamic and kinetic models applied to a downdraft fixed bed. The model presented in this work is made up from three constituent sub-models which attempt to simulate each of the zones namely pyrolysis, oxidation and reduction zones. These are then combined to form a complete model using both single and double air feed to the gasifier. Whilst there are many studies in literature on biomass gasification based on equilibrium and kinetic models, this technology is still not very commercially viable due to the challenges related to the gasification of biomass to produce clean gas for internal combustion engines and gas turbines as well as severe constraints in terms of gas quality and lack of flexibility in the type of biomass. It is in this context that this work has relevance in attempting to explore various approaches for modeling and simulation. In one approach to simulation the three zones were all assumed to reach thermodynamic equilibrium and each zone was simulated using a Gibbs Reactor. In another approach an assumption was made that the third zone, the Reduction Zone, could be simulated using a chemical rate approach. This required chemical equations to be presented that could theoretically represent the formation and disappearance of species in the Reduction Zone. In HYSYS this zone was represented by a PFR. Whilst this operation requires the presentation of chemical kinetic data it also integrates over a stated tubular reactor to produce a unique solution according to the conditions calculated by the previous zone, the oxidation zone represented by a Gibbs Reactor. Using such an approach for this type of problem; simulation of a biomass gasifier is unique.

Chapter 3 Modelling and Simulation of Biomass Gasification Process

Operating a biomass gasifier efficiently depends on a number of complex chemical reactions such as fast pyrolysis, partial oxidation of the pyrolysis products, gasification of the resulting char, conversion of tar and lower hydrocarbons, water-gas reaction and methane formation etc. Development of mathematical models are required due to the complexity of the reaction processes, sensitivity of the product distribution, rate of heating and residence time in the reactor in other effectively design and operate a particular gasifier[25].

Mathematical simulation is a very important aspect of research and development of the Gasification technology. Simulation may not provide a very accurate prediction of system performance however, it may provide guidance on the effect of design, operating conditions and input variables. Also, modelling may provide a less expensive means of evaluating the benefits and the accompanying risks in the real time situation [80]. Understanding of chemical and physical mechanisms of biomass gasification processes is essential to optimize the gasifier designing and operating biomass gasification systems[127].

The importance of mathematical simulations can be summarized as follows [80]

- Allows optimizing the operation or design of the plant using available experimental data from a plant or large-scale plant.
- Provide information on extreme operating conditions where experiments and measurements are difficult to perform.
- Identify operating limits and related risks.
- Aid in scale-up of the gasifier from one successfully operating size to another and from one feedstock to another.
- Assist in interpretation of experimental results and analyse anomalous behaviour of the gasifier.

Gasification simulations models may be classified into thermodynamic equilibrium model, kinetic model, computational Fluid dynamics (CFD) model and artificial neural work. These models are based on different methods to assess and predict gas fractions and the effects of operating conditions of a particular design including the utility and limitations. Modelling of the gasification process using a particular approach may consider the following reaction which are the basic gasification reactions [128]:

Bouordard reaction (R1) $C + CO_2 \rightarrow 2CO$ (3.1)

Water- gas reaction (R2) $C + H_2O \rightarrow H_2 + CO$ (3.2)

Methane Formation (R3) $C + 2H_2 \rightarrow CH_4$ (3.3)

Steam reforming reaction (R4) $CH_4 + 2H_2O \rightarrow 4H_2 + CO_2$ (3.4)

3.1 Thermodynamic Equilibrium Models

Thermodynamic equilibrium models are based on the chemical and thermodynamic equilibrium which are determined by implication of equilibrium constants and minimization of Gibbs free energy**.** The idea of chemical equilibrium is based on the second law of thermodynamics when applied to reacting systems [54]. At chemical equilibrium, the species of a reacting system is at a stable composition as it does not experience a net change in concentration over time [94]. Equilibrium models are suitable simulation tools for processes whose duration are in most cases quite long with regard to the reaction timescale [81]. The thermodynamic equilibrium calculations are suitable for studying the influence of fuel and process parameters such as temperature [58].

Some major assumptions of thermodynamic equilibrium models can be presented as follows:

- The reactor is considered as zero dimensional.
- There is perfect mixing of materials and uniform temperature in the gasifier even though different hydrodynamics are observed in practice.
- The rates of reactions are fast enough and residence time is long enough to attain equilibrium.

By employing the governing equations describing the behaviour of such state, one can formulate an equilibrium model. These fundamental equations stated in Tigabwa et al [94] are following equations.

Overall mass balance:

$$F_{in} \sum in\, n_{K,i}\ X_i\ =\ F_{out} \sum out\, n_{K,i} X_i \tag{3.5}$$

Where $n_{k,i}$ is the number of atoms *k* of a molecule *i*, and x_i is the molar fraction of a component *i*.

Overall energy balance:

$$F_{in} \sum in\, X_i H_i(T_{in}, P) =\ F_{out} \sum out\, X_i H_i(T_{out}, P) \tag{3.6}$$

3.1.1 Stoichiometric Equilibrium Models

Stoichiometric models are based on the use of equilibrium constants where specific chemical reactions used in the calculations are defined; it follows that appropriate chemical reactions are selected and information regarding the equilibrium constants are required [107]. The equilibrium constant of a reaction *j* is

$$K_j = \prod_i (\frac{P_i}{P_0})\ vi, j \tag{3.7}$$

These sets of selected chemical reactions can be associated with the Gibbs free energy change related to temperature:

$$\text{-RTln}K_j = \Delta G^0 j \tag{3.8}$$

The disadvantage of this method lies in the fact that a set of non- linear algebraic equations are solved for the mole numbers of each specie and this mostly difficult if the system is large [108]. In order to predict the gasification process in a downdraft gasifier, Zainal et al used stoichiometric equilibrium method to model the gasification process in a downdraft gasifier different biomass materials [112]. The equilibrium model predicts the calorific value of the gasifier reasonably well and compares well the experimental values available in the literature for wood. However, the amount of oxygen in that model was eliminated by defining it in terms of components in the producer gas but was not shown when they compared their model with their experimental data, this is what makes this model different. The thermodynamic

equilibrium model based on equilibrium constants was developed and used to predict the composition of the producer gas in a downdraft waste gasifier. The model can predict the reaction temperature given the amount of air and vice versa. The equilibrium constant is multiplied by coefficients obtained from the comparison of experimental and predicted results from other works to improve the model. The modified model when used to simulate the gasification of Thailand MSW (municipal solid waste) showed that with increased moisture content, the hydrogen content increases gradually, while carbon monoxide decreasing. Methane which has a low percentage in the producer gas decreases [128]. Syed et al also used thermodynamic equilibrium methodology to obtain the product composition of the producer gas and to calculate the maximum cold gasification efficiency of the gasification process in an entrained flow environment. The results show that on dry and ash free basis the maximum gasification efficiency is achieved when most of the solid carbon present in the feedstock is converted into carbon monoxide. It shows that increasing O/C and H/C ratio directly affects the cold gasification efficiency. CGE increases as the both ratios increase [129].

Stoichiometric equilibrium models incorporate the thermodynamic and chemical equilibrium of the chemical species involved. The model can be designed either for a global gasification reaction or can be divided into sub-model for drying, pyrolysis, oxidation and reduction [25].

Single step stoichiometric equilibrium model

This model embodies the several complex reactions of gasification into one generic reaction as mentioned in the below equation. It assumes that one mole of biomass CH_hO_o based on a single atom of carbon that is being gasified with *w* mole of water/steam in presence of *a* mole of air:

$$CH_hO_o + wH_2O + a(O_2 + 3.76N_2) = n_cC + n_{H2}H_2 + n_{co}CO + n_{CO_2}CO_2 + n_{CH4}CH_4 + n_{H_2O}H_2O + 3.76aN_2 \quad (3.9)$$

Here *w* is the amount of water per kilo mol of wood, *m* is the amount of oxygen per kilo mol of wood. Subscripts, n_C, n_H, n_{CO}, n_{CO2}, n_{CH4}, n_{H2O}, are the coefficients of the products.

In the reaction shown above, *w* and *a* are the variables and can be varied to obtain the desired amount of product. Based on the stoichiometric balance of carbon, hydrogen and oxygen from the generic equation (3.9) the mass balance equations are formed to obtain the six unknowns which include:

Carbon: $n_C + n_{CO} + n_{CO_2} + n_{CH_4} \rightarrow 1$ (3.10)

Hydrogen: $2n_{H_2} + 4n_{CH_4} + 2n_{H_2O} \rightarrow 2w + h$ (3.11)

Oxygen: $n_{CO} + 2n_{CO_2} + n_{H_2O} \rightarrow w + 2a$ (3.12)

Reactions R1 to R4 which are Boudouard reaction, water-gas reaction, methane formation and steam reforming reaction respectively are considered the major reaction of gasification. The equilibrium constants(K_{eq}) are defined as shown below [130]:

$$K_{eq,1} = \frac{n^2 CO}{nCO_2} \quad (3.13)$$

$$K_{eq,2} = \frac{n_{H_2}\, n_{CO}}{n_{H_2O}} \quad (3.14)$$

$$K_{eq,3} = \frac{n_{CH_4}}{n^2 H_2} \quad (3.15)$$

$$K_{eq,4} = \frac{n_{H_2} nCO_2}{n_{CO} n_{H_2O}} \quad (3.16)$$

When the gasification process is assumed to be adiabatic then the energy balance of the gasification reaction brings about a new set of equations which in turn determine the final temperature of the system [68] and [131]:

$$\sum_i n_i \left[h^0{}_{f,i} + \Delta H^T_{298}\right]_{i,Reactant} = \sum_i n_i \left[h^0{}_{f,i} + \Delta H^T_{298}\right]_{i,Product\ loss} \quad (3.17)$$

Modifying the above equation (3.17) by considering equation (3.9) we obtain

$$h^0_{f,wood} + w\left(h^0_{f,H_2O(1)} + h_{vap}\right) + a h^0_{f,O_2} + 3.76 a h^0_{f,N_2} = n_c . h^0_{f,c} + n_{H_2} h^0_{f,H_2} + n_{CO} h^0_{f,CO} + n_{CO_2} + n_{CH_4} h^0_{f,CH_4} + n_{H_2O} h^0_{f,H_2O} + 3.76 a h^0_{f,N_2} + \Delta T(n_C C_{p,C} + n_{H_2} C_{p,H_2} + n_{CO} C_{p,CO} + n_{CO_2} C_{p,CO_2} + n_{CH_4} C_{p,CH_4} + n_{H_2O} C_{p,H_2O} + 3.76 a C_{p,N_2} \quad (3.18)$$

Here $h^0{}_f$, $C_{p,C}$, h_{vap}, represent heat of formation of corresponding chemical species, specific heat capacity and enthalpy of vaporization of water, respectively, and ΔT is the difference between the gasification temperature and the initial temperature of the biomass feedstock. The heat of formation of biomass wood; $h^0_{f,wood}$ can be estimated by the application of Hess law. Single step stoichiometric equilibrium model may be formulated by the application of the chemical equilibrium state and the reaction stoichiometric condition.

Equilibrium models are further categorized as stoichiometric models and non-stoichiometric models. Stoichiometric models are based on equilibrium constants.

Sub-models for the stoichiometric equilibrium model

The stoichiometric equilibrium model comprises separate sub-models to describe each of the zones such as the drying, pyrolysis, oxidation and reduction. These models are combined together to form the complete model. The output from one sub-model becomes input for the following model's sub-model [52]. The sub-models can be used employing several combinations as shown in Figure 3.1 below.

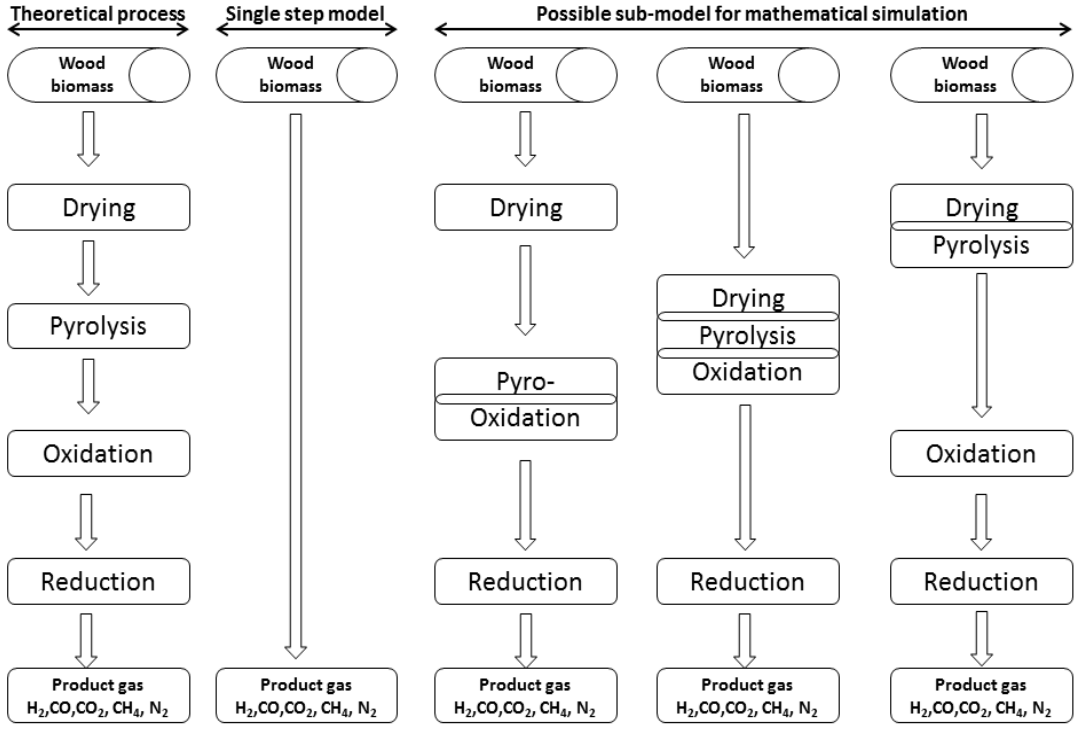

Figure 3.1 Sub-models for conversion of biomass to producer gases

Many researchers have developed the thermo-chemical equilibrium gasification models to describe gasification process either by considering the gasifier as a single or global process system. In the study for modelling and simulation of the combined pyrolysis and reduction zone for a downdraft gasifier by Ningbo Gao et al, the pyrolysis and the reduction zones are combined to simulate the global biomass gasification process [132]. In another study the downdraft biomass gasification model was developed by Dejtrakulwong et al [133], which was divided into modules for drying, pyrolysis, oxidation and reduction. The one-dimensional kinetic finite rate model was applied to the reduction module. Figure 3.2 shows the view of the physical model of the downdraft gasifier including the reactions that are occurring in the various zones.

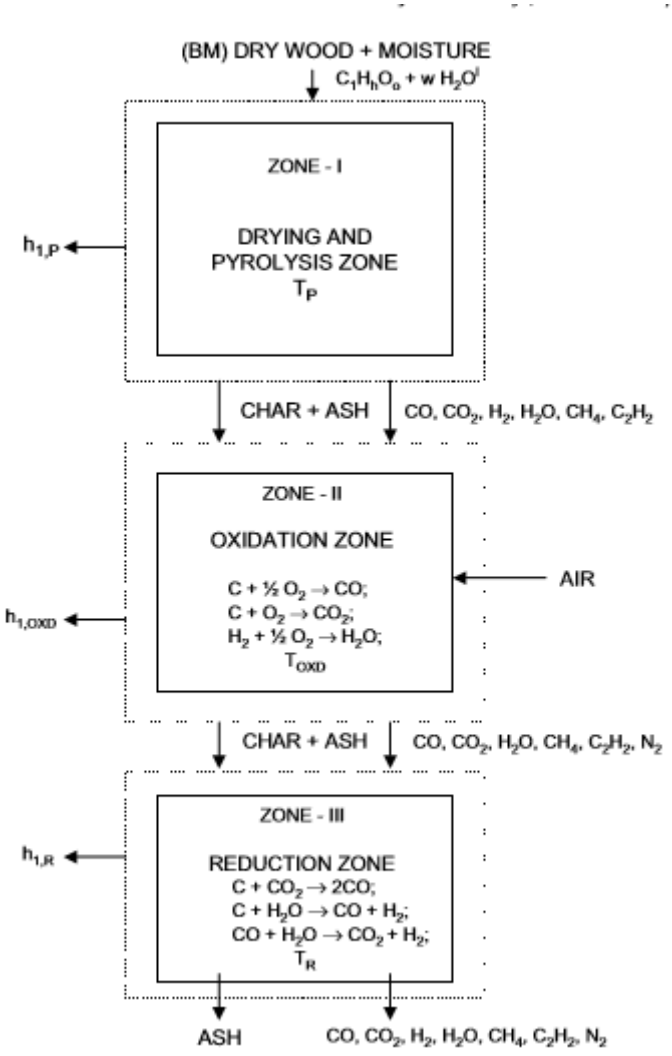

Figure 3.2 Three zone equilibrium and Kinetic model of downdraft gasifier [133]

Here drying and pyrolysis zones are combined together. The products of this zone are assumed to be char, CO, CO_2, H_2, H_2O, C_2H_2 and CH_4. The drying and pyrolysis zone is where the moisture in the biomass is released as steam and where the ligno - cellulosic material is thermally decomposed. The decomposition of this ligno-cellulosic material is transformed into gaseous volatile species mainly composed of CO_2, H_2, CH_4, C_2H_2, CO as well as char. These substances then move to the oxidation zone where it contacts with air and partial combustion of the volatile species takes place. The pyrolysis products are then transformed into the oxidation products which consist of CO, CO_2, CH_4, H_2, N_2, steam tar and char. The heat generated from the oxidation zone is used to drive the reactions in both drying and reductions zones. In the reduction zone, oxidation products react to form CO, CO_2, H_2, CH_4, N_2 and water vapour.

3.1.2 The Model development and assumptions

The model formulated in this work consists of three constituent sub-models to describe each of the zones i.e. pyrolysis, oxidation and reduction zone. These are then combined together to form a complete model. The sub-models are taken from Centeno et al [134] and Roy et al [57]. The pyrolysis and oxidation zones are modelled using the chemical equilibrium. Mass balance equations are used to calculate the amounts of pyrolysis products. These are solved using assumptions from Centeno. The single energy balance equation is from Roy et al and is applied across both zones to calculate the reaction temperature at the entry into the reduction zone.

Assumptions

- The gasifier operates under atmospheric temperature.
- All gaseous species are treated as ideal gases.
- The char is modelled as carbon graphite (non-volatile carbon).
- Only the volatile part of the biomass undergoes the pyrolysis process. The non-volatile carbon and biomass moisture proceed to the oxidation zone.
- Since the affinity between hydrogen and oxygen is higher than that of oxygen and carbon, it is assumed that 80% of fuel oxygen i.e. 4/5 of the supplied oxygen is associated with fuel hydrogen in the form of water while the remaining 20% i.e. 1/5 of oxygen is associated with carbon in the biomass and releases as CO and CO_2.

- The ratio of moles of CO and CO_2 formed is inversely equated to their molecular masses i.e. CO/CO_2 =44/28.
- Fifty percent of the hydrogen in the fuel is given off as H_2 upon decomposition and the remaining fifty percent is given off in the form of CH_4 and C_2H_2.
- The ratio of moles of CH_4 and C_2H_2 is inversely related with their molecular masses i.e. CH_4/C_2H_2 = 26/16.

Formulation of the model

From the ultimate analysis data, moist biomass can be presnted as sum of volatiles, non-volatile and components of water plus some amount of incombustible materials such as ash:

Biomass = $C_{bC}H_{bH}O_{bO}$ + w$H_2O + ash \rightarrow C_{bvC}H_{bvH}O_{bvO} + C_{bnvc} + wH_2O + ash$ (3.19)

Here, wH_2O is moles of water in the feedstock moisture; bvC is volatile moles of Carbon; bvH is volatile moles of Hydrogen; bvO is volatile moles of Oxygen; $bvnC$ is non-volatile moles of Carbon

Pyrolysis Zone

The process taking place in the pyrolysis zone can be represented symbolically as

Biomass + heat → volatile components + water vapour + char + ash (3.20)

The above chemical reaction is written as

$C_{bvC}H_{bvH}O_{bvO} \rightarrow X_{pC}C + X_{pCO_2}CO_2 + X_{pCO}CO + X_{pCH_4}CH_4 + X_{p_{C_2H_2}}C_2H_2 + X_{pH_2}H_2 + 2X_{pH_2O}H_2O$ (3.21)

Pyrolysis zone mass balance equations are:

Carbon: $bvC = X_{pc} + X_{pCO_2} + X_{PCO} + X_{p_{CH_4}} + 2X_{p_{C_2H_2}}$ (3.22)

Hydrogen: $bvH = 4X_{pCH_4} + 2X_{p_{C_2H_2}} + 2X_{pH_2} + 2X_{pH_2O}$ (3.23)

Oxygen: $bvO = 2X_{pCO_2} + X_{pH_2O} + X_{PCO}$ (3.24)

Parameter X_p in above equations represent amounts of products from pyrolysis zone

Oxidation zone

The oxidation zone reaction can be represented symbolically by

$$Volatiles + char + air \rightarrow H_2O + CO + H_2 + CO_2 + CH_4 + N_2 \ + char + tar \quad (3.25)$$

Assumptions

- Acetylene formed during the pyrolysis process is fully oxidized.
- If oxygen is supplied in sufficient amount, the hydrogen formed in the pyrolysis zone is fully oxidized and converted to water because of its high burning rate.
- If any oxidation remains after oxidation of hydrogen and acetylene, methane formed during this process is converted to water and carbon dioxide depending on the availability of oxygen
- Any remaining oxygen is consumed in oxidation of char.
- Concentrations of CO and CO_2 are assumed to be inversely proportional to the ratio of exothermicity of the corresponding reactions i.e. the less the exothermic reaction, the more the product formation.
- It is assumed that CO_2, CO and H_2O produced during oxidation are added to the products from the pyrolysis zone.
- N_2 form entering the oxidation zone is inert.

Products calculated from the pyrolysis zone X_p react with air in the oxidation zone and products from the oxidation zone X_o are calculated as:

$$X_{pC}C + X_{pCO_2}CO_2 + \ X_{pCO}CO + X_{pCH_4}CH_4 \ + X_{pH_2}H_2 + X_{pC_2H_2}C_2H_2 + 2X_{pH_2O}H_2O + a(O_2 + 3.76N_2) \rightarrow X_{oC}C + \ X_{oCO_2}CO_2 + \ X_{oCO}CO + X_{oCH_4}CH_4 + \ X_{oH_2}H_2 \ + X_{oC_2H_2} + \ X_{oH_2O}H_2O \ + 3.76aN_2 + bnvC \quad (3.26)$$

Mass balance equations can be written as follows.

Carbon:

$$bnvC + X_{pC} + X_{pCH_4} + \ \ X_{pCO} + \ X_{pCO_2} + \ 2X_{pC_2H_2} = X_{oCO_2} + X_{oCO} \ + \ X_{oCH_4} + X_{oC} \quad (3.27)$$

Hydrogen:

$$2X_{pC_2H_2} + 4X_{pCH_4} + 2X_{pH_2} + 2X_{pH_2O} = 4X_{oCH_4} + 2X_{oH_2} + 2X_{oH_2O} \quad (3.28)$$

Oxygen:

$$X_{pCO} + X_{pCO_2} + X_{pH_2O} + 2a = X_{oCO} + 2X_{oCO_2} + X_{oH_2O} \quad (3.29)$$

Products amounts are calculated from the mass balance and using the following assumption: 4/5 of the supplied oxygen is associated with fuel hydrogen in the form of water while the remaining 20% i.e. 1/5 Oxygen is associated with carbon in the biomass and releases as CO and CO_2.

To perform calculations in MATLAB, these expressions are written thus considering the assumptions;

$$xpH_2O = 0.8 * bvO + wH_2O \quad (3.30)$$

$$xpCO = 0.2 * bvO * 44/(44 + 28) \quad (3.31)$$

$$xpCO_2 = 0.2 * bvO * 28/(44 + 28) \quad (3.32)$$

Fifty percent of the hydrogen in the fuel is given off as H_2 upon decomposition and the remaining fifty percent is given off in the form of CH_4 and C_2H_2

$$xpH_2 = 0.5 * (bvH - 2 * 0.8 * bvO) * 0.5 \quad (3.33)$$

$$xpCH_4 = 0.5 * (bvH - 2 * 0.8 * bvO) * 26/(26 + 16) \quad (3.34)$$

$$xpC_2H_2 = 0.5(bvH - 2 * 0.8 * bvO) * 16/(26 + 16) \quad (3.35)$$

Energy balance

Both exothermic and endothermic reactions occur in the gasifier. Examples of such reactions are partial oxidation and Boudouard reactions, respectively. Some of the heat generated from the exothermic reaction is used by the endothermic reaction and the rest is converted to sensible heat, affecting the temperature. The reaction temperature is an important parameter that influences the both chemical reactions and thermodynamic calculations. It is therefore necessary to know the reaction

temperature. In order to obtain this value, the first law of thermodynamics or energy balance is applied for the description of gasification process [107].

Once the composition of the pyrolysis products has been obtained from solving the mass balance, they can be used to solve the energy balance across the pyro- oxidation zone for the reactor temperature at entry to the reaction zone:

$$x_{biomass}\, h_f^o + a\int_{T_o}^{T_a} \bar{c}_{p,O_2}\, dT + 3.76a\int_{T_o}^{T_a} \bar{c}_{p,N_2}\, dT + w h_{f,H_2O}^o + \dot{Q}_{loss} =$$
$$\sum_{x=1}^{6} x_{ox}\left[h_{f,x}^o + \int_{T_o}^{T} \bar{c}_{p,x}\, dT\right] + x_{oC}\bar{c}_{p,c}(T - T_o) + \dot{m}_{ash}\bar{c}_{p,ash}(T - T_o) \quad (3.36)$$

Reduction zone

The kinetic model predicts the gas yield and product composition that a gasifier achieves after a finite time or in a finite volume in the case of a flowing medium [6]. The model is able to predict the temperature profiles and gas composition inside the gasifier, taking into account the gasifier operating conditions and the gasifier configuration. It also considers both the kinetics of gasification reactions and the hydrodynamics of the gasifier. The reaction kinetics requires reaction rates, knowledge of bed hydrodynamics, mass and energy balance to obtain gas yields, tar and char at a given operating condition while the reactor hydrodynamics involves the knowledge of the physical mixing process [77].

3.2 Kinetic model

The reduction of the chemical species from the oxidation zone takes place in the gasifier's reduction zone. The products from oxidation zone are taken as initial input for the first compartment of reduction zone. The reactions of the reduction zone are slow, reversible and endothermic so they cannot be assumed to have reached equilibrium. For this reason, a finite rate kinetic model originally presented by Giltrap et al is employed which considers the following reactions taking place.

Bourdouard reaction:

$$C + CO_2 \leftrightarrow 2CO \qquad \Delta H = 172 kJ/kmol \text{ (endothermic)} \qquad (3.37)$$

Water gas reaction:

$$C + H_2O \leftrightarrow CO + H_2 \qquad \Delta H = 131.4 kJ/kmol \text{ (endothermic)} \qquad (3.38)$$

Methanation reaction:

$C + 2H_2 \leftrightarrow CH_4$ ΔH =-74.9kJ/kmol (exothermic) (3.39)

Steam Reforming:

$CH_4 + H_2O \leftrightarrow CO + 3H_2$ ΔH = 206.4kJ/kmol (endothermic) (3.40)

The values of the equilibrium constants for the four above reactions are calculated from Gibbs free energy

$$K_p = \exp\left(\frac{-\Delta G_T}{RT}\right) \quad (3.41)$$

The expressions for the equilibrium constants for the four reactions are given by

$$K_1 = exp\left(-2\frac{g_{CO}}{RT} + \frac{g_{CO_2}}{RT}\right) \quad (3.42)$$

$$K_2 = exp\left(-\frac{g_{CO}}{RT} - \frac{g_{H_2}}{RT} + \frac{g_{H_2O}}{RT}\right) \quad (3.43)$$

$$K_3 = exp\left(-\frac{g_{CH_4}}{RT} + 2\frac{g_{H_2}}{RT}\right) \quad (3.44)$$

$$K_4 = exp\left(-\frac{g_{CO}}{RT} - 3\frac{g_{H_2}}{RT} + \frac{g_{CH_4}}{RT} + \frac{g_{H_2O}}{RT}\right) \quad (3.45)$$

Rates of four reactions in the reduction zone are evaluated using Arrhenius type kinetic rate equations, see Table 3.1

Table 3.1 Rates of four reactions in the reduction zone are evaluated using Arrhenius type kinetic rate equations

Reaction No	**Reaction**	**Reaction rate Mol/m^3.s**	**Ai (1/s)**	**Ei (kJ/mol)**
R1	Boundouard reaction: $C + CO_2 \leftrightarrow 2CO$	$r_1 = C_{RF} A_1 exp^{\left(\frac{-E_1}{RT}\right)} . \left(y_{CO_2} - \frac{y_{co}^2}{K_{eq.1}} \right)$	3.616 x 10^1	77.39
R2	Water gas reaction $C + H_2O \leftrightarrow CO + H_2$	$r_2 = C_{RF} A_2 exp^{\left(\frac{-E_2}{RT}\right)} . \left(y_{H_2O} - \frac{y_{CO} . y_{H_2}}{K_{eq.2}} \right)$	1.517 x 10^4	121.62
R3	Methane formation: $C + 2H_2 \leftrightarrow CH_4$	$r_3 = C_{RF} A_3 exp^{\left(\frac{-E_3}{RT}\right)} . \left(y^2{}_{H_2} - \frac{y_{CH_4}}{K_{eq.3}} \right)$	4.189 x 10^4	19.21
R4	Steam formation $CH_4 + H_2O \leftrightarrow CO + 3H_2$	$r_4 = C_{RF} A_4 exp^{\left(\frac{-E_1}{RT}\right)} . \left(y_{CH_4} - \frac{y_{CO} . y_{H_2}^3}{K_{eq.4}} \right)$	7.301 x 10^{-2}	36.15

In equations in Table 3.1, *CRF* is the char reactivity factor, a variable that accounts for the active sites on the surface of the char in the zone. Babu and Sheth yielded their best results with an exponentially increasing *CRF*.

According to their study the expression *CRF = Cexp(bz)*

where *C* and *b* are constants set in order that the model is tuned to estimate a gas exit temperature comparable to an experimental results and *z* is the length of the reduction zone.

Also, r_i is the rate of the reaction *i* in the $mol.m^{-3}.S^{-1}$; A_i is the frequency factor for reaction *i*; E_i is the activation energy of the reaction in$J.mol^{-1}$; *R* is the constant in $J.mol^{-1}K^{-1}$; *T* is the temperature in K; K_i is the equilibrium constant of reaction i.

A system of nine coupled ordinary differential equations is derived from mass and energy balance equations, the ideal gas law and the Ergun equation for calculating the pressure drop of fluid across a packed bed of particles. The sub model of the reduction zone assumes a cylindrical form of the reduction zone with uniform cross-sectional area. The creation and destruction of any species in finite kinetic rate model for reduction zone is generally dependent on several factors such as the length, temperature and even flow [25]. Then, the net formation or destruction of any species in the next compartment may be estimated as a function of gas velocity and rate of formation of corresponding species as expressed in equations (3.38-3.39) [25, 27].

The modelled reactions for the reduction zone are:

$$\frac{dnx}{dz} = \frac{1}{v}\left(R_x - n_x \frac{dv}{dz}\right) \quad (3.46)$$

Here n_x is the molar density of species x in $mol.mol^{-3}$, R_x is the net rate of formation of species x by chemical reactions in $mol.mol^{-3}.s^{-1}$; v is the superficial gas velocity in m/s.

Equation (3.46) can be used to generate the molar concentrations of each of the six gaseous species (CO_2, CO, H_2O, H_2, CH_4, N_2) considered. Also, the total molar density of all gases, *n*, can be expressed as the sum of the molar densities of each of the six component gases. Once the rate of modeled reaction (R_i) is estimated, the rate of formation of each gaseous species (R_x) involved in gasification reaction is estimated as in Table 3.2.

Table 3.2 Rate of formation of species per unit volume in terms of the rates of reaction

Species	**Rx (mol./m^3.s)**
CO	$2r_1 + r_2 + r_4$
H_2	$r_1 - 2r_3 + 3r_4$
CO_2	$-r_1$
CH_4	$r_3 - r_4$
H_2O	$-r_2 - r_4$
N_2	0
Total no of gaseous species	$r_1 + r_2 - r_3 + 2r_4$

The species created or used up are then estimated as a function of the gas velocity (V) and the rate of rate of formation (R_x).

The overall rate of gasification reaction is also dependent on the gasifier temperature at z-nth section and chemical equilibrium constants of individual gasification reactions

$$\frac{dT}{dz} = \frac{1}{v\sum n_x c_{p_x}}\left(-\sum_i ri\Delta H_i - v\frac{dP}{dZ} - P\frac{dv}{dz} - \sum R_x\, c_{p_x} T\right) \quad (3.47)$$

The first two equations (3.46) and (3.47) give a total of seven differential equations when all six gaseous species are considered. Equation 3.46 was used to generate six expressions for the molar concentrations of each of the six species considered in MATLAB code. However, the state of the gasifier is also described by the concentration of the gas species, the temperature and the superficial gas velocity so to complete the system of differential equations we still expressions for the pressure gradient and the gas velocity which are shown below

$$\frac{dv}{dz} = \frac{1}{\sum_x n_x\, c_{p_x} + nR}\left(\frac{\sum_x n_x\, c_{p_x}\, \sum_x R_x}{n} - \frac{\sum_i r_i\, \Delta H_i}{T} - \frac{dP}{dz}\left(\frac{v}{T} + \frac{v\sum_x n_x c_{p_x}}{P}\right) - \sum_x R_x c_{p_x}\right) \quad (3.48)$$

$$\frac{dP}{dz} = 1183\left(\rho_{gas\frac{V^2}{\rho_{air}}}\right) + 388.19v - 79.896 \quad (3.49)$$

These derivatives were solved using the ODE45 function in MATLAB which employs the Runge-Kutta scheme to evaluate the effect of several variables such as temperature and the final composition of the gas, pressure etc.

3.3 Non-Stoichiometric equilibrium model: the thermodynamic basis for the Gibbs reactor in HYSYS

The non – stoichiometric equilibrium model is solely based on minimizing Gibbs free energy of the system. Generally, the non- stoichiometric model can be applied for simulating various gasifier configurations as they are not dependent on the gasifier design and not limited to a specified range of operating conditions [95]. However, moisture content and elemental composition of the feed is required and can be obtained from the ultimate analysis data of the feed. This method is therefore well suited for solid fuels like biomass whose exact chemical formula is not definitely known [25].

The Gibbs Reactor in the HYSYS simulation package is employed when it is thought that multi-reactions are going to equilibrium at a fixed temperature and pressure or it is required to know the maximum possible conversion for multi-reactions at a given temperature and pressure. In the treatment presented here it is assumed that the reactions proceed in the Gaseous Phase. The treatment given below presents the necessary thermodynamic equations and also outlines the standard mathematical approach for the solution of the multi equations generated.

If multi- reactions are involved, in theory, it is possible to adopt the equilibrium constant based approach. However, such an approach requires the calculation of individual equilibrium constants and a mathematical method for solving equations based on equilibrium constants. The use of equilibrium constants also obviously assumes knowledge of the chemical reactions occurring in the simulated system. This knowledge is often not to hand and hence the approach outlined below is the only realistic approach that can be adopted.

The approach requires a knowledge of Gibbs Energies and an ability to calculate Chemical potentials. Some of the required data are held in a simulation package database and some of the quantities are calculated using the Property Package specified when the calculations are to be carried out. The multi-reaction Gibbs Reactor is based on the fact that, at equilibrium, the Total Gibbs Energy of the system is a MINIMUM

The Gibbs free energy, G_{total} for the gasification product which consists of *N* species where (*i=1.... N*) is represented as in the equation below:

$$G_{total} = \sum_{i=1}^{N} n_i \Delta G_{f,i}^{0} + \sum_{i=1}^{N} n_i \, RTln\left(\frac{n_i}{\sum n_i}\right) \qquad (3.50)$$

Here, $n_i \Delta G_{f,i}^{0}$ is the standard Gibbs energy of *i* species, *R* is gas constant. The solution of Eq. (3.50) for unknown values of n_i is approached to minimize G_{total} of the overall reaction considering the overall mass balance, though, non-stoichiometric equilibrium model does not specify the reaction path, type or chemical formula of the fuel, the amount of total carbon obtained from the ultimate analysis must be equal to sum of total of all carbon distributed among the gas mixtures and unburnt char [135]:

$$\sum_{i=1}^{N} a_{i,j} n_i \quad = \mathrm{A} \qquad (3.51)$$

Here $a_{i,j}$ is the number of atoms of the j element and A_j is the total number of atoms of j^{th} element in reaction mixture. The objective of this approach is to find the values of n_i such that the G_{total} will be minimum [136]. Thus, the Lagrange function (L) can be defined as

$$L = G_{total} - \sum_{j=1}^{K} \lambda j \left(\sum_{i=1}^{N} a_{i,j} n_i - A_i\right) \quad (3.52)$$

where λ is Lagrangian multipliers. The equilibrium is achieved when the partial derivatives of Lagrange function are zero. i.e.

$$\left(\frac{\partial L}{\partial n_i}\right) = 0 \quad (3.53)$$

$$\left(\frac{\partial L}{\partial n_i}\right) = \frac{\Delta G_{f,i}^0}{RT} + \sum_{i=1}^{N} ln\left(\frac{n_i}{n_{total}}\right) + \frac{1}{RT}\sum_{j=1}^{K} \lambda j \left(\sum_{i=1}^{N} a_{i,j} n_i\right) = 0 \quad (3.54)$$

The standard Gibbs free energy of each chemical species can be obtained by subtracting the standard enthalpy form the standard entropy multiplied by a specific temperature of the system [6]:

$$\Delta \bar{G}_{j,i}^0 = \Delta \bar{H}_{f,i}^0 - T\Delta \bar{S}_{f,i}^0 \quad (3.56)$$

Here $\Delta \bar{S}_{f,i}^0$ is the standard entropy of i species. According to first law of thermodynamics, the energy balance of the non- stoichiometric equilibrium model is [137].

$$\sum_{r=reactant} n_r \bar{H}_r^0(T_r) + Q_{loss} = \sum_{pt=product} n_p \, \bar{H}_{pt}^0\left(T_{pt}\right) + \Delta H \quad (3.57)$$

Chapter 4 Implementation of the developed mathematical Models for simulation of a biomass gasifier

4.1 Biomass gasification in a downdraft gasifier using HYSIS simulator and MATLAB solver

This Chapter describes the simulation of biomass gasification in a downdraft gasifier using Aspen HYSYS and MATLAB in detail. Process description, components, physical properties and block specifications are provided below.

4.2 HYSYS

HYSYS is a powerful engineering simulation tool created with respect to program architecture, interface design, engineering capabilities and interactive operation. The integrated steady state and dynamic capabilities, where the same model can be evaluated from either perspective with full sharing of process information represent a significant advancement in the engineering software industry. The software seeks to give appropriate mathematical models of a range of operations used in the process industries. These operations can be mathematically modelled in isolation or can originally or subsequently be combined to give a Process Flow Diagram (PFD). The algorithms used to carry out the mathematical modelling are not made available as part of the modelling although the methods used are often. Since there is no specific gasifier model ready for use in Aspen HYSYS there is the need to separate the entire process into different blocks that can be simulated with the existing models provided by Aspen HYSYS.

According to the features of Aspen HYSYS and the thermodynamic equilibrium model used for this simulation, the following assumptions were made in the current simulation of the biomass gasification process:

- Steady state operation
- Zero-dimensional
- Particle size is not considered
- Uniform temperature distribution for the biomass particle
- Pressure drops are neglected
- All elements that compose the biomass yield into C, H, O and N

- Tar formation is not considered
- Heat loss for the reactors are neglected
- Char is 100% carbon
- Equilibriums for all the reactions is reached in the gasifier

Biomass is fed as a non-conventional component into a reactor such as conversion or Gibbs reactor which converts the biomass into conventional components so that the ultimate and proximate analysis can be calculated. The downdraft gasifier is model based on reaction kinetics or minimization of Gibbs free energy using sets of reactors (see Figure 4.1).

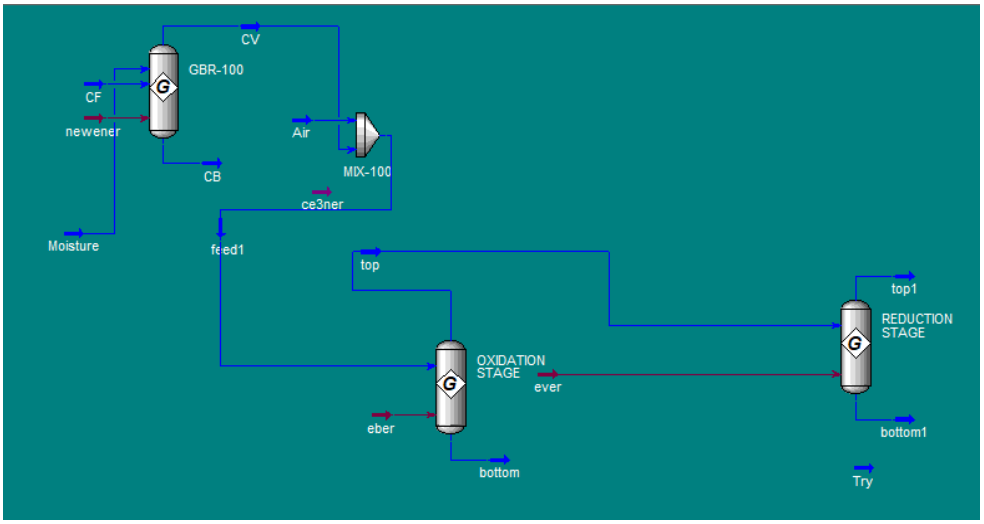

Figure 4.1 Flow sheet of biomass gasification process in a downdraft gasifier

The proposed model was developed following different steps which involved identification of the process phases, selection of the model blocks available in Aspen HYSYS for representing each phase, link between the selected blocks and setting of the operative parameters. Figure 4.1 shows the process flow from the pyrolysis to the reduction stage using the Gibbs reactors. Table 4.1 shows components identification with their names and types.

Table 4.1 Components identification, name and type

Component ID	Type	Component name	Formula
Biomass	Non-conventional		
C	Solid	Carbon graphite	C
CO_2	Conventional	carbon dioxide	CO_2
CO	Conventional	Carbon monoxide	CO
H_2	Conventional	Hydrogen	H_2
H_2O	Conventional	Water	H_2O
CH_4	Conventional	Methane	CH_4
N_2	Conventional	Nitrogen	N_2
O_2	Conventional	Oxygen	O_2

4.3 Physical property method

The basis of the modelling is to recognize that, in most cases, process operations are being carried out using a FLUID phase. In general processes can exist in one or more of 3 phases, GASEOUS, LIQUIDUS or SOLIDUS. Thus, the first requirement of the software is to have equations available that enable the calculation of Pressure (*P*), Temperature (*T*) and Volume (*V*). If one of these Intensive/Extensive properties is in input data, then the equation(s) can calculate/iterate the other properties. HYSYS makes an entire range of such equations available and attempts to give advice as to which of the equations is suitable for the fluid(s) that it is proposed for investigation. Thus, the specific fluids to be investigated must first be specified.

Initially, HYSYS makes a component list available; all components that are considered likely to take part in the operations can be specified at this initial point. If the desired component cannot be found in the database, then a hypothetical component can be made up whose properties will be estimated. Thus, the first requirement of HYSYS is that a component list has been specified. Once this is in existence, HYSYS requires that the equation(s) to be used in estimating the *P, V, T* data be specified. This does require some specialist knowledge of thermodynamics but many of the components specified have their *P, V, T* calculated using the thermodynamic EQUATIONS OF

STATE (EoS). This is an area of study that occupies many textbooks but one of the favoured equations is that due to PENG-ROBINSON (named after the originators).

This equation was made more 'accurate' in representing polar gases and liquids by incorporating the proposed changes due to Styrek and Vera. The final equation is referred (unsurprisingly) to as PRSV. This equation was used in this work because the presence of solid carbon was only acknowledged in one of the Unit operations (Pyrolysis) and its presence could be counted in the overall mass balance.

4.3.1 The Peng-Robinson Stryjek-Vera Equation

The Peng-Robinson Stryjek-Vera (PRSV) equation of state is a two-fold modification of the PR equation of state that extends the application of the original PR method for moderately non-ideal systems. It has been shown to match vapour pressures curves of pure components and mixtures more accurately than the PR method, especially at low vapour pressures. It has been successfully extended to handle non-ideal systems giving results as good as those obtained using excess Gibbs energy functions like the Wilson, NRTL or UNIQUAC equations. One of the proposed modifications to the PR equation of state by Stryek and Vera was an expanded alpha, "α", term that became a function of acentricity and an empirical parameter, κi, used for fitting pure component vapour pressures [138].

The PRSV equation of state which is formally similar to the cubic equation state proposed by Peng Robinson [139] and is represented as;

$$P = \frac{RT}{v-b} - \frac{a}{v^2+2bv-b^2} \tag{4.1}$$

where

$$a = (0.457235\ {R^2T^2}/{P_c})\alpha_i \tag{4.2}$$

$$\alpha_i = [1 + k(1 - T_r^{0.5})]^2 \tag{4.3}$$

and

$$b = 0.07776\ {RT_c}/{P_c} \tag{4.4}$$

$$k_i = K_{Oi} + k(1 + T_{ri}^{0.5})(0.7 - T_{ri}^{0.5}) \tag{4.5}$$

$$k_{Oi} = 0.378893 + 1.4897153\omega_i - 0.17131848\omega_i^2 + 0.0196554\omega_i^3 \quad (4.6)$$

ω_i = acentric factor (4.7)

Here ki is characteristic pure component adjustable parameter, k is a function of acentric factor and reduced temperature, K_{Oi} is a function of acentric factor, α_i is a function of temperature and acentric factor, P_c and T_c are critical pressures and temperature respectfully.

Once the component list and Property Package have been specified (see Table 4.2), HYSYS allows access to either modelling of a single operation, multiple operations in isolation from each other or combine operations into a Process Flow Diagram (PFD). HYSYS makes the Unit Operations that can be mathematically modelled available in an Operations Palette. This is a symbolic display of the various operations. Each identified symbol can then be loaded into the PFD as required. Operations can be combined by making their Inputs/Outputs common to each required operation. Each operation can have the operating conditions, stream flows and compositions input as appropriate. If any stream flows or conditions require iteration, then HYSYS will perform the operation to the accuracy specified by the user.

HYSYS will not make recommendations as to what changes should be made to conditions/flows. It will issue warnings about flow imbalances for both mass and energy. Through colour coded bars it will warn about what stage of the modelling is the progress. Red indicates most vital parameters, which have not been specified. Yellow indicates that some vital parameters have not been specified with indication of these parameters. The green colour indicates a successful simulation using the operations specified. Overall HYSYS is a powerful mathematical modelling tool that can be used to simulate whole processes. This makes it extremely popular in carrying out some Process Design. It is accepted that HYSYS carries out simulation through mathematical modelling and does not represent the use of actual physical modelling of the unit operations available.

Table 4.2 Block specification

HYSYS reactor family	**Scheme**	**Reactor use**	**Description**
Gibbs	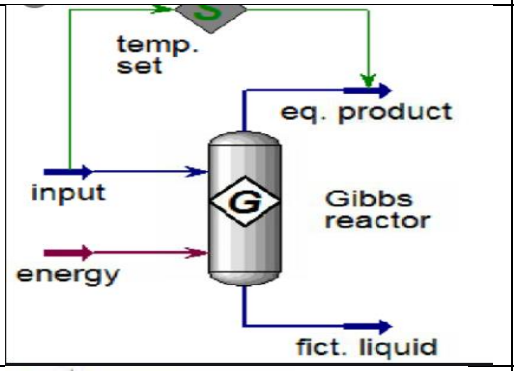	Pyrolysis oxidation/gasification	This reactor models the char gasification processes
Conversion	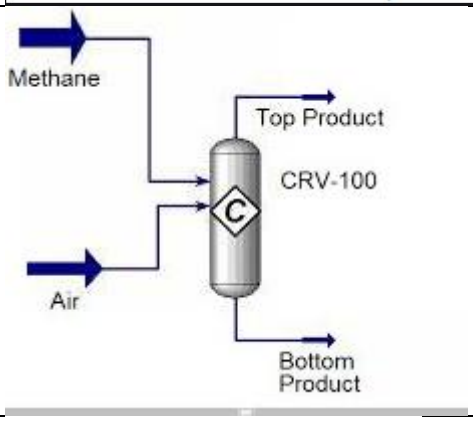	Pyrolysis	Models the decomposition of biomass which is a hypothetical component into a conventional constituent component.
Mixer		Inlet to the oxidation	Models the mixing of different streams inlet into a block
PFTR	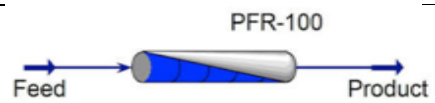	Reduction	

4.3.2 Process description

Biomass is a non-conventional component which is converted into conventional components by calculating its ultimate and proximate analysis. It was assumed that there are 3 important stages in the process that can be modelled. After biomass drying there is a pyrolysis stage where the Carbon, Hydrogen, Oxygen bearing volatiles can be taken into the vapour phase with an energy input. The products from the Pyrolysis stage can then be considered to enter an oxidation stage where the products from the Pyrolysis stage are mixed with oxygen-bearing air and oxidation takes place at elevated temperatures. Subsequently the products from this stage are considered to enter a

reduction stage where the proportions of Carbon monoxide, Carbon dioxide and Hydrogen are altered - particularly the amount of Carbon monoxide being reduced. This is usually then considered to be a useable Syngas.

In terms of appropriate Unit Operations available to mathematically model these Stages, the oxidation and reduction stages are considered to be dependent on reactions that go to chemical equilibrium although the reactions that can occur are not necessarily well defined. This is a classic thermodynamic problem where a Gibbs Free Energy Minimisation technique can be employed. In simple terms, this technique uses the composition, pressure and temperature of the stream entering a specified reactor system. The temperature and pressure of the exit product stream are also specified. The technique calculates the total Gibbs energy of the entering stream at the specified conditions and composition using a database of Formation Gibbs energies. The component Formation Gibbs energies are also available for the exit stream because the temperature and pressure of this stream are specified. To satisfy the thermodynamic requirement that the total input and output Gibbs energies are equal the technique has minimisation functions available e.g. Lagrange Multipliers.

Ultimately the Gibbs energies are equalised by finding the appropriate output component compositions that meet the requirement of equal input and output total Gibbs energies. Such a reactor is classically known as the Gibbs Reactor and such an operation is available in HYSYS. The oxidation and reduction stages were specified as GIBBS reactors and loaded into the HYSYS PFD. The pyrolysis section is more equivocal for modelling in the version of HYSYS used (Version 6). Basically, a mathematical statement of the amount of C, H and O forced into the vapour phase by application of energy is required. If this was to be modelled the biomass available from the drying process would need to be presented to the unit operation chosen and a phase change introduced into the model. The version of HYSYS used has no directly applicable model for this situation. The Pyrolysis was eventually presented using a conversion reactor. This is a reactor model that basically asks for a reaction; reaction stoichiometry and expected reaction conversion. This did not appear particularly promising in modelling the pyrolysis. The Biomass was fed to the reactor as $C_xH_yO_z$ where *x, y* and *z* were calculated from the ultimate analysis of the specific biomass (wood chips, wood pellets and rubber wood). A reaction was required rather than a

simple phase change, so it was assumed that water, H_2O, was formed in the reactor. However, the reactor conversion was specified as a small amount (usually <0.5%). This had the effect of making the bulk of the unconverted C, H and O appear in the output streams together with a small amount of water. These output streams could then be fed forward to the Gibbs Reactor simulating the oxidation stage. To make it easier to adjust the air flow into the oxidation stage; a HYSYS mixer was used to receive the outputs from the Conversion Reactor together with a specified air Input stream, HYSYS mass balances these streams and outputs them as a single stream which is taken as the input stream to the oxidation stage. By the nature of the reactor and the assumptions made about its operation it was not possible to add a moisture stream and expect realistic outputs.

Conversion reactor

It has been demonstrated that a basic model of a Gasifier based on a simple 3 zone model of the gasifier can be put together using Aspen HYSYS software. In one approach, the model takes 2 basic operations available in HYSYS, the Gibbs Reactor and the Conversion Reactor, and makes assumptions about the thermodynamic conditions in the 3 zones. The Conversion Reactor simply requires the statement of a reaction (or reactions) occurring in a reaction together with the expected conversion. This reactor in HYSYS was used which was developed by M. Bassyouni et al [140] in a paper where they tried to simulate the gasification of date palm waste. Based on the reaction conditions set and the expected conversion, the HYSYS operation gives an expected output. To use this operation a simple reaction of hydrogen with water with an extremely low conversion was set. The operating pressure and temperatures were set at values normally encountered in this stage of the operation. The effect of this operation was to, in effect, produce a pyrolysed stream for components in the vapour phase. A number of calculations were carried out with this reactor in place. As calculations proceeded, it became necessary for the moisture content of the input stream to be varied.

Gibbs reactor

In previous attempts at modelling and simulating the pyrolysis stage it has been assumed that the stage can go to thermodynamic equilibrium and the outputs calculated on this basis. In HYSYS there are 2 possibilities available for handling this situation,

an Equilibrium Reactor and a Gibbs Reactor. The Equilibrium Reactor requires the expected reactions within the reactor to be supplied. The Gibbs Reactor does not require this; it simply need the details of the input stream and the conditions of the stream. Based on Gibbs free energy calculations, the output stream compositions and conditions can be calculated. This approach has the advantage that no reactions occurring in the reactor have to be explicitly stated. When a moisture stream was added, this type of reactor was used to simulate the Pyrolysis stage. In various approaches to modelling the 2nd and 3rd zones, the Combustion (Oxidation) and Reduction zones have been modelled assuming thermodynamic equilibrium with, in some cases, various chemical reactions occurring, explicitly assumed. An approach has been adopted where both these zones have been assumed to approach thermodynamic equilibrium and have been simulated using Gibbs reactors where no explicit statement of the reactions occurring is required. The use of the 3 Gibbs Reactors allow Input and Output streams to be incorporated. For the first Gibbs Reactor (the Pyrolysis Stage) the addition of an extra Input Stream to the reactor allows to set amount of moisture to be added to the system as water and this can also be varied to allow greater or lesser moisture contents.

4.4 The Kinetic Reactor in HYSYS using Plug flow reactor PFR

Design equations exist (and can be derived) for a PFR (Plug Flow Reactor). The important design equations are:

$$\frac{V}{F_A} = \int_0^{z_A} \frac{dz_A}{-r_A} \tag{4.8}$$

and

$$\tau = C_{A_0} \int_0^{z_A} \frac{dz_A}{-r_A} \tag{4.9}$$

Here V is a reactor volume, F_A is a reactant flow rate, z_A is a reactant conversion, $-r_A$ is a reaction rate, τ is a space time and C_{A0} is an initial reactant concentration.

Conversion within the reactor depends on the relative rates of the reactions taking place. Reaction rate constants and a stoichiometric equation have to be supplied for each reaction. It is assumed the reacting stream passes through the reactor in Plug flow i.e. the stream passes through without mass or energy gradients and there is no radial

mixing. The conversion achieved by the reactor is computed by integrating the relevant differential equations and energy equations over the length of the reactor. Constant gas density for the reactants is not assumed and the density is rigorously corrected as the reactions proceed.

In the computation, it is necessary to supply the composition and flow rate of the inlet stream and the pressure and temperature of this stream. The reactor can be operated isothermally, adiabatically or the outlet temperature can be specified.

Integration in the reactor is carried out numerically, both the equations listed above can be solved for multiple reactions. The numerical integration requires difference equations to be solved within a series of calculation 'strips'. The larger the number of strips the nearer the differential equation solution is to the requirement of an infinitely small strip. HYSYS allows the number of strips to be specified up to a maximum of 10000. In the PFR used in the kinetic model the number of strips was usually set at 1000. No significant differences were observed when the longer calculations were carried out for 10000 strips. In HYSYS it is also necessary to specify a reactor length and reactor diameter, in the kinetic model these parameters were varied.

For a chemical reaction to be represented in HYSYS it normally requires the equation to be represented as a reversible reaction. Typically, the reaction would be:

$$aA + bB = cC + dD \tag{4.10}$$

where *A, B* are reactants and *C, D* are products. The terms *a, b* and *c, d* are the appropriate stoichiometric coefficients for the reaction. In HYSYS the reversible reaction would be represented as:

$$r_1 = k_1 C_A^a C_B^b \ldots - k_2 C_C^c C_D^d \tag{4.10a}$$

Here k_1 and k_2 are the Rate Constants for the forward and reverse reactions. These can be calculated using the ARRHENIUS EQUATION which takes the form:

$$k = Ae^{\frac{-E}{RT}} \tag{4.11}$$

where A is Collision Frequency Factor and *E* is the Activation Energy.

In HYSYS the rate constants are not normally specified directly. The required data are the Collision Frequency Factors, *A*, for the forward and reverse reactions and the Activation Energies *E* for the forward and reverse reactions. In terms of the data available, the form of the equation input required by HYSYS was not immediately available in the form required. The data available were for an equation of the form:

$$r = k_1\left(C_A^a C_B^b - \frac{C_C^c C_D^d}{K}\right) \tag{4.12}$$

The parameters are the same as previously defined: k is an equation Equilibrium Constant. The equilibrium constant can be written in an appropriate form:

$$K = \frac{k_1}{k_2} \tag{4.13}$$

The data available did not give values of *K* as a function of temperature and it was necessary to generate these data. This would require the generation of *K* values as a function of temperature for 4 reactions. No tables of *K* values vs Temperature were available for the 4 reactions. The first approach to obtaining the necessary values was to find values of ΔG_f^θ, the Standard Gibbs Free Energy of Formation, for all the species in the 4 reactions. These values were available at various temperatures from JANAF tables. Once these values were available, the following equation could be used:

$$\Delta G_T^\theta = \sum\left(\Delta G_f^\theta\right)_{Products} - \sum\left(\Delta G_f^\theta\right)_{Reactants} \tag{4.14}$$

Where ΔG_T^θ is the Standard Gibbs Free Energy Change for the reaction at a given temperature. Using these values for the given reaction we can use the Equilibrium Reaction Isotherm to find values of the Equilibrium ConstantK_a:

$$\Delta G_T^\theta = -RTlnK_a \tag{4.15}$$

The amount of data garnering required here was considerable. An alternative approach in generating values of the equilibrium constant was to use the Integrated Gibbs-Helmholtz Equation. The form used assumed that the Standard Enthalpy Change for a given reaction was independent of temperature. If this assumption is made, then the Gibbs-Helmholtz can be written as:

$$\frac{\Delta G_{T_2}^\theta}{T_2} - \frac{\Delta G_{T_1}^\theta}{T_1} = \Delta H^\theta\left(\frac{1}{T_2} - \frac{1}{T_1}\right) \tag{4.16}$$

Thus, if the value of the Standard Gibbs Free Energy Change at 298 K is known then it is possible to generate values of the Standard Gibbs Free Energy Change at temperature T_2 provided that the value of ΔH^{θ} at 298 K, which is assumed independent of the temperature, is known.

Using these generated values, equation (4.16) can be used to generate values of the Equilibrium Constant over a range of temperatures (see Table 4.3). This was done using values of ΔG^{θ}_{298} and the following data obtained for 4 reactions proposed to model the reduction stage within the Biomass Gasifier.

Table 4.3 Values of equilibrium constant obtained at different temperatures

	Kp			
Reaction				
Temperature (^{0}C)	400	800	1200	1600
1	5.03 E-14	0.0092	52.16	3928.98
2	7.26 E-11	0.0272	19.62	526.75
3	361354.941	4.69	0.11	0.02
4	2.01 E-16	0.0058	178.22	31220.90

The value of K_a is represented in terms of partial pressures as K_P, the 4 columns are for data at the specified temperatures.

The 4 reactions referred to are:

Reaction 1 (Boudouard)

$$C + CO_2 \leftrightarrow 2CO \tag{4.17}$$

Reaction 2 (Water Gas)

$$C + H_2O \leftrightarrow CO + H_2 \tag{4.18}$$

Reaction 3 (Methanation)

$$C + 2H_2 \leftrightarrow CH_4 \tag{4.19}$$

Reaction 4 (Steam Reforming)

$$CH_4 + H_2O \leftrightarrow CO + 3H_2 \tag{4.20}$$

With these data available, the data required for representing the kinetics in HYSYS could be calculated. Data in Table 4.4 was available to calculate k_1.

Table 4.4 Collision factor and Activation energies for the Reactions 1-4

Reaction	**Ai (1/s)**	**Ei (kJ/mol)**
1	36.16	77.39
2	15170	121.62
3	4.189×10^{-3}	19.21
4	7.301×10^{-2}	36.15

Once a value of k_1 is calculated, then equation (4.13) together with the calculated values of the equilibrium constant can be used to calculate k_2. Once the appropriate values of k_2 had been calculated it was necessary to use these values, and the corresponding temperatures, to calculate values of A and E for the reverse reaction.

This was done using equation (4.11) and taking logs of both sides giving an equation

$$\ln(k_2) = \ln(A) - \frac{E}{RT} \qquad (4.21)$$

A plot of k_2 vs $1/T$ yield a slope equal to $-E/R$ and intercept of ln (A). Values of E and A can then be found for the reverse reaction and all the data requirements of HYSYS are then fulfilled.

The values calculated are presented in Table 4.5

Table 4.5 Calculated values for K_1 and K_2 at different temperatures

Reaction 1				
Temperature (K)	400	800	1200	1600
K_1	2.82×10^{-9}	3.2×10^{-4}	0.0155	0.1076
K_2	56259.05	0.0348	2.97×10^{-4}	2.74×10^{-5}
Reaction 2				
Temperature (K)	400	800	1200	1600
K_1	1.99×10^{-12}	0.0002	0.0771	1.623
K_2	0.027	0.0064	0.0039	0.0031
Reaction 3	400	800	1200	1600
K_1	1.3×10^{-5}	2.33×10^{-4}	6.11×10^{-4}	9.88×10^{-4}
K_2	3.59×10^{-11}	4.98×10^{-5}	5.55×10^{-3}	0.059
Reaction 4				
Temperature (K)	400	800	1200	1600
K_1	1.39×10^{-6}	3.18×10^{-4}	1.95×10^{-3}	4.82×10^{-3}
K_2	6.91×10^{9}	$5.48\ 10^{-2}$	1.09×10^{-5}	1.54×10^{-7}

The corresponding values of *E* and *A* are given in Table 4.6.

Table 4.6 Activation energies for the reactions 1- 4

	Reaction 1	**Reaction 2**	**Reaction 3**	**Reaction 4**
E (J/mol)	77390	121620	19210	36150
E’ (J/mol)	-95084	-9486	94057	-17003
A (1/s)	36.16	15170	4.189×10^{-3}	0.073
A’ (1/s)	2.15×10^{-8}	1.49×10^{-3}	68.95	4.35×10^{-13}

Here

E: Activation energy of the forward reaction

E’: Activation energy of the reverse reaction

A: Frequency factor of the forward reaction

A’: Frequency factor of the reverse reaction

These values were used during modelling in HYSYS software.

It is worth noting that for Reactions 1, 2 and 4 the activation energies for the reverse reactions are negative i.e. the rate constants for the reverse reactions decrease with temperature. One of the problems related to HYSYS when using the kinetics to simulate the reduction stage is that little or no methane gas is formed. If data is examined, it can be seen that Reaction 3 is an equation representing methane formation. The rate constants for the forward reaction (methane formation) are very low over the temperature range considered. The rate constants for the reverse reaction are greater than for the forward one at higher temperatures, this mirrors the conditions encountered in the gasifier. These results are consistent with the values of the equilibrium constant. The other reaction where methane is involved is Reaction 4. At higher temperatures, the forward rate constant is higher than the reverse one. This would indicate that any methane would be favoured to disappear at higher temperatures. HYSYS indicates that this is so. The simulation of the reduction stage cannot be carried out in HYSYS simply through kinetics and mass balancing. Simulation is carried out using the simulation of an actual operation, thus, a Plug Flow Tubular Reactor was used in calculations.

4.5 Double air stream model

Previously for single stream operation the approach adopted had assumption that the system could be considered in 3 sections; a pyrolysis section, a combustion section and a reduction section. The pyrolysis section was simulated using a conversion reactor where the components were vaporised prior to entry into the combustion section. The combustion and reduction sections were simulated using Gibbs reactors i.e. it was assumed that both these sections reached thermodynamic equilibrium. In this case, air stream was directly input to the Combustion Section.

For using HYSYS to simulate the air entering as a double stream, the simulation of the Pyrolysis section had to be changed. Of the reactors available, HYSYS require the reactions occurring to be specified. The Gibbs Reactor balances the input and output Gibbs Energies without requiring the designation of specific reactions, this means that the output streams are considered to be at equilibrium. The original Conversion Reactor was replaced by another Gibbs Reactor and the air stream was split. One part of the stream was input to the Gibbs Reactor that was designated as the first (Pyrolysis)

section. The other part of the stream was input to the Gibbs Reactor that was simulating the combustion section.

The addition of the 3rd Gibbs Reactor influences the simulation. The simulation calculates possible reactions in the presence of the new air stream, and these reactions are not just due to the presence of this stream, but other reactions are possible for the Carbon, Hydrogen and Oxygen entering as the Eucalyptus Wood. In fact, the simulator indicated that as well as hydrogen, carbon monoxide and carbon dioxide are being formed and there was considerable methane. However, the overall simulation stream exiting the reduction section indicates figures close to experimental results provided by Martinez et al [69] and the simulated system operates within the temperature regions reported experimentally.

It is noteworthy that the split stream of air does not affect composition of the stream leaving the combustion section. This composition does not depend on the flow ratios of the 2 air streams. However, this ratio does affect the composition of the stream leaving the 1st Gibbs Reactor that has been added. For a system based on data given by Martinez et al [69] with the temperatures set within the experimentally measured ranges, typically for a 50% ratio (1:1), the output stream for the 1st Gibbs Reactor is shown in Table 4.7. The air ratio of 16Nm^3/h and temperatures 450^0C and 500^0C are used for G1 and G2 respectively to test for the effect of the split air stream.

Table 4.7 Products from Pyrolysis and Combustion reactors at AR = 50%

Component	**G1**	**G2**
H_2O	0.078	0.0567
CO	0.1345	0.1668
CO_2	0.2166	0.1252
C	0	0
H_2	0.0592	0.1575
CH_4	0.1506	0.0047
O_2	0	0
N_2	0.4212	0.4831

If the ratio is changed to 85% (first stream/second stream) then the results become as presented in Table 4.8.

Table 4.8 Products from Pyrolysis and combustion reactor when air ratio is changed to 85%

Component	**G1**	**G2**
H_2O	0.0403	0.0567
CO	0.0757	0.1668
CO_2	0.2118	0.1252
C	0	0
H_2	0.0764	0.1575
CH_4	0.0800	0.0047
O_2	0	0
N_2	0.5164	0.4831

The output from G2 (the Combustion Section) is the same for both cases – this must be the case because the output from G2 for both cases is based on the calculation of products based on the same overall air flow (Stream 1 plus Stream 2). As has been stated, the final stream from the Reduction Stage gives simulated results close to the experimental results reported by Martinez.

4.6 Numerical simulation of a biomass gasifier using codes in MATLAB

MATLAB is a high-performance language for technical computing which integrates computation, visualisation and programming in an easy-to-use environment. The typical uses of MATLAB include Algorithm development, Math and computation, data analysis, scientific and engineering graphics, modelling and simulation etc. MATLAB is among the most suitable environments for the creation of simulation models. It allows the implementation of various data types; it also provides the right environment for model formation and provides a library for the solution of various mathematical tasks for example calculating a system of differential equations. MATLAB provides a refined input/output graphical interface for the creation of simulation environments.

The idea for a complex model for the gasification of biomass is derived from the initial process analyses, which was suggested as a synthesis of elementary process models. The synthesis is possible because of the basic thermal exchange between biomass and gas elements. It is based on the accumulation of heat which is relative to the difference between input and output heat flow created by the source or heat consumption. In the case of elementary models, the following models are described: pyrolysis model,

oxidation model and reduction model. The three models include thermal breakdown of biomass, release of gasses and the burning of the solid by product [141].

4.6.1 Procedure for numerical simulation

The biomass gasifier is divided into four stages. Five files was created in MATBLAB for the Input data, Pyrolysis zone, Oxidation zone, Energy balance and Reduction zone (see codes in the Appendix section). First, the initial input values for both the constant and variable parameters for the feedstock to be used were determined, initial temperatures in all cells were set. The molar fraction of the hydrogen, carbon and oxygen were determined and process models were independently implemented with codes in a MATLAB environment as individual m-functions.

Input file

Here, a function is declared that accepts all the input data. This file describes input data for all sections of the gasifier such as feed stock, pyrolysis, oxidation and reduction zones. Within the feed stock section, the type of wood and the outside temperature is specified. In the pyrolysis and oxidation sections of input file, the conductivity of the walls, measurements of the zones are specified. The reduction zone of this section specifies the diameter of the chamber and the temperature.

Pyrolysis zone file

The input function for this file is called the pyro. It contains the molar masses of the carbon, hydrogen and oxygen, mass flow rates of ash, moisture and fixed carbon in the feed stock. The equation derrived asnd based on the assumptions made and mass balance equations are specified here. The input data from the imput file is specified in this pyrolysis file. With data from the input file, assumptions and mass balances, the product amounts of CO, CO_2, H_2, H_2O, CH_4 and C_2H_2 and char are calculated**.**

Oxidation zone file

The input function for this file is the ‘oxi’ wih the moles of oxygen and nitrogen entering the zone, masses of products from the pyrolysis zone. The input function of the pyrolysis file ‘pyro’ is also specified here. The overall composition and temperature in this zone is obtained through mass and energy balance; the energy balance is a function of the initial temperatures, dimensions of oxidation zone,

conductivity of the walls of the oxidation zone, product amounts from pyrolysis zone etc. This gives the temperature leaving the oxidation zone and entering the reduction zone including products from the oxidation zone which are CO, CO_2, H_2, H_2O, CH_4 and C_2H_2 and char.

Reduction zone file

The Reduction zone is the final stage of the biomass gasifier where the pressure, temperature, velocity and molar concentrations of the gas constituents from the pyrolysis zone and oxidation zone were processed and ODE 45, which is a code in MATLAB to solve differential equations, was used to integrate their respective functions. Then the gas compositions, pressure and temperature in the oxidation zone were detemined along the depth of the oxidation chamber and the final wet and dry gas compostions were produced. The algorithm was written and modified accordingly in MATLAB in order to generate required outputs.

Energy balance calaculation file

The energy balance evaluates the temperature at the exit of the oxidation zone and entry to the reduction zone from the energy balance equation across the pyrolysis and oxidation zones. The temperature is then solved by Newton-Raphson Method code, which is for solving non linear equations for number of variables.

Chapter 5 Modelling Approach and Data Used in Numerical Simulations on Properties of Various Biomass Feedstock

5.1 Introduction

This Chapter describes the simulations carried out for validating the models developed in this study for various biomass feedstock utilized. Mathematical modelling of gasification is a very complex. As described above MATLAB and ASPEN HYSYS software were deployed to obtain numerical results. Kinetic and equilibrium models have been programmed in HYSYS and MATLAB to describe operation of the downdraft gasifier.

Five feeds, namely wood chips, wood pellets, rubber wood, palm oil fronds and eucalyptus woods were used as biomass in the downdraft gasifier. These woody biomass feeds were chosen as they have been investigated by other researchers and experimental and theoretical results exists for comparison. For each of these feeds, the effects of a number of parameters are investigated theoretically and each of the output results is compared with the theoretical and/or experimental results published by other authors. Biomass feedstock is characterised in order to evaluate their suitability for thermochemical conversion process operations. The analysis and methods required to find the characteristics of the feedstock are ultimate, lignocellulosic, proximate, caloric value, pH and thermogravimetric. Proximate analysis is carried out to identify the moisture content, volatile matter, fixed carbon content of the feedstock and ash content. Ultimate analysis is normally carried to determine the elemental composition of carbon, hydrogen, nitrogen, sulphur and oxygen. The feedstocks with low sulphur and nitrogen content produces low non- environmental gases during the thermochemical conversion process [142]). Carbon, hydrogen and oxygen are the main constituents of the carbohydrate chains in an organic structure and their percentages affect the calorific value of the feedstock. The heating value of a biomass fuel may be reported on either the higher heating value (HHV) or lower heating value (LHV) property. The higher heating value indicates the heat release upon combustion of fuel with the original and generated water in the condensate state while the lower heating value is based on gaseous water as the product [143].

5.2 Interactive components in HYSYS modelling

When using the PFD approach in HYSYS simulations, the accuracy of results depends on the accuracy of data used. Component data is normally supplied in HYSYS through an appropriate property package. This requires the components present in the PFD to be listed. HYSYS retains a pure property data base but normally uses predicted interactive properties for mixtures. The predicted properties are crucially determined by the predictive equations employed. In the case of the biomass gasifier simulation it was considered that the bulk of the material would exist in the vapour/gaseous phase. This is pre-determined by HYSYS based on the components encountered in the mixtures and the conditions under which simulation will take place (e.g. high or low temperatures and pressures). Under the conditions, and components that were to be simulated, the most effective predictive equation was the original equation of Peng-Robinson as modified by Styrek-Vera, PRSV. Essentially, this equation will account for molecular interactions in the vapour phase and make appropriate adjustments. Corrected volumes and corresponding compositions for stated temperature and pressure will be generated. Basically, HYSYS recognises the existence of a solid phase as dictated by the pure component properties at a given temperature and pressure but does not calculate any interactive parameters. This is considered to be acceptable for the systems investigated and the phases likely to be present. If solid phase interactions were required to be simulated as well, then a different property package would have to be used but this would be inappropriate for gaseous phase components which do dominate the systems to be simulated. Once HYSYS has been supplied with the property package to be used the various unit operation algorithms then use the property package to supply the necessary properties.

In the software, the biomass fed into the gasifier is characterised by the ultimate and proximate analysis and by its chemical formula as it is classified as a non-conventional stream [118]. In Aspen HYSYS a combination of two or more blocks was necessary to use for modelling the downdraft gasifier. The gasification process was modelled through a combination of Gibbs/ Conversion blocks or Gibbs and PFR blocks. Gibbs block calculates chemical equilibrium and phase equilibrium by minimizing the Gibbs free energy of the system. A Mixer block was used to mix the products of the pyrolysis with the flow of air.

5.2.1 Process flow diagrams

The process flow diagram (PFD) shows the sequence of flow through a system through the various equipment (such as piping, instrumentation, and equipment design) and details of the stream connections, stream flow rates and compositions and operating conditions through the plant layout.

The Pyrolysis section of the gasifier was initially presented using a CONVERSION REACTOR model because the pyrolysis stage converts a solid phase to a vapour phase without notable change of composition. This type of reactor normally has 3 mass flow streams attached to it: an Input Stream and 2 Output Streams. In such the reactor, the temperature and reaction stoichiometry are specified together with a stated conversion. The temperature does affect the reaction through a polynomial equation within the algorithm that allows the stated conversion to be varied with temperature. In the PFD, (see Figure 5.1), the Input Stream CF is input as the biomass using a formula of the type $C_xH_yO_z$. The components input was organised from the HYSYS database as C, H and O. This sort of operation requires two Output Streams that allow the existence of a gas phase, Stream CV and a liquid or gas solid phase CB.

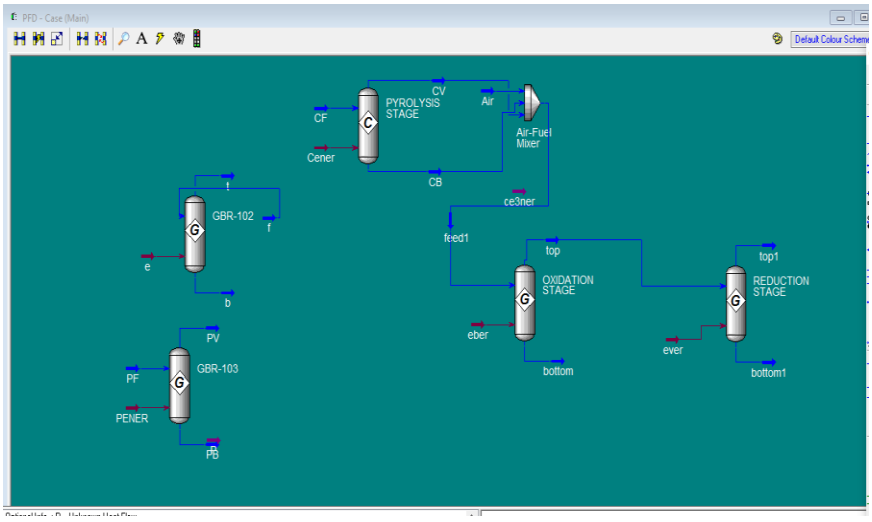

Figure 5.1 Process flow diagram with conversion and Gibbs reactors and Mixer

In Figure 5.2, Feed 1 and air goes through the mixer which mixes the various streams; the air and the pyrolysis products. The products from the mixer then enters the Oxidation Stage as an input to a HYSYS Gibbs Reactor. Such the Reactor requires at least 2 Outputs which can be a Gas Output Stream and a Liquid or Solid Output stream.

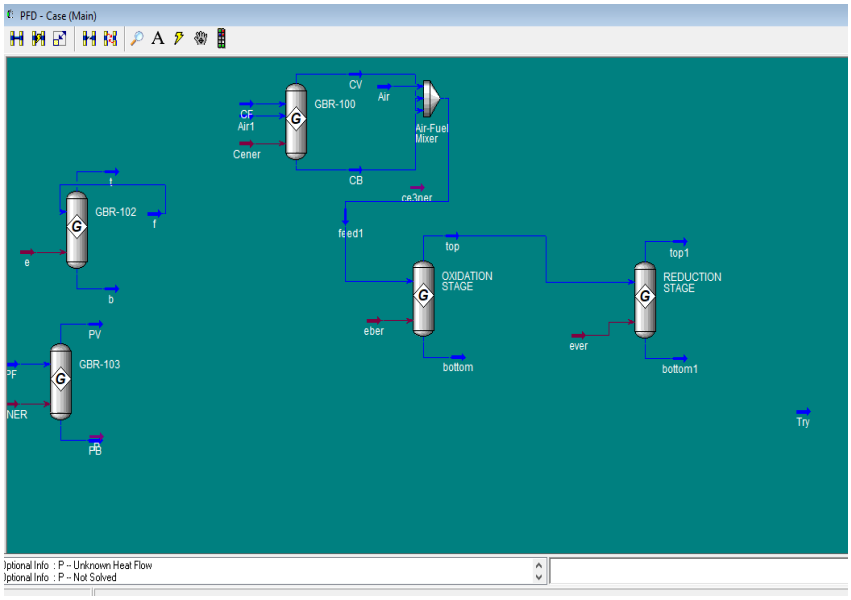

Figure 5.2 Process flow diagram with Gibbs reactors and mixer

In this case, the gaseous output is the top stream and HYSYS calculated all the output as gaseous fractions, so all the mass enters stream top. This stream then becomes the Input Flow Stream to the reduction Stage which is either the plug flow reactor (PFR) or Gibbs reactor (the 2nd Gibbs Reactor) which again requires 2 Output stream which are top1 and bottom1 as shown in Figure 5.3.

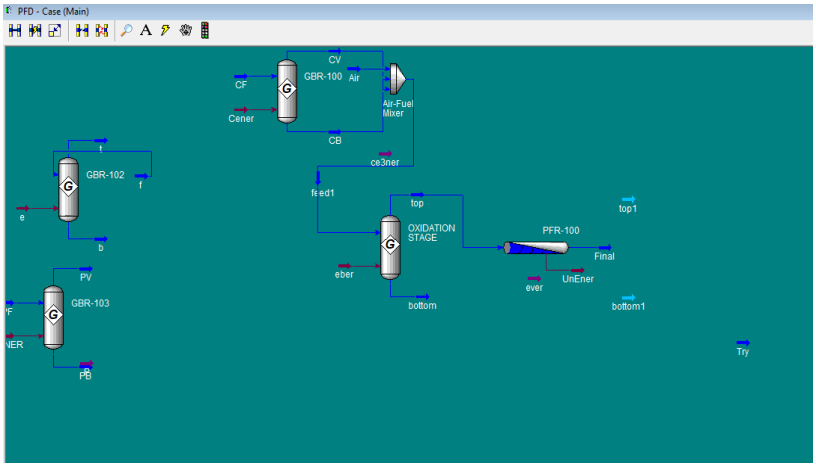

Figure 5.3 Process flow diagram with Gibbs reactors and mixer and Plug flow reactors

All the Output is in the gas phase, so the output results required are those for Output Stream top. Both Gibbs Reactors also have Energy streams. These can be included in the reactor calculations and they have the effect of allowing Isothermal operation of the reactor. HYSYS does the necessary energy balancing to maintain the temperature constant within the reactor.

5.3 Principles of the gasifier operations for modelling in MATLAB

The downdraft gasifier was presented as three distinct reaction zones: (1) drying and pyrolysis, (2) oxidation and (3) reduction. The drying and pyrolysis zone is where the moisture in the biomass is released as steam, and where the ligno-cellulosic material that is the biomass thermally decomposes. It is during this decomposition phase that the lingo-cellulosic material is transformed into gaseous volatile species, mainly comprised of CO, CO_2, H_2, CH_4, C_2H_2, as well as char (carbonised biomass) and more steam. These substances then move to the oxidation zone where air is introduced, and partial combustion of the volatile species and char takes place. The pyrolysis products are now transformed into the oxidation products, which mostly consist of CO, CO_2, H_2, CH_4, N_2, steam, char and tar. The heat generated by the combustion reactions in the oxidation zone is used to drive the reactions in the pyrolysis zone and the reduction zone.

In Matlab code modelling the following stages can be distinguished:

- ✓ Gasifier was divided into 3 zones; pyrolysis, oxidation and reduction zones.
- ✓ From ultimate chemical analysis data, moist biomass can be represented as a sum of the volatile, non-volatile and water components.
- ✓ Mass balance equations are used to calculate the amounts of pyrolysis and oxidation products.
- ✓ A single energy balance equation is then applied across both zones (as a single pyro-oxidation zone) to calculate the reactor temperature at entry into the reduction zone.
- ✓ Once the molar flow rates have been obtained from solving the mass balances, they are used to solve the energy balance across the combined pyro-oxidation zone for the core reactor temperature (T) at entry to the reduction zone.
- ✓ A finite-rate kinetic model is employed, which considers the four main reactions taking place in the reduction zone.
- ✓ A system of ordinary differential equations is made up by the mass and energy balance equations, the ideal gas law and the Ergun equation
- ✓ The system of derivatives was solved using the ODE45 function in MATLAB

The MATLAB model results were tested against the published experimental results using the corresponding biomass properties, gasifier specifications and operating conditions

5.4 Biomass feedstock modelled

Various types of biomass used in this study and their characteristics are discussed in this section.

5.4.1 Wood chips

The quality of wood chips is determined by water content, tree species, the quality of wood itself, particle size, the amount of dirt such as stones, soil, plastics etc. (see Table 5.1 and Fig. 5.4). These parameters have an important influence on bulk density, caloric value, and share of ash. For production of wood chips, only low quality and small diameter round wood, forest residues and wood wastes are used. Typical areas of application for wood chip plants are agricultural and wood processing companies, commercial companies, apartment buildings and public buildings as well as micro and local heating systems. The biggest disadvantage of wood chips is their lower energy density, which is caused by the lower bulk density of this type of fuel. All of this will influence the size of storage needed**.** Wood chips have a sub-rectangular shape with a length of between 5 and 50 mm and a low thickness compared to other dimensions.

Table 5.1 Characterisation of wood chips

Biomass: Wood chips	
Proximate analysis % wet basis	
Moisture content	7.36
Volatile matter	75.00
Fixed carbon	17.30
Ash	0.34
Ultimate analysis (% dry basis by mass)	
Carbon	48.00
Hydrogen	6.00
Oxygen	46.00
Consumption	3.1 kg/h
Equivalence ratio	3.00

Figure 5.4 Chipped woody biomass in the form of pieces with a defined particle size produced by mechanical treatment with sharp tools such as knives

5.4.2 Wood Pellets

Wood pellets for non-industrial use normally have a diameter 6 mm and a length of 1-4 cm, see Figure 5.5. Besides this type of wood pellet, industrial pellets can also be bought on the market. The quality of industrial pellets is lower; they have a diameter of 6, 8 or 10 mm; their ash content can be over 3 percent. Mechanical durability is not an important issue. For normal and efficient operation of smaller boilers, use of standardized and certified pellets is recommended.

Figure 5.5 Light and dark wood pellet

The colour of pellets does not determine the quality classes of pellets. Darker colour (see Figure 5.5.) is caused by proportion of bark and tree species. Usually in this case the ash percentage is higher.

Small particles in the bag, see Figure 5.6, are usually caused by lower mechanical durability of pellets. In some cases densified biofuel is used which is made as wood pellets from pulverised woody biomass with or without additives, usually in cylindrical form, of various lengths but typically 5 to 40 mm. Typical characteristics of wood pellets as a fuel are presented in Table 5.2.

Figure 5.6 Wood pellets with particles

Figure 5.7 Densified biofuel made from pulverised woody biomass with or without additives

Table 5.2 Characterization of wood Pellets

Biomass: Wood pellets	
Proximate analysis % wet basis	
Moisture content	8.55
Volatile matter	82.88
Fixed carbon	8.00
Ash	0.57
Ultimate analysis (% dry basis by mass	
Carbon	50.00
Hydrogen	6.67
Oxygen	42.76
Consumption	2.9 kg/h
Equivalence ratio	2.8

5.4.3 Eucalyptus Wood

Eucalyptus wood species are mostly from Australia but grown extensively worldwide as short rotation hardwoods for various products and ornaments. Eucalyptus is the most valuable and widely planted hardwood in the world. Eucalyptus is known to contain major amounts of polyphenols of both condensed and hydrolysable ranges [144]. The Eucalyptus wood usually cut in cylindrical shapes with dimensions less than 6 cm in both diameter and height; see Figure 5.8. The moisture and heating value of the wood are shown in the proximate and ultimate analysis, see Table 5.3

Figure 5.8 Eucalyptus wood chips [144]

Table 5.3 Characterization of Eucalyptus wood [144]

Proximate analysis (wt %)	
Ash	1.87
Volatile	83.02
Fixed carbon	15.02
Ultimate analysis (wt %)	
Carbon	44.31
Hydrogen	5.63
Nitrogen	3.23
Sulfur	0.91
Oxygen	44.05

5.4.4 Rubber wood

The rubber tree is the one of most important biomass in Thailand which had a plantation area of about 2.72 million ha in 2000 [145]. The main product of rubber tree is natural rubber latex, which Thailand produces about one third of the world's natural rubber. Rubber tree is cut when it is 25-30 years; about 3–4% of the rubber growing area is cut down for replanting annually. Every year, about 14.7-19.6 million tons of rubber tree are cut down. The rubber wood becomes raw material for sawmills and wood product factories, e.g., furniture, kitchenware and wooden toys. By-products from rubber wood processes are sawdust, wood shaving and rubber wood chips which have potential use as raw material for gasifier. The properties of rubber wood residues were analysed in term of moisture content, heating value, proximate analysis and ultimate analysis. The typical analysis results for rubber wood are shown in Table 5.4.

Table 5.4 Characterization of rubber wood [145]

Proximate analysis (wt %)	
Volatile matter	80.10
Fixed carbon	19.20
Ash	0.70
Ultimate analysis (wt %)	
Carbon	50.60
Hydrogen	6.50
Nitrogen	42.20
Moisture content (% by mass)	16.00
HHV	19.6 MJ/kg

5.4.5 Palm oil Fronds

Malaysia is one of the major planters of oil palm trees in the world. As the main exporter of palm oil, the country has significantly large plantation areas. There are

more than 4.5 million hectares of oil palm plantations in Malaysia. Almost all the parts of oil palm trees, see Figure 5.9, are commercially utilized, mainly in energy and manufacturing sectors. However, oil palm fronds (OPF) have very limited usage. The contribution of oil palm fronds (OPF) constituted 46.71% (97 million tons per year) of the total oil palm wastes. Currently, fronds are dumped in the plantation site without significant contribution except for the use of erosion control and soil conservation [146]. Thus, OPF can be used as alternative energy source to produce producer gas through gasification. Recently, high temperature air gasification of biomass waste has received high attention because of the improvement gained in the quality of producer gas and reduction of tar compared to that of the conventional process [147].

Figure 5.9 Oil Palm Tree [148]

Figure 5.10 shows illustration of an OPF. It mainly consists of the hard and fibrous petiole and the leaflets. The average bulk density of OPF was reported to be about 700 kg/m^3 and the weight of each frond was between 15 and 20 kg depending in the age of the palm tree. Characteristics of OPF as a fuel are presented in Table 5.5.

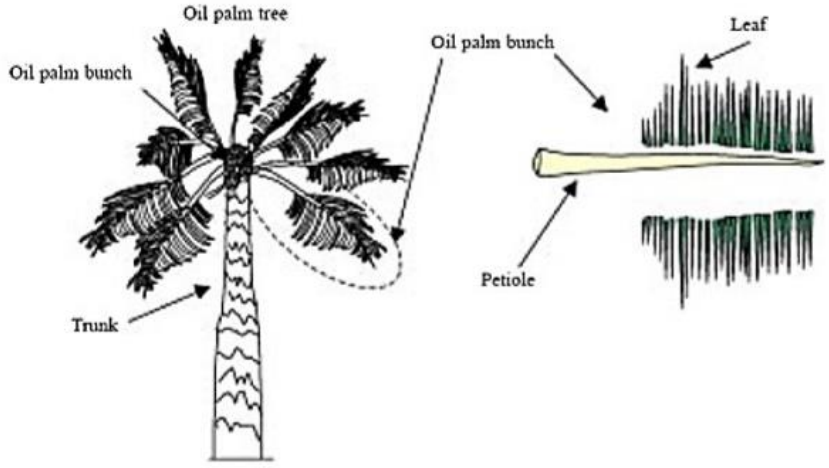

Figure 5.10 Oil palm fronds [148]

Table 5.5 Characteristics of oil palm fronds [148]

Proximate analysis (% dry basis)	
Volatile matter	83.50
Fixed carbon	15.20
Ash	1.30
Ultimate analysis (% dry basis)	
Carbon	44.58
Hydrogen	4.53
Oxygen	48.80
Nitrogen	0.71
Sulfur	0.07
HHV (MJ/kg)	17.00
Moisture content (wb)	0.10

Chapter 6 Description of Obtained Numerical Results and Their Discussion

6.1 Introduction

This chapter presents the results obtained from modelling the gasification of various biomass feedstock such as wood chips, wood pellets, rubber wood and Eucalyptus wood and oil palm fronds.

The robustness, performance and utility of mathematical models can be estimated by comparing the numerical results with experimental data obtained under similar process parameters. In the present models, the governing process parameters are moisture content and air to fuel ratio or equivalence ratio and temperature of the reaction zone. The composition of the product gas is mainly determined by the chemical composition of the biomass, moisture content and the operating conditions. Therefore, based on similar process parameters and similar biomass chemical composition, robust mathematical models should yield amounts of products identical to that in experimental data. The composition of the product gas mainly consists of methane, hydrogen, carbon dioxide, and water. These final producer gas compositions are mainly expressed on dry basis that is, without the water content.

Theoretical results obtained in this Chapter are compered to experimental data published by various authors.

6.2 Modelling and simulation results of biomass using MATLAB

Mathematical model is developed to simulate the behaviour of a downdraft gasifier operating in the steady state. To validate this model, predicted results from this model is tested against published experimental data. The model is developed to describe processes in each of the three reaction zones of the reactor, which are pyrolysis, oxidation and reduction zones. The analysis in the pyrolysis and the oxidation zones is based on the chemical equilibrium whilst the reduction zone processes are considered based on finite rate chemical kinetics. The model is tested against published experimental results from literature, namely by Chawdhury et al. [29] obtained from the design and testing of a small downdraft gasifier JRB-1 at Durham University, UK. The design of the JRB-1 gasifier was based on the Fluidyne gasifier. It slightly

modified for simplicity and to give more flexibility in operation. The capacity of the model was 6-7 kW (thermal output). The model was also tested against the experimental data by Matthew et al [149] obtained from the design of an inexpensive biomass downdraft gasifier run on pine wood chips. The gasifier was constructed from commercially available stainless-steel vacuum flask-style thermos bottle (see Figure 6.1). The model was compared with these experimental data as the gasifiers run on wood chips and operate within the same range operating conditions. The JRB-1 also runs on wood pellets.

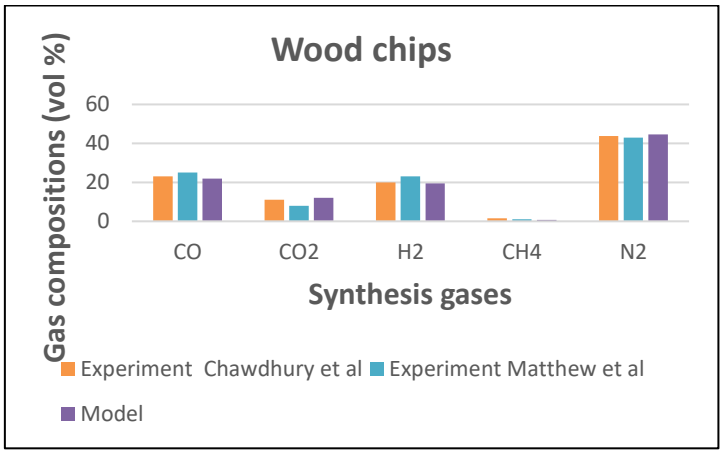

Figure 6.1 Comparison of producer gas composition predicted by the developed model against experimental data

The temperature of the reaction zone in the JBR-1 gasifier is within 950-1150 ^{0}C, the primary air flow rate is 0.0015 m^3/s and the biomass moisture content is about 7.36%. The adiabatic temperature of the inexpensive inverted downdraft gasifier by Matthew et al [134] is around 673-952K with the 10% moisture content. The calculated temperature of the model is 986 ^{0}C, the moisture content of the wood chips is 10% and the air entering the oxidation zone is 0.0127 mol. The model produced reasonable agreement with the experimental results for CO, CO_2, H_2 and N_2 which seems to agree more with the experimental result of Chawdhury et al [24]. CH_4 was under-predicted under these conditions since at higher temperatures the endothermic reaction($CH_4 + H_2O \leftrightarrow CO + 3H_2$) favours the formation of CO and H_2 and the depletion of CH_4.

Further validation was carried out by testing the model against the experimental results of Barrio et al [8] who performed gasification experiments with wood pellets as feedstock with a stratified downdraft gasifier operating at 750 ^{0}C at various moisture contents of 6.38%, 6.67%, 6.9%, and 7.02% and air/fuel ratios being 1.66, 1.63, 1.707

and 1.684, whilst the calculated equivalent ratios are 0.265, 0.26, 0.272 and 0.269, respectively. Figures 6.2 to 6.5 show the comparison of the model to these four sets of experimental results.

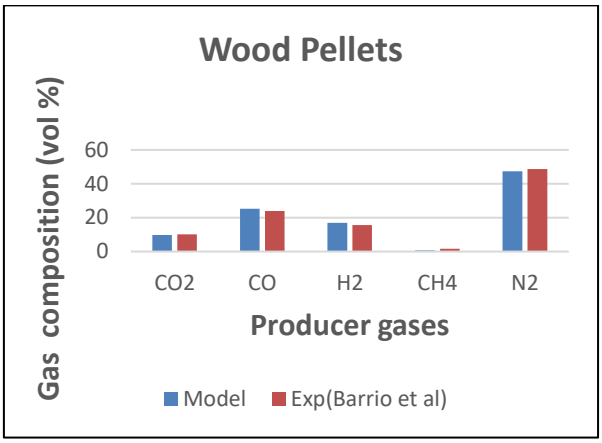

Figure 6.2 Comparison of producer gas composition predicted by model against the experimental results of Barrio et al. with wood pellets: the calculated equivalent ratio is 0.265

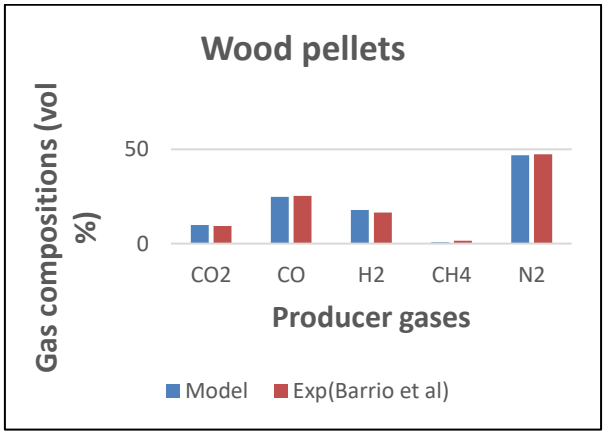

Figure 6.3 Comparison of producer gas composition predicted by model against the experimental results of Barrio et al. with wood pellets as fuel: the calculated equivalent ratio is 0.26

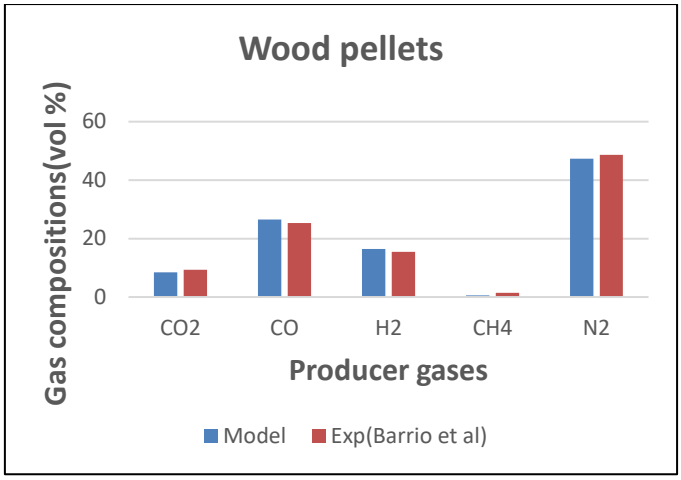

Figure 6.4 Comparison of producer gas composition predicted by model against the experimental results of Barrio et al. with wood pellets as fuel: the calculated equivalent ratio is 0.272

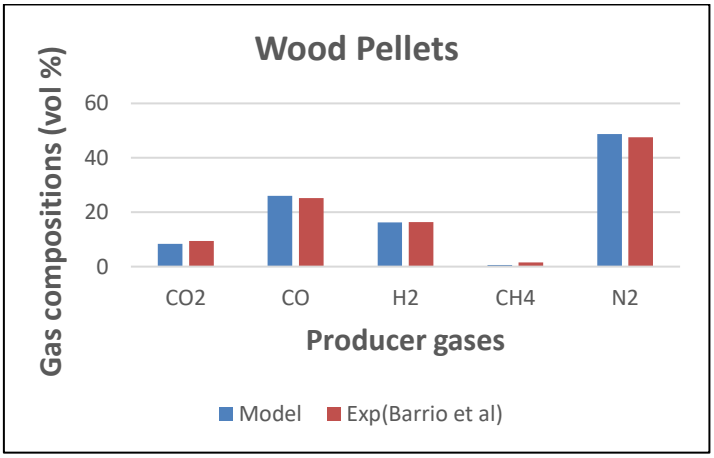

Figure 6.5 Comparison of producer gas composition predicted by model against the experimental results of Barrio et al. with wood pellets: the calculated equivalent ratio is 0.269

In Figures 6.2 - 6.5, data shows that the predicted results are generally in good agreement with experimental data for CO_2, CO, H_2 and N_2, except for the composition of CH_4, which was under-predicted. Exothermic reactions favour the formation of methane. Under the conditions of the pyrolysis and combustion process, exothermic reaction for the formation of CH_4 would not be favoured, this explains why in the equilibrium approach adopted, the amount of CH_4 is very small. Under-predicted values of CH_4 are not only present in this model but also in the models of other researchers: Zainal et al [112] and Bacon et al [150], who confirmed that the CH_4 in the product is higher than would be estimated from the equilibrium calculation. In the calibrated

model of Jayeh et al the predicted CH_4 was adjusted in such a way that it was equal to the amount of methane measured in the product gas. In using MATLAB codes, the calculated error values are in a range of 4 -12% for CO_2, 3 -15% for H_2, 2 -13% for CO, 1- 4% for N_2 but for CH_4, this value was between 50- 64%.

6.3 Comparison and validation of results with thermodynamic equilibrium modelling (Aspen HYSYS)

Aspen HYSYS is used to set up a non-stoichiometric equilibrium model for the downdraft gasifier to predict the synthesis gas production. The model simulates various zones of the downdraft gasifier. The process flow diagram (PFD) with Gibbs reactors represent the simulation procedure which models gasification of wood chips, wood pellets, rubber wood and palm fronds using a set of equilibrium air stream gasification reactions to obtain synthesis gas composition. This model predicts the performance of the gasifier with the results shown in Figures 6.6 – 6.11.

Figure 6.6 shows the comparison of product gas composition with the experimental data of Matthew et al. at 10% of moisture content and 952 K reaction zone temperature obtained from gasification of pinewood chips in a small inexpensive wood gasifier. The errors between the experimental data and the model is reasonable for CO, CO_2, H_2 and N_2, however, CH_4 is under predicted. In the study of the effect of moisture content and equivalence ratio on the gasification process for different biomass fuel carried out by Manish et al [151], the methane percentage in the gas composition from their modelling result was taken as zero because the predicted amount was negligible.

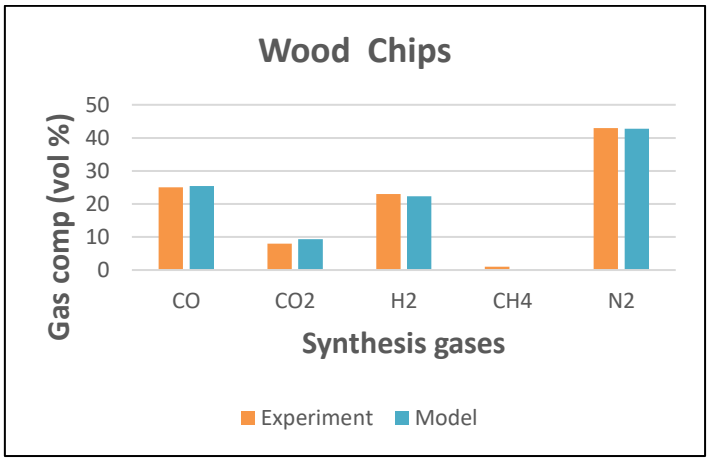

Figure 6.6 Product composition comparisons with experimental data of Matthew et al. [149]

The model was also tested against the experimental results by Duleeka et al [152] obtained from the testing of the 10 kW downdraft gasifier with varying throat diameters and the experimental data by Jayah et al [104]. The throat diameter of the gasifier is 125 mm, ER is 0.352. The moisture content is 0.2226 by weight fraction from the test run by Jayah et al [114] and the experimental work by Duleeka et al [138] used 14,7% moisture content and A/F =1.96 (ER = 0.352).

Figure 6.7 presents comparison of the present model and experimental data using the same conditions. The dry gas composition has been represented by the volume percent of varied species. The H_2 concentration has been somewhat over predicted while CH_4 was slightly under predicted when compared with the experimental value. The predicted concentrations of CO, CO_2 and N_2 agree reasonably with the corresponding experimental results.

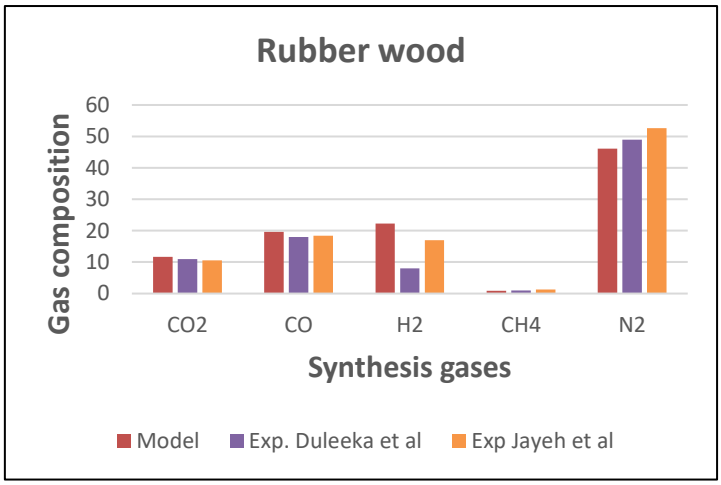

Figure 6.7 Dry gas composition comparisons of present model with experimental data

Considering that pyrolysis products are cracked in oxidation zone where the temperature is high and in the presence of O_2 in the air, it is possible that some of the CH_4 produced went through combustion. This trend was also found in the thermodynamic equilibrium model presented by Jarungthammachote et al [153], where H_2 was over-predicted and CH_4 was under-predicted. To modify the model in their study, a coefficient of 11.28 was introduced which was calculated from the average value of the ratio of CH_4 in the experiment series of 9 cases in the work of Jayah et al [104] and one case in Zainal et al [46]. After the modification of the model, the amounts of the H_2 significantly reduced and the amounts of CH_4 increased to became of similar levels to the experimental values in all cases.

To further test the reliability of this model with wood pellets as the feed stock, the validation of this model is tested against the experimental data measured by Chawdhury et al [29] and Barrio [8] using the following conditions; T= 650 – 670 ^{o}C, A/F =1.52 for wood pellets (see Figure 6.8).

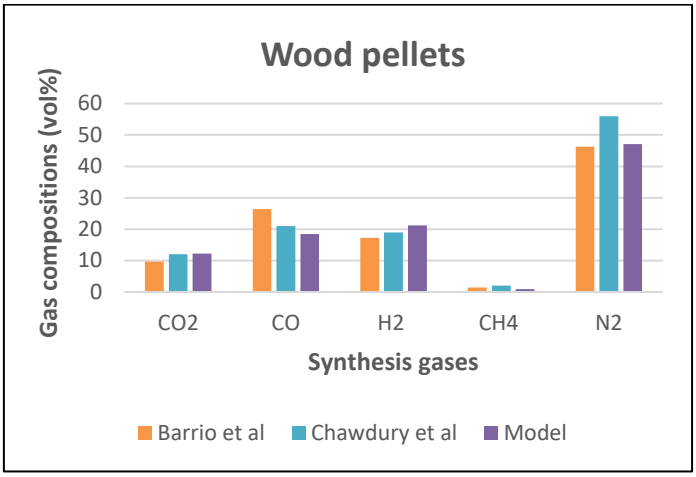

Figure 6.8 Comparison of dry gas composition by the model against experimental data

Figure 6.8 shows the model results compared with experimental data in Barrio et al [8] at A/F=1.52, MC =8% and Chawdury et al [29] with MC = 8.55% for wood pellet. The predicted gas compositions for CO_2, CO, N_2 and H_2 are fairly comparable to experimental data, however, the predicted CH_4 is slightly lower than experimental data.

Palm fronds, also known as oil palm fronds, are ones of the feed stocks used to test for the validity of this model. Comparison between the model predictions and experiments was carried out for a range of values of the equivalence ratio. There are quite a few studies on oil palm fronds and some of experimental data provided does not include all the gas compositions, therefore the predicted results were compared with the gas compositions results, made available in open literature. The equilibrium model prediction was tested against experimental data obtained from downdraft gasification of OPF carried out by Samson et al. [50] with ERs of 0.41 to 0.51 and temperatures ranging from 600 ^{0}C to 900 ^{0}C, as shown in Figures 6.9 and 6.10.

Figure 6.9 compares the predicted model with experimental data for CO_2, CO, H_2 and N_2 composition in the product gas for ER of 0.41 with temperature of 900^{0}C; this present mathematical model is tested with experimental data using the same operating conditions. The mathematical model reasonably predicts the composition of CO, CO_2 and does predict N_2 fairly well. The H_2 concentration predicted by the model is slightly

higher than the experimental data. Such H_2 over-prediction from equilibrium model has been reported in other studies as well [50].

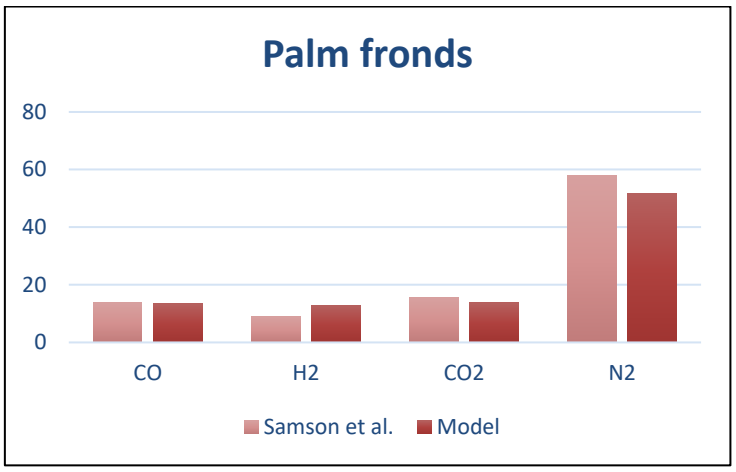

Figure 6.9 Comparison of the predicted synthesis gas composition of oil palm fronds with experimental data by Samson et al. [41] at ER of 0.41

Figure 6.10 compares the predicted model with experimental data for CO_2, CO, H_2 and N_2 composition in the product gas for ER 0.51 at 700 ^{0}C. The concentrations of CO_2, CO are better predicted for ER 0.51. Again, H_2 prediction is higher than that of the experiment data, this could be attributed to the reduction reactions responding to zone temperatures; at temperatures around 750-800 ^{0}C, the endothermic nature of H_2 production reactions results in an increase in H_2 content and decrease in CH_4 [154].

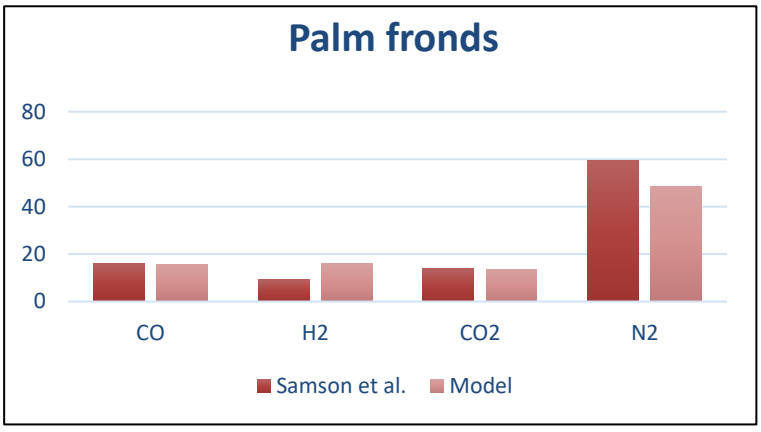

Figure 6.10 Comparison of predicted synthesis gas composition of oil palm fronds with experimental data by Samson et al. [41] at ER of 0.51

Eucalyptus wood is used to test the validity of the non-stochiometric equilibrium model. Martinez et al [60] presented an experimental study of the gasification of eucalyptus wood in a moving bed type of downdraft gasifier with two air supply stages. The configuration was implemented to improve the quality of the producer gas by reducing its tar content by varying the air fed into the gasifier and the distribution of the gasification air between the zones (AR). The predicted results of the mathematical model are compared with the experimental tests carried out with air fed into a single stage and double stage gasifier. The total air flows range from 16 to 24 Nm^3/h and temperatures ranging from 600 to 750 ^0C. Figures 6.11 to 6.13 show the gas compositions with varying air flow ratios fed into a single stage gasifier.

In Figure 6.11, H_2 predicted compositions fairly agrees with the experimental data. From 16 Nm^3/h to 20 Nm^3/h, H_2 increases from 15.5% to 16%, with further increase in air flow ratios from 22 Nm^3/h to 24 Nm^3/h, H_2 decreases from 14.5% to 13.9%. The equivalence ratio shows two opposing effects on gasification process. Increasing ER favours gasification by increasing the temperature which in turn favours the production of H_2. However, beyond a certain limit, the oxidation reaction predominates due to availability of O_2 in the air and the yield of H_2 drops [155].

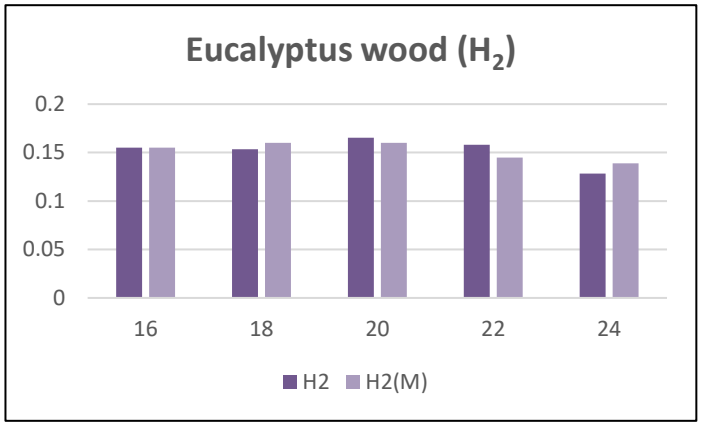

Figure 6.11 Comparison of predicted H_2 gas composition of Eucalyptus wood with experimental data of Martinez et al [60] (single stage air supply)

In Figure 6.12, the predicted CO compositions produced compares reasonably well with the experimental data. It is observed that with an increase in the air flow ratio from 16 Nm^3/h to 18 Nm^3/h CO increases from 16.2% to 17.1%. It is also observed that with further increase from 20 Nm^3/h to 24 Nm^3/h, CO gradually decreases from 17% to 16.9% and then to 15%. This indicates that, initially, CO increases due to increase in the conversion of fuel but after attaining the optimum value its production begins to decrease.

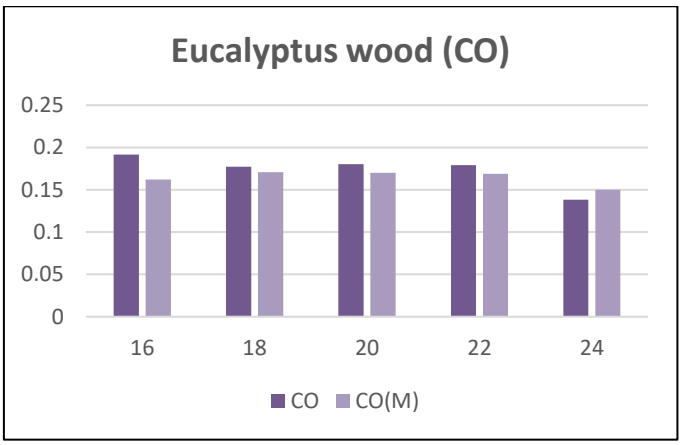

Figure 6.12 Comparison of predicted CO gas composition of Eucalyptus wood with experimental data of Martinez et al [60] (single stage air supply)

In Figure 6.13, the predicted CH_4 is seen to be consistently higher than the values of the experimental data however, it follows a reasonable pattern; decreasing as the air ratio increases. Using the model, the higher concentrations of the CH_4 are formed in the pyrolysis zone, as it goes into the oxidation zone. However, as it leaves the oxidation it is reduced, this shows the effect of the temperature on the formation of methane.

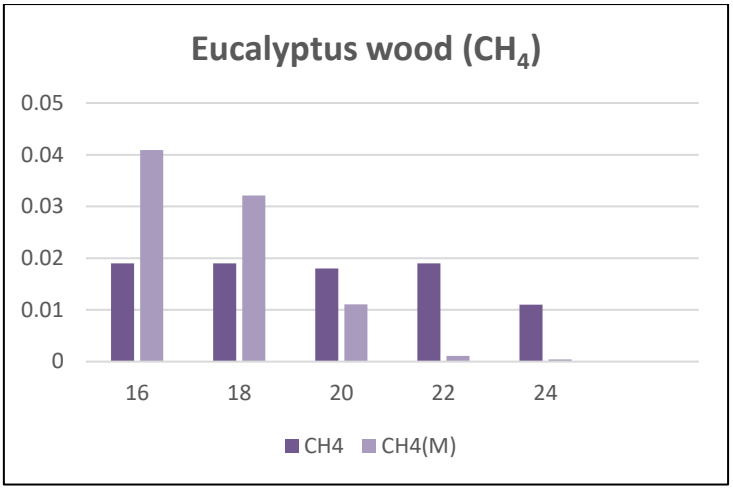

Figure 6.13 Comparison of predicted CH4 gas of Eucalyptus wood with experimental data of Martinez et al [60] (single stage air supply)

6.4 Biomass equilibrium and kinetic modelling

In much of the work using HYSYS, the gasification zone was simulated by assuming that thermodynamic equilibrium was reached. To try and produce a kinetic based simulation, the reduction zone analysis was based on kinetic modelling using a PFR in HYSYS. The first two zones, pyrolysis and combustion, were analysed using a thermodynamic equilibrium approach with Gibbs reactors. This model is tested for both single and double air operations using Rubber wood, wood chips and Eucalyptus wood. The predicted results using this kinetic model have been validated using published experimental data, see Figures 6.14 -6.20.

The model is tested against the experimental results from Duleeka et al [152] obtained from the testing of the 10 kW downdraft gasifier with varying throat diameters and the experimental data from Jayah et al [104]. In data published by Jayah et al [104], the throat diameter of the gasifier is 125 mm, ER is 0.352, and moisture content is 0.2226 by weight fraction. The experimental work of Duleeka et al [138] uses 14.7% moisture content and A/F =1.96 (equivalent to E.R 3.52). These gasifiers ran on rubber wood**.** The three sets of results have similar quantitative amounts of the gases. In Fig. 6.14, the gas compositions of CO, CO_2, CH_4, H_2 and N_2 obtained from the simulation using both Gibbs and plug flow reactors compares fairly well with these experimental data. However, the H_2 and CH_4 was slightly under-predicted. The relatively low percentage of H_2 could be attributed to the some of the reactions suggested not adequately

favouring the formation of H_2 and CH_4. When the reverse reaction of water gas becomes dominant in terms of the reaction rate, the formation of H_2 is not favoured. The reactions representing the reduction zone for the formation of CH_4 is not favoured.

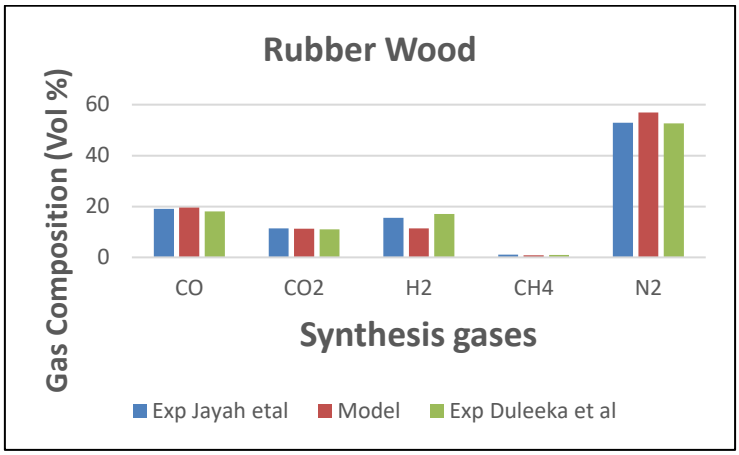

Figure 6.14 Comparison of Rubber Wood gas composition by model against the experimental results (Equilibrium and Kinetic Modelling)

The model is also tested against the experimental results from Chawdhury et al [29] obtained from the design and testing of a small downdraft gasifier JRB-1 at Durham University with the flow rate of air at 0.0015 m^3/s and the temperature in the reaction zone is 950-1150 ^0C. It was also tested on the inverted downdraft gasifier studied by Matthew et al [149] with the moisture content of 10% and the temperature of 679 ^0C. This model used the equivalent ratio of 0.2 and the temperature of 850 ^oC which is within the operating conditions of the experimental data. The comparison is shown in Figure 6.15 below.

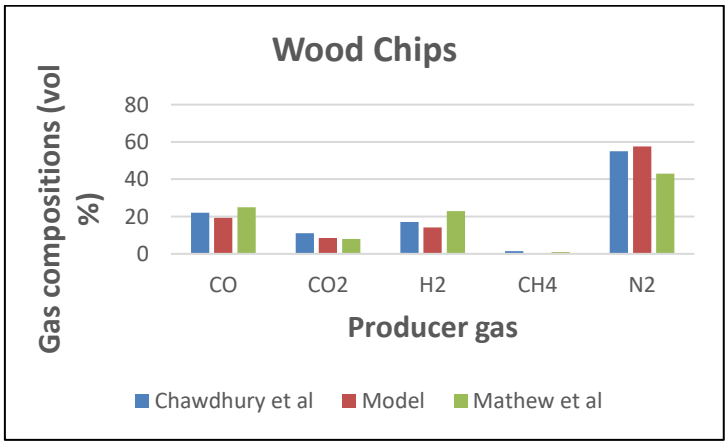

Figure 6.15 Comparison of gas Wood Chips composition by model against experimental data (Equilibrium and Kinetic)

In Figure 6.15, the graph shows the concentrations of CO, CO_2, CH_4 and N_2 compared with the experimental results of Chawdury [25] and that of Matthew [149]. Results for prediction of CO, CO_2, CH_4 and N_2 produce the better fit as they are not too deviated from the experimental data. The main deviation from the experimental data is CH_4. This sort of trend seems to be reproducible even with different biomass feeds. As explained before, this could also be attributed to the reaction that produces the methane in the reduction zone not being favoured.

The mathematical model is also tested using eucalyptus wood for the double air supply gasification operation. In the paper, published by Martinez et al [60], experimental results are presented for the gasifier working at an AR of 80% and at various total air flows of 16, 18, 20, 22 and 24 Nm^3/h. Results reported include temperature profiles, relating to the Pyrolysis, Combustion and Reduction stages. These were listed as Runs C1 to C5, see Table 6.1. The two-stage air gasification operation was implemented using both thermodynamic and kinetic models, hence the simulation was represented with two Gibbs (model Gibbs) and a PFR (model kin) reactors. The theoretical results obtained from modelling are compared to experimental data in Figures 6.16-6.20 for the above runs C1 to C5.

Table 6.1 Experimental planning of gasification test

Test	First stage (Nm^3/h)	Second stage (Nm^3/h	Total (Nm^3/h	AR (%)	T0(C)
C1	7.11	8.89	16	80	570.61
C2	8	10	18	80	642.72
C3	8.89	11.11	20	80	642.61
C4	9.78	12.22	22	80	733.14
C5	10.67	13.33	24	80	702.73

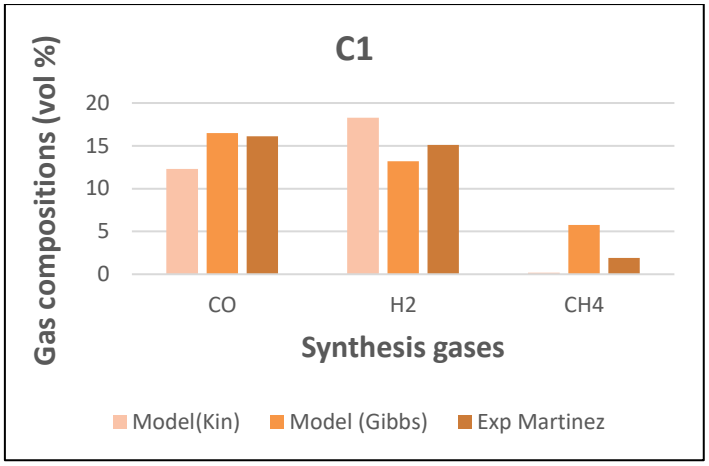

Figure 6.16 Comparison of gas composition by model against the experimental results (C1)

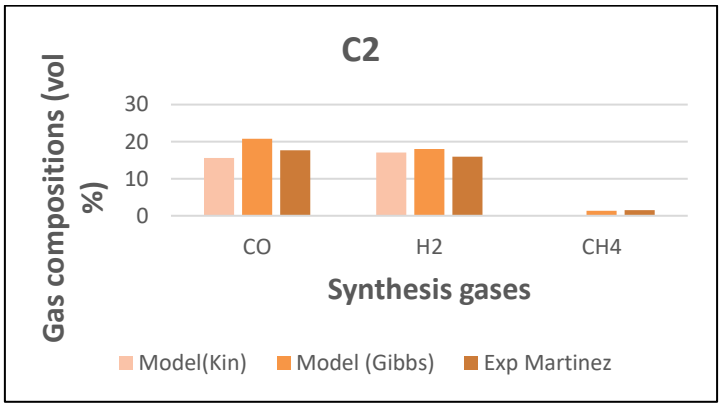

Figure 6.17 Comparison of gas composition by model against the experimental results (C2)

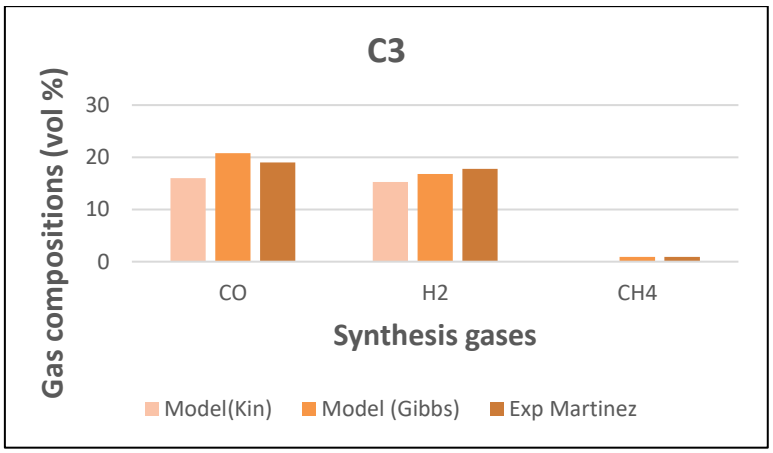

Figure 6.18 Comparison of gas composition by model against the experimental results (C3)

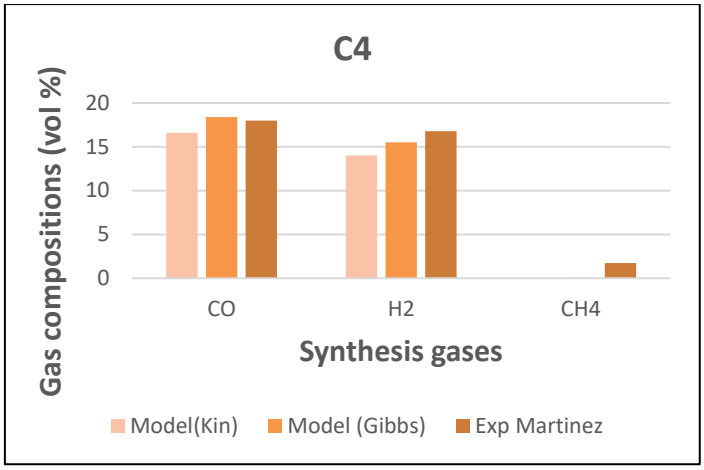

Figure 6.19 Comparison of gas composition by model against the experimental results (C4)

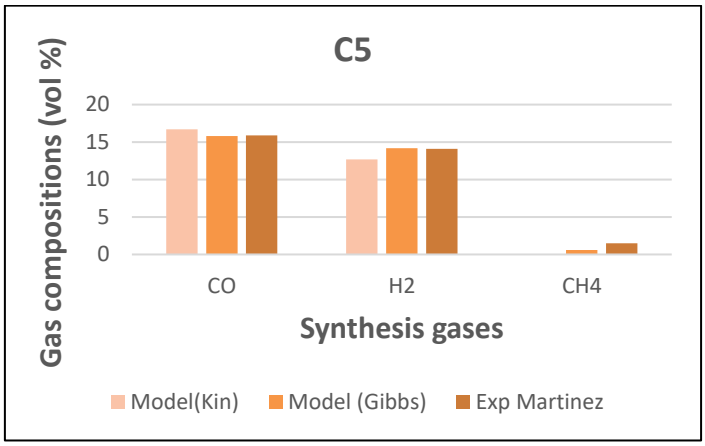

Figure 6.20 Comparison of gas composition by model against the experimental results (C5)

Figures 6.16-6.20 show the CO, H_2, and CH_4 concentrations profiles of the producer gas for air ratio (AR) of 80% and 16–24 Nm^3/h of total air flow for runs C1 to C5. The concentrations of the gases produced by the model fairly agrees with that of the experiment with some minimal errors. The trends obtained in this model is consistent with those reported in the study of Martinez et al [69], especially for CO and H_2. The concentration of CO increases from 16.5% to 20.8% with the air flow increase from 16N m^3/h (C1) to 18 Nm^3/h (C2). Above this point, CO begins to decrease from 18.5% to 15.8% with the increase in total air flow from 20 Nm^3/h (C3) to 24 Nm^3/h (C5). As explained above, initially, CO increases due to the increase in the conversion of fuel but after attaining the optimum value then its production begins to decrease. With the thermodynamic model, H_2 increases from 13.2% to 18% with the increase in total air ratio from 16 Nm^3/h to 18 Nm^3/h and then slowly decreases from16.8% to 14.2% with

the air flow increase from 20 Nm^3/h to 24 Nm^3/h. With the kinetic model, H_2 decreases continuously from 18.3% to 14.2% as the total air flow increases from 16 to 24 Nm^3/h. In terms of the thermodynamic predictions, the Gibbs model does not deal with individual equations but in the region of high temperatures, the peak in composition is produced by the formation of other species being favoured as the amount of oxygen in the air increases. At lower temperatures, hydrogen formation could be favoured which would explain the peaking. Considering the kinetic approach and the four equations representing the reduction zone as the temperature of this zone increases, HYSYS indicates that under the conditions used, the Boudouard reaction and the reverse water gas reaction become dominant in terms of the reaction rate. Thus, for the reverse water gas reaction, CO and H_2 are removed by the reaction. The Boudouard reaction produces CO, so the net effect is that the H_2 composition should reduce while CO increases. In the case of using ASPEN HYSYS, the calculated error values of product gases at various conditions are in the range of 6-26% for CO_2, 2 -30% for CO, 3 – 23% for H_2, 2 – 16% N_2 but for methane this value was within 51-66%.

6.5 Parametric studies

After successfully validating the predictions from the developed mathematical model using the experimental results, the model was applied to perform parametric studies with different operating parameters such as moisture content, equivalence ratio and temperature.

6.5.1 Influence of moisture content

Almost all biomass fuels contain a high percentage of moisture, see Werther et al [156]. The moisture may be inherent in biomass and may also be due to the prevailing weather condition. The moisture content in biomass is one of the important parameters that affect the performance of the gasifier through the variation in the producer gas composition and conversion efficiency. The concentration of gases obtained from the equilibrium and kinetic modelling of the three zones of the downdraft gasifier is presented in Figures 6.21-6.23. In the present work, results have been calculated for three biomass fuels (wood pellets, chips and rubber wood) and variation of composition with increase in moisture content in fuel from 0 to 30%, ER at 0.25 and temperatures from around 750^0C, 800^0C and 850 ^{0}C respectively. Figures 6.21 to 6.23

show the compositions of the gases with variation of moisture content for various biomass feeds.

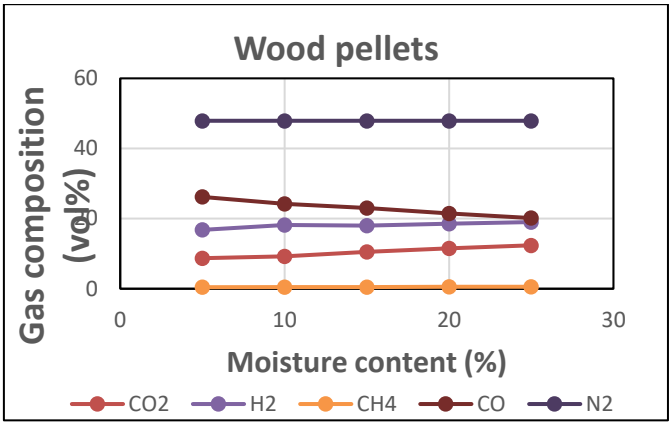

Figure 6.21 Effect of moisture content on Wood pellets gas composition

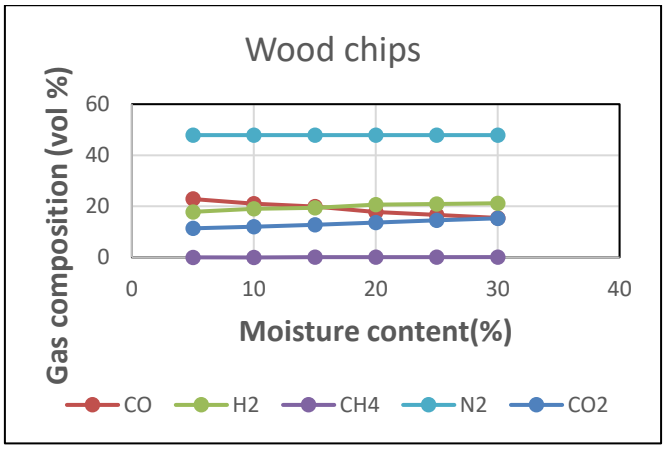

Figure 6.22 Effect of moisture content on Wood chips gas composition

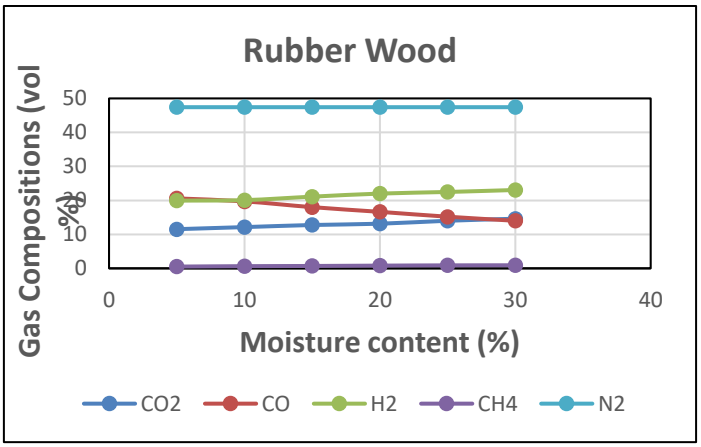

Figure 6.23 Effect of moisture content on Rubber woods gas composition

It can be observed in these Figures that with the increase in the moisture content, the H_2 and CO_2 content in the gas increases. Hydrogen percentage increases from 17% to

20% for wood pellet, from 17.82 to 21.69% for wood chips and from 19.93 to 25.58% for Rubber wood. The CO_2 percentage changes from 9 to 12% for wood pellets, from 11.15 to 15.31% for wood chips and from 11.12 to 15.81% for rubber wood for the increase in moisture content from 5 to 30%. The increasing formation of H_2 can be attributed to the fact that with the increased amount of moisture, the water gas reaction contributes more than the Boudouard reaction in converting the char in the reduction zone [57]. Thus, the increased production of H_2 from the water gas reaction increases the concentration of H_2 in the producer gas. The fuel moisture content in the fuel has the negative effect on the CO content as CO is consumed producing H_2 and CO_2, causing the decrease in CO and the increase in CO_2, accordingly. Even though the percentage of CH_4 is less than 1%, the concentration of CH_4 in the gas is observed to gradually increase with increase in the moisture content and this indicates that at lower temperatures the formation of CH_4 is favoured while N_2 concentration of the gas remains almost constant for all wood types.

The moisture content of the biomass affects the synthesis gas composition as most of the heat evolved in the oxidation will be lost to the evaporation of the moisture when it should be raising the temperature required for the reduction reactions. This effect on the combustible gases subsequently affects the calorific values of the synthesis gas. Figure 6.24 shows the variation of synthesis gas composition and LHV over the moisture content range.

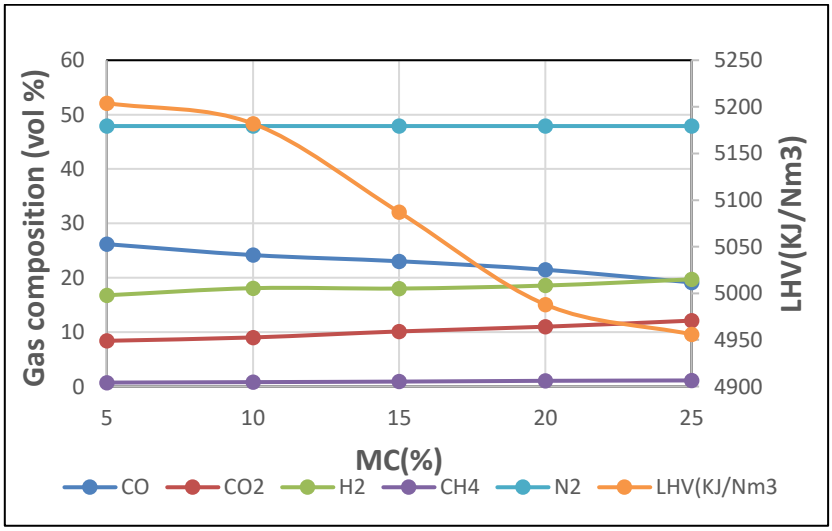

Figure 6.24 Effect of moisture content on Rubber Wood composition and LHV

With increase in the moisture content, the LHV decreases continually due to the decrease in the temperature of the system which affects the production of the combustible gases that contribute to the energy content of the synthesis gas. With increase in the moisture content, the equilibrium of the reduction reaction shifts towards the production of CO_2 whilst CO decreases. H_2 has the tendency to either increase or decrease depending on the favoured reaction between the water gas reaction and the methanation reaction. Methane increases slightly with the increased moisture content, however the concentration of methane is quite small. Thus, with the production of higher concentration of less calorific mixes of CO_2 and N_2 (which is normally higher), the energy content of the synthesis is expected to decrease.

6.5.2 Effect of equivalence ratio

In the downdraft gasifier, air is added in the equivalence ratio being in the region of 0.25 [38]. The equivalence ratio gives an idea of the air to fuel ratio at which a gasifier should be operated. However, in the study carried out by Babu et al. [157], it was shown from the three studies carried out that the optimum equivalence ratio depends on the composition of the biomass, design and operation of the gasifier. This section shows the effect of varying ER on the gas compositions and the lower heating value (LHV) using wood pellets, wood chips and rubber wood feed stocks. ER has been varied from 0.2 to 0.62, moisture content is around 10-17% to show the predictability of this model. The gasification temperature is around 750- 800 ^{0}C. Figures 6.25 – 6.27 shows the effect of ER on the gas composition.

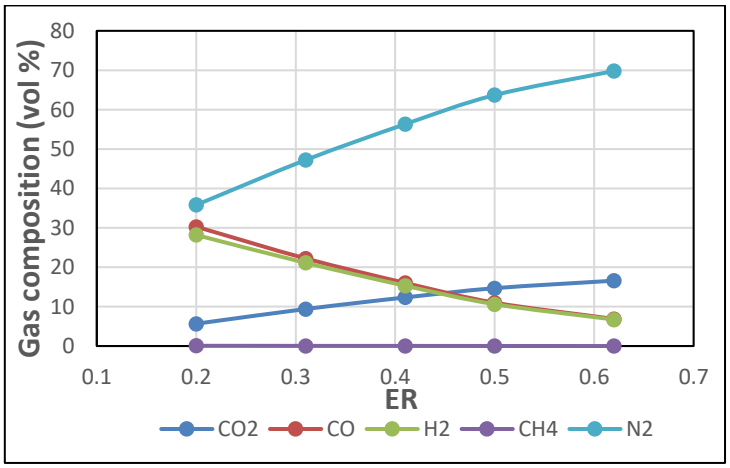

Figure 6.25 Effect of ER on wood pellet synthesis gas composition

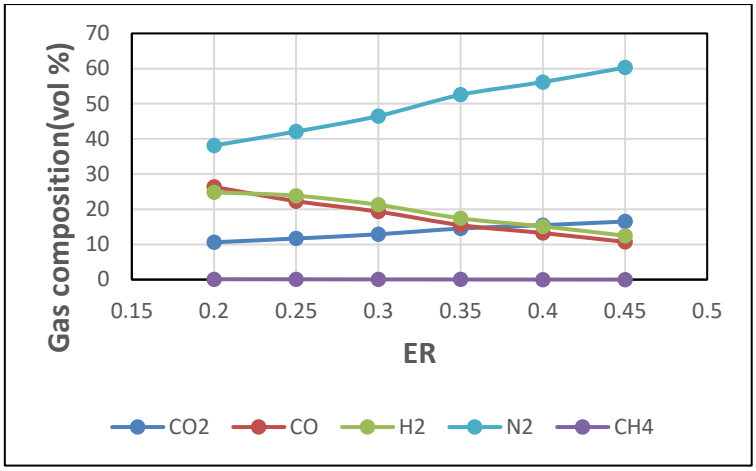

Figure 6.26 Effect of ER on wood chip synthesis gas composition

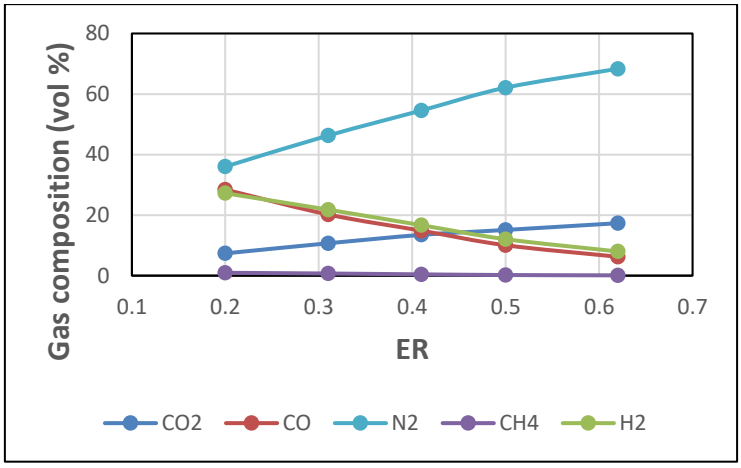

Figure 6.27 Effect of ER on rubber wood synthesis gas composition

Figures 6.25 to 6.27 describe the effect of varying equivalence ratio on the gas compositions for wood pellets, wood chips and rubber wood, respectively. The yield of hydrogen predicted by the developed model is observed to follow a decreasing trend with increasing ER. With the increasing ER, the concentration of CO_2 rises significantly, while combustible species such as CO and H_2 and CH_4 show an inverse relation. A similar trend is reported by other researchers like Turn et al [56]. The increase in CO and H_2 can be attributed to the endothermic water gas reaction. When the ER increases from low values, the temperature of the system increases, ensuing in a marked increase in generation of H_2. However, beyond a certain limit, the oxidation reaction predominates due to availability of excess oxygen and the yield of H_2 drops for conversion of H_2 to H_2O; this trend is reported by Lv et al. [51]. CO_2 shows increasing trends for all three biomasses; the percentage of CO_2 is observed to increase with the increase in ER, like the trend established by Altafini et al [109]. The trend of CO_2 could be correlated with the trend opposite to that for CO and the effect of ER on

CO_2 production varies in many studies. The results show a decreasing trend of CH_4 as ER increases, Mansaray et al. [50] inferred that increasing the ER results in a decrease in concentrations of methane and other light hydrocarbons, which have relatively high heating values. The concentration of N_2 is observed to increases with increase in ER. When ER is increased, more oxygen is supplied into the gasifier, but it also brings with it N_2 thus there is the increase in N_2.

The effect of air to fuel ratio (AR) was also investigated on palm oil frond gas composition on a wet basis (see Figure 6.28). Air to fuel ratio was varied from 0.1 to 2 at 800 ^{0}C.

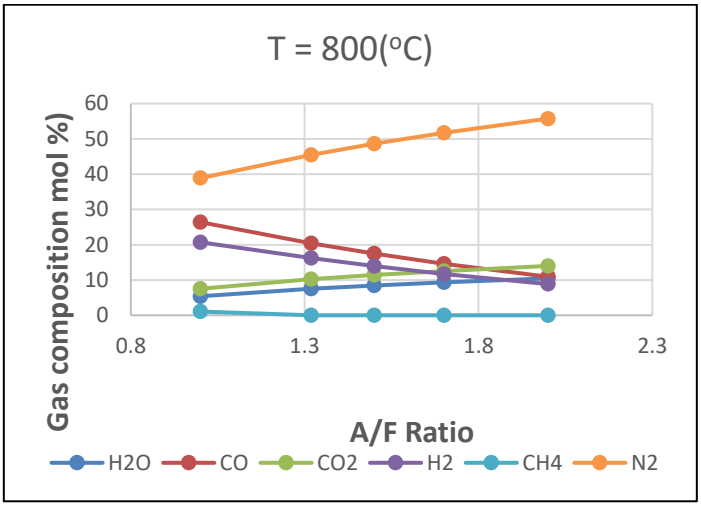

Figure 6.28 Effect of A/F ration on palm oil frond gas composition

The simulation results in Figure 6.28 show that the molar fraction of CO is higher at lower air fuel ratios. CO_2 increased slightly as the air fuel ratio increased. The decreasing CO and increasing CO_2 with increasing air fuel ratio is due to oxidation of CO at the higher air ratio. The H_2 composition is reducing with increasing the air to fuel ratio and this could be explained by the fact that hydrogen is involved in the water gas shift reaction in which the reverse reaction consumes H_2 and CO_2 and produces CO and H_2O. N_2 as expected increases as it comes in with the air supplied to the gasifier.

Figure 6.29 shows CO, CH_4 and H_2 concentration profiles as well as LHV as a function of the total air fed into the zones. The predicted result is obtained from the double air supply operation using the thermodynamic equilibrium model. From the chart, high amounts of CH_4 were obtained from the first run at 16 Nm^3/h, thus affecting the LHV of the gas for that run. Thus, disregarding the first run, at 18 Nm^3/h, the highest LHV

of 4551 kJ/Nm^3 is obtained and this coincides with the highest concentrations of CO, H_2 and CH_4. This is expected as the combustible gases are the contributors of the energy content of the gas. From this total air flow, the process is observed to be favoured by combustion given the operating conditions, thus the rise of air flow from 20 Nm^3/h to 24 Nm^3/h results in the LHV continually decreasing to the 3143 kJ/Nm^3, which also matches lower concentrations of the gases.

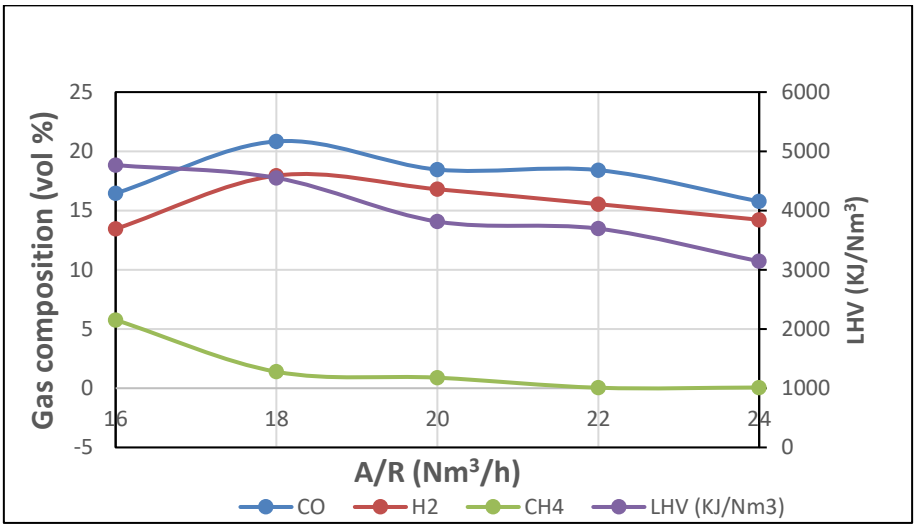

Figure 6.29 Effect of A/R on LHV and Eucalyptus wood gas composition

6.5.3 Influence of temperature

Temperature has an intense effect on the producer gas composition, this is due to gasification being a temperature-controlled reaction; temperature thus controls the equilibrium of the reaction. Some reports show that achieving a high carbon conversion of the biomass and a low tar content requires a high operating temperature greater than 800 ^oC in the gasifier. By increasing the temperature, combustible gas content, gas yield and heating value all increase significantly, while the tar content decreased sharply [158]. This section shows the effect of varying temperature on the gas compositions for wood pellets, wood chips, rubber wood and palm fronds feed stocks see Figures 6.30 - 6.33 respectively.

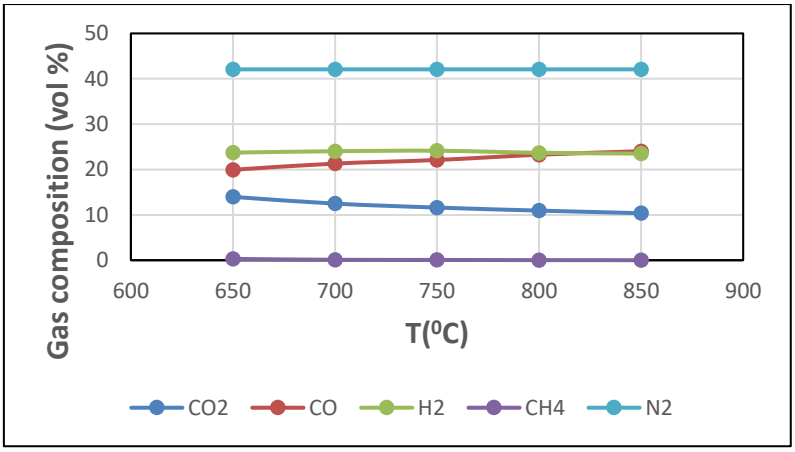

Figure 6.30 Wood chips gas compositions versus temperature

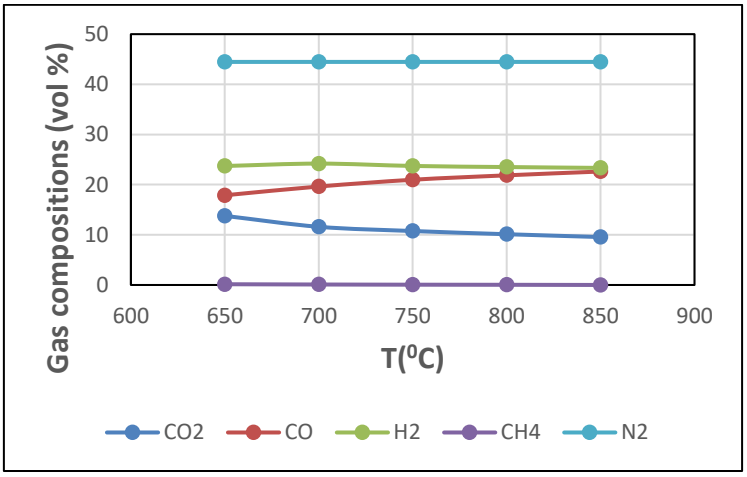

Figure 6.31 Wood pellets gas compositions versus temperature

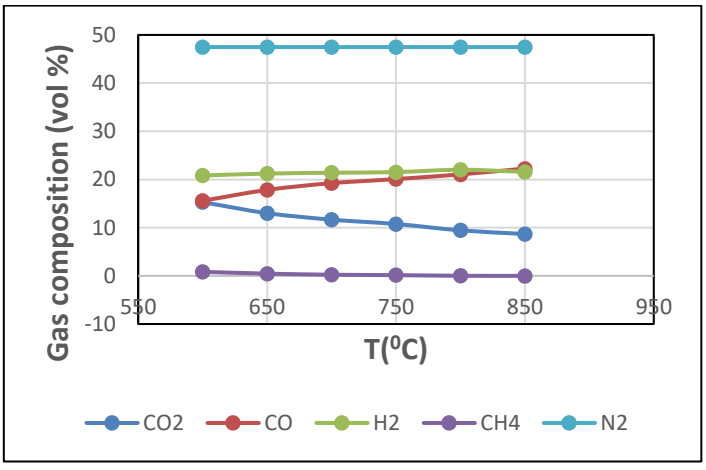

Figure 6.32 Rubber wood gas compositions versus temperature

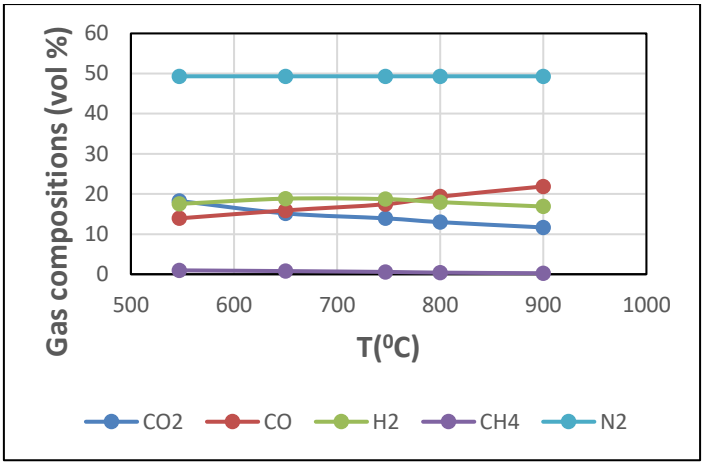

Figure 6.33 Palm frond gas compositions versus temperature

In Figures 6.30 to 6.33, it can be seen that the CO_2 and CH_4 concentrations show decreasing trends while H_2 and CO shows increasing tendency for formation. The gasification temperature influences the equilibrium of the chemical reactions. As the temperature increases, the CO_2 level falls and the CO level rises and this would indicate that as the temperature is rising, the endothermic reactions are being favoured. Thus, the reaction such as water-gas reaction, which is endothermic, could be favoured and producing CO and H_2 at the higher temperatures. This sort of behaviour is noted in other syngas production reactions such as the Boudouard where at the higher temperature, the more stable CO_2 molecule can be 'broken down' to produce the less stable CO molecules, hence the reason for increase in CO and decrease in CO_2. In terms of the hydrogen production, it is noted that the peak in H_2 composition is observed at around 650 and 750 ^{0}C and at higher temperatures, the amount of H_2 starts to fall. Hence H_2 exhibits both increasing and decreasing tendencies of production. This is because the H_2 yield is dominated by both the char gasification reaction and water-gas shift reaction; the char gasification reaction is endothermic reaction while the water-gas shift reaction is exothermic. An increase of the gasification temperature moves the equilibrium point forward in the endothermic reaction resulting in the increase in the H_2 yield. But for the water-gas reaction, the equilibrium point moves to the left, which results in the decrease of H_2 [159]. This also agrees with the findings of Mahishi et al [160]. Mahishi et al. report that hydrogen at chemical equilibrium initially increased with the temperature and when it reaches the maximum, it then gradually decreases at the higheer temperatures. The temperature affects not only the amount of tar formed but also the composition of tar by influencing the chemical

reactions involved in the gasification network. It could be inferred from the results that the reason for the drop in CH_4 at higher temperatures and increase in CO and H_2 is due to the utilization of CH_4 in the endothermic reaction; ($CH_4 + H_2O \leftrightarrow CO + 3H_2$). This trend agrees with that obtained by Turn et al. [161]. Also, at low temperatures, methane and unburnt carbon are present in the producer gas but at elevated temperatures, carbon is converted to carbon monoxide in accordance with Boudouard reaction ($\boldsymbol{C + CO_2 \leftrightarrow 2CO}$). Methane on the other hand, is converted into hydrogen by reverse methanation reaction ($\boldsymbol{C + 2H_2 \leftrightarrow CH_4}$). This brings about the increase in the operating temperature of the gasifier which in turn favours the formation of carbon monoxide and hydrogen [55].

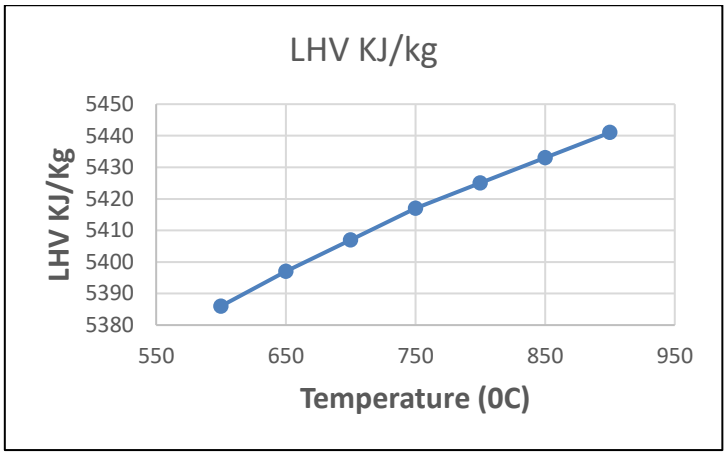

Figure 6.34 Effect of gasification temperature on LHV (A/F =1)

The graph in Figure 6.34 shows that the LHV increased with increase of gasification temperature. The highest LHV is obtained between 850- 900 ^{0}C at a low A/F =1. The increase of temperature results in the increase of LHV of the syngas as it raises the proportions of the combustible gases. However, the reverse effect is obtained if too much air is involved in the process as it will come with more N_2 which dilutes the gases and hence reduces the LHV.

6.6 Summary

- The underestimation of the CH_4 could be attributed to the fact that, in the real gasification processes, the producer gas does not achieve the complete equilibrium conditions inside the gasifier [162]. For this reason, to prevent the complete consumption of methane in theoretical results, in some models, described in literature, a correction coefficient is introduced to move the methanation reaction

to the CH_4 production (avoiding its consumption). Other studies do not include a fraction of CH_4, formed during the pyrolysis process, in the combustion-gasification stage bypassing it to the gasifier outlet [163].

- The reaction ($C + 2H_2 \rightarrow CH_4$) is exothermic, which means that the temperature increase results in the production of CH_4 being decreased, leaving more H_2 in the gas.
- The reaction ($CO_2 + C \rightarrow 2CO$) is endothermic; therefore, the temperature increases the amount of CO_2 reacted with char to produce more CO.
- The reaction ($C + H_2O \rightarrow H_2 + CO$) is endothermic, which means for increasing temperature CO and H_2 production are also increased and more char and H_2O are consumed.

- For the different biomass feeds considered the temperature at which the various sections operate can be seen to have an effect. That said, the H_2 and CH_4 levels do not vary significantly; as expected the main variation is in the CO_2 and CO levels, the latter tending to increase with temperature and the former decreasing. In a model that is using an equilibrium approach for reactions it is inevitable that endothermic reactions will be favoured as the temperature increases. This is consistent with the observations made above.
- The variation of LHV is best summarised by reference to Figure 6.34 where it has been observed that the LHV increase with temperature. This is consistent with the observations made on the CO formation with increasing temperature but the situation is obviously complicated by the impossibility of methane formation at the higher temperatures but the general trend of LHV with temperature is consistent with the observation made in the sense that overall, the quantity of combustible gas has been increased.

Chapter 7 Conclusions and Recommendations

7.1 Conclusions

- The two types of the mathematical model for simulation of a biomass downdraft gasifier and its operation was considered using different configurations, biomass feedstock and operational conditions.
- The gasification of wood chips, wood pellets, rubber wood, Eucalyptus and oil palm fronds were investigated. The gasification of these solid fuels was simulated in a downdraft gasifier with pyrolysis, oxidation and reduction zones.
- Kinetic and thermodynamic equilibrium models (based on both stoichiometric and non-stoichiometric methods) were implemented in order to predict various biomass gasification product gases using air as the oxidizing agent in a downdraft gasifier. These were implemented in MATLAB and ASPEN HYSYS. ASPEN HYSYS was used since it was possible to consider biomass gasifier with two stages of air supply (separately to pyrolysis and oxidation zones). MATLAB model in addition to composition of product, predicts the temperature in the reduction zone, whilst this temperature is an input in ASPEN HYSYS. Due to assumptions made, MATLAB code provides more accurate predictions in performance of the gasifier. The percentage error values calculated from the use of MATLAB codes are in a range of 4 -12% for CO_2, 3 -15% for H_2, 2 -13% for CO, 1- 4% and 50- 64% CH_4, while the predictions from ASPEN HYSYS gives error values in the range of 6-26% for CO_2, 2 -30% for CO, 3 – 23% for H_2, 2 – 16% N_2 and 51-66% for methane.
- The thermodynamic equilibrium model was deployed using an Aspen HYSYS software in which stoichiometry is not considered and various required specie's enthalpies and Gibbs Free Energies of formation are calculated automatically by Aspen HYSYS.
- The kinetic model was deployed with Aspen HYSYS plug flow tubular reactor (PFTR) model, the equilibrium constants and considering the dimensions of the reactor.
- In MATLAB, this was implemented by solving differential equations of mass and energy balances in gasifier zones, using some empirical assumptions and equilibrium constants to obtain the PVT of the system and gas compositions.

- In the models presented in this work, operating conditions such as temperature, equivalence ratio, moisture content and LHV were studied. The analysis show that higher temperatures favoured the formation of CO and H_2, while CH_4 and CO_2 reduce depending on the reaction that prevails.
- Moisture content in the biomass also affects the composition of the gases and the energy content. Increasing MC reduces the temperature of the system and the LHV, also the composition of H_2 and CO_2 increases, CH_4 increases to a certain extent while CO decreases.
- The proposed equilibrium model displayed a variable ability for the prediction of various product yields with this being a function of the feedstock studied. It also demonstrated the ability to predict product gases from various biomasses using both single and double stage air input. In the case of gasification with double air stage supply, higher amounts of methane are obtained with specific tendencies of the gases reaching a peak at certain conditions.
- The total air quantity fed to the pyrolysis and combustion zones ranges from 16 – 22 Nm^3/h at 80% of AR (runs C1-C5). The composition of gas components in the exit, predicted by the developed model, is comparable to the experimental data published by various authors. The simulations indicate that for each of the above runs, there are certain conditions at which there is a peak achieved in formation of each of the combustible gases.
- In the single stage air supply gasification, feed stocks such as rubber wood, wood chips, wood pellets and palm fronds were used. Both thermodynamic and kinetic models of gasification have been deployed as written codes in MATLAB and simulations in Aspen HYSYS. The numerical results have been validated and they reasonably compare with the published experimental data
- The double stage air supply gasification model seemed to produce more CH_4. The kinetic model can only produce CH_4 at very low temperatures. In the equilibrium model, lesser amounts of CH_4 were obtained but at higher temperatures than the kinetic model.

- There were two vital components of the kinetic modelling of biomass reactors in this work. To incorporate the kinetics into the HYSYS simulation it was necessary to introduce a unit operation that incorporated reaction kinetics. This work used a Plug Flow Reactor (PFR). This required some investigation into the length of such

a reactor and necessary adjustment to fit in with the results obtained. Secondly, a presentation of the modelling chemical equations was required that could realistically represent all the known products. Four equations were used, and it was necessary to have Rate Constants and Arrhenius equations for each reaction and to transform these data into a form useable by HYSYS. Once this was achieved the Reduction Section of the Gasifier could be represented by a PFR.

- The kinetic model achieved some success in that it did predict results comparable with experimentally published results for a range of conditions. There were discrepancies particularly with CH_4 formation and the operating temperatures required to produce results comparable with experimental values were usually consistently lower than those actually used experimentally. The use of the PFR, however, did show promise for the use in further modelling.
- The weakness of the kinetic approach is its need for reliable kinetic data. Unlike thermodynamics kinetic data have to be measured and there is a shortage of reliable measured data for relevant reactions that could be used to simulate/model gasification reactions.

7.2 Recommendations

- Further experimental work needs to be carried out for both single and double stage air supply gasification using various biomass feedstock as this provides extended opportunities for detailed testing and validation of the developed mathematical models of the biomass gasifiers.
- Accurate measurements of the chemical composition of the producer gas, generated by the biomass gasifier, using modern technological facilities and of other operating parameters, such as temperatures, velocities and pressures, inside the gasifier are necessary for improvement of the developed mathematical models of biomass gasifiers.
- Computational Fluid Dynamics methods could be further applied for modelling of operation of biomass gasifiers to obtain additional information on flow and heat transfer inside the biomass gasifiers.
- Further detailed kinetic data is required for the kinetic model that incorporates PFR.

- Dynamic neural network-based model for gasification is a type of dynamic modelling that can help curb the issues related to gasification process efficiency that partly prevents biomass gasification technology to become more economically viable. The deployment of Neural network model has the potential to predict process parameters during plant operation with variable operating conditions.
- Effect of flow conditions such as SV should also be considered to measure the performance controlling the gas production rate and the rate at which air as well as gas passes through the gasifier. This will consequently exercise a primary effect of heat transfer around each particle during flaming pyrolysis of the volatiles, combustion of the of the tars and gasification of the charcoal.

REFERENCES

1. Kumar, A., D.D. Jones, and M.A. Hanna, *Thermochemical Biomass Gasification: A Review of the Current Status of the Technology.* Energies, 2009. **2**(3): p. 556-581.
2. Malik, A. and S.K. Mohapatra, *Biomass-based gasifiers for internal combustion (IC) engines-A review.* Sadhana-Academy Proceedings in Engineering Sciences, 2013. **38**(3): p. 461-476.
3. Baruah, D. and D. Baruah, *Modeling of biomass gasification: a review.* Renewable and Sustainable Energy Reviews, 2014. **39**: p. 806-815.
4. Bridgwater, A.V., *Renewable fuels and chemicals by thermal processing of biomass.* Chemical Engineering Journal, 2003. **91**(2-3): p. 87-102.
5. Felipe Centeno, K.M., Electo E. Silva Lora, Rubenildo V. Andrade, *Theroretical and experimental investigations of a downdraft biomass gasiifer -spark ignition engine power system.* 2012.
6. Basu, P., *Biomass Gasification and Pyrolysis Practical design and Theory*. 2010, Elsevier Inc.: 30 Corporate Drive, Suite 400 Burlington, MA 01803, USA.
7. Young-Il Son, S.J.Y., Yong Ku Kim, Jae-Goo Lee, , *Gasification and power generation characteristics of woody biomass utilizing a downdraft gasifier, Biomass and Bioenergy.* 2011. **35**(10,): p. 4215-4220.
8. Barrio, M., *Experimental investigation of small-scale gasification of woody biomass.* PhD thesis , Faculty of Engineering Science and Technology, Department of Thermal Energy and Hydro Power, The Norwegian University of Science and Technology 2002: p. 204-232.
9. Pieratti, E., *Biomass gasification in small scale plants: experimental and modelling analysis*. 2011, University of Trento.
10. Programme, U.N.E., *Technologies for converting waste Agricultural Biomass to Energy*. 2013, International Environment Technology Centre: Osaka Japan.
11. Arvind, K.A., *Biomass as Fuel in Small Boilers*. 2009, Asian Productivity Organisation: Tokyo, Japan. p. 4-52.
12. Mohammad, M.N.B., P., *Photosynthesis: How and Why?* Advances in Photosynthesis-Fundamental Aspects, ed. M.N.B. Mohammad, P. Vol. 9. 2012, China: Intech. 598.
13. Agbontalor, E.A., *Overview of various biomass Energy Conversion routes.* American -Eurasian Journal, 2007. **6**(2): p. 662-671.
14. Twidell, J., *Biomass energy.* Renewable Energy World, 1998. **1**(3): p. 38-39.
15. Report, G.S., *Renewables 2016 Global Status Report*. 2016. p. 272.
16. Hull, S., *Wisconsin sustainable planting and harvest guidelines for nonforest biomass*. 2011: Wisconsin Department of Agriculture, Trade, and Consumer Protection.
17. Comission, E.-E. *Biomass Green Energy for Europe.* 2005.
18. (PI), J.S.T., *Biomass Engineering: Size reduction, drying and densification.* Bioenergy Technologies Office, 2015.
19. Zafar, S., *Waste to Energy Conversion Routes.* Bioenergy Consult, 2016.
20. Tran, K.-Q., et al., *Stump torrefaction for bioenergy application.* Applied energy, 2013. **112**: p. 539-546.
21. Van Essendelft, D., X. Zhou, and B.-J. Kang, *Grindability determination of torrefied biomass materials using the Hybrid Work Index.* Fuel, 2013. 105: p. 103-111.
22. Chen, W.-H., J. Peng, and X.T. Bi, *A state-of-the-art review of biomass torrefaction, densification and applications.* Renewable and Sustainable Energy Reviews, 2015. 44: p. 847-866.
23. Rousset, P., et al., *Enhancing the combustible properties of bamboo by torrefaction.* Bioresource Technology, 2011. **102**(17): p. 8225-8231.

24. Antonopoulos, I.S., et al., *Modelling of a downdraft gasifier fed by agricultural residues.* Waste Management, 2012. **32**(4): p. 710-718.
25. Puig-Arnavat, M., J.C. Bruno, and A. Coronas, *Review and analysis of biomass gasification models.* Renewable & Sustainable Energy Reviews, 2010. 14(9): p. 2841-2851.
26. Giltrap, D.L., R. McKibbin, and G.R.G. Barnes, *A steady state model of gas-char reactions in a downdraft biomass gasifier.* Solar Energy, 2003. 74(1): p. 85-91.
27. X. Li, J.R.G., A.P. Watkinson, C.J. Lim, A. ErguÈdenler, *Equilibrium modelling of gasification: a free energy minimizaion approach and its application to a circulating fluidized bed coal gasifier.* 2000: p. 197 -207.
28. Baxter, M.J., *Downdraft gasification of biomass.* PhD thesis , Birmingham, UK: Aston University, 1994.
29. M. A. Chawdhurya, K.M., *Development of a Small Downdraft Biomass Gasifier for Developing Countries.* 2011. **3**(1): p. 51-64.
30. Samy, S., P. E *Pyrolysis*. 25.
31. K., Y.C.M., *Thermal Conversion of Biomass, Pyrolysis and Gasification: A Review.* The International Journal of Engineering And Science (IJES), 2013. **2**(3): p. 11.
32. Sinha, S., et al., *Modelling of pyrolysis in wood: a review.* SESI Journal, 2000. **10**(1): p. 41-62.
33. Lysenko, S., S. Sadaka, and R.C. Brown, *Comparison of the cost of hydrogen from air-blown and thermally ballasted gasifiers.* Biofuels, Bioproducts and Biorefining, 2012. **6**(6): p. 673-685.
34. Soltes, E.J., T. Elder, and I. Goldstein, *Organic Chemicals from Biomass*. 1981, CRC Press, Pyrolysis.
35. Molino, A., S. Chianese, and D. Musmarra, *Biomass gasification technology: The state of the art overview.* Journal of Energy Chemistry, 2016. **25**(1): p. 10-25.
36. Nuno Coutoa, A.R., Valter Silvaa, Eliseu Monteiro*b, Khalid Bouziane, *Influence of the biomass gasification processes on the final.* elsevier, 2013(36): p. 596 – 606.
37. Rauch, H.B.R., *Review of applications of gases from biomass gasification*, in *Syngas production and utilisation" in the Handbook Biomass Gasification*. 2006: The Netherlands JUNE.
38. Knoef, H. and J. Ahrenfeldt, *Handbook biomass gasification*. 2005: BTG biomass technology group The Netherlands.
39. Henham, A. and M. Makkar, *Combustion of simulated biogas in a dual-fuel diesel engine.* Energy Conversion and Management, 1998. **39**(16-18): p. 2001-2009.
40. Monteiro, E., et al., *Syngas application to spark ignition engine working simulations by use of rapid compression machine.* Internal Combustion Engines, 2012: p. 51-74.
41. Krigmont, H.V., *Integrated biomass gasification combined cycle (IBGCC) power generation concept: The gateway to a clearer future.* A White Paper, Allied Environmental Technologies, 1999.
42. Szewczyk, M. and T. Trzepieciński, *Application of biomass-powered Stirling engines in cogenerative systems.* ECONTECHMOD: An International Quarterly Journal on Economics of Technology and Modelling Processes, 2012. **1**: p. 53-56.
43. Paper, F.F., *Wood gas as fuel engine*. 1986, FAO Forestry Department Rome Italy. p. 139.
44. Hagen, C.Y.W.B.E.B., *Biomass Conversion and Technology*. Vol. m 1996, Baffins Lane, Chichester West Sussex PO 19 UD, England: John Wiley and Sons 203.
45. S.A Channiwala, P.P.P., *A unified correlation for estmating HHV of solid, liquid and gaseous fuels.* elsevier, 2001. 81: p. 1051-1063.
46. Selvig, W.A., Gibson, F. H., *Calorific of coal*, in *Chemistry of coal utilization*. J. Wiley and Sons: New York.
47. Jenkins, B. and J. Ebeling, *Correlation of physical and chemical properties of terrestrial biomass with conversion.* 1985.

48. Niessen, W.R., *Combustion and incineration processes: applications in environmental engineering*. 2010: CRC Press.
49. Graboski, M. and R. Bain, *Properties of biomass relevant to gasification [Fuel gas production].* Biomass gasification; Principles and technology (USA), 1981.
50. Atnaw, S.M., S.A. Sulaiman, and S. Yusup, *Influence of fuel moisture content and reactor temperature on the calorific value of syngas resulted from gasification of oil palm fronds.* The Scientific World Journal, 2014. 2014.
51. Bhattacharya, S., D. Albina, and A.M. Khaing, *Effects of selected parameters on performance and emission of biomass-fired cookstoves.* Biomass and Bioenergy, 2002. **23**(5): p. 387-395.
52. J.K Ratnadhariya, S.A.C., *Three zone equillibrium and kinetic free modelling of biomass gasifier- a novel approach.* Renewable & Sustainable Energy Reviews, 2009: p. 1050-1058.
53. Kaupp, A., and Goss, J. R.,, *State of the Art for small Scale (to 50 kW) Gas Producer-Engine Systems,*, in *First International Producer Gas Conference*. March 1981, , U.S.D.A., Forest Service: Colombo, Sri Lanka, .
54. Madhukar R. Mahishi, D.Y.G., *Thermodynamic optimization of biomass gasifier for hydrogen production.* International Journal of Hydrogen Energy, 2007. **32**(16): p. 3831–3840.
55. Zainal, Z.A., et al., *Experimental investigation of a downdraft biomass gasifier.* Biomass & Bioenergy, 2002. **23**(4): p. 283-289.
56. A.M, S., *Operating and Performance Gasfication Process Parameters* International Journal of Science and Research(IJSR), 2013: p. 1-8.
57. Roy, P.C., A. Datta, and N. Chakraborty, *Modelling of a downdraft biomass gasifier with finite rate kinetics in the reduction zone.* International Journal of Energy Research, 2009. **33**(9): p. 833-851.
58. Melgar, A., Perez, J. F., Laget, H., Horillo, A., *Thermodynamic equilibrium modelling of a gasifying process.* energy Conversion and Management, 2007. **1**(48): p. 59-67.
59. Ian Narva´ ez, A.O.o., † Maria P. Aznar,‡ and Jose´ Corella, *Biomass Gasification with Air in an Atmospheric Bubbling.* 1996. **35**: p. 2110-2120.
60. Ajay Kumara, b., Kent Eskridgec, David D. Jonesb, Milford A. Hanna, *Steam–air fluidized bed gasification of distillers grains: Effects of steam to biomass ratio, equivalence ratio and gasification temperatureFluidized Bed. Effect of Six Operational Variables on the Quality of.* elsevier, 2009. **100**(6): p. 2062-2068.
61. T. B. Reed., R.W., S. Ellis, A. Das, and S. Deutche,, *Superficial velocity - the key to downdraft gasification*, in *4th Biomass conference of the Americas, Oakland*. 1999: Oakland, California, USA,.
62. Takashi Yamazaki, † Hirokazu Kozu,† Sadamu Yamagata,† Naoto Murao,† and S.S. Sachio Ohta, ‡ and Tatsuo Ohba‡, *Effect of Superficial Velocity on Tar from Downdraft Gasification of Biomass.* Energy and Fuel, 2005. **19**: p. 1186-1191.
63. M. Siedlecki, W.d.J., *Biomass gasification as the first hot step in clean syngas production process – gas quality optimization and primary tar reduction measures in a 100 kW thermal input steam–oxygen blown CFB gasifier.* Biomass and Bioenergy, 2011. **35**(supplement 1): p. 540 -562.
64. Meng, X.M., et al., *Biomass gasification in a 100 kWth steam-oxygen blown circulating fluidized bed gasifier: Effects of operational conditions on product gas distribution and tar formation.* Biomass & Bioenergy, 2011. **35**(7): p. 2910-2924.
65. Fabry, F., et al., *Waste gasification by thermal plasma: a review.* Waste and Biomass Valorization, 2013. 4(3): p. 421-439.
66. Lettner, F., H. Timmerer, and P. Haselbacher, *Biomass gasification–State of the art description.* Intelligent Energy Europe, Austria, 2007.
67. Warnecke, R., *Gasification of biomass: comparison of fixed bed and fluidized bed gasifier.* Biomass and Bioenergy, 2000. 18(6): p. 489-497.

68. Held, J., *Gasification–Status and technology.* Swedish Gas Centre, 2012.
69. Juan Daniel Martínez, E.E.S.L., Rubenildo Viera Andrade, René Lesme Jaén, *Experimental study on biomass gasification in a double air stage downdraft reactor.* Biomass and Bioenergy, 2011. **35**(8): p. 3465-3480.
70. Juan Daniel Martinez, K.M., Rubenildo V. Andrade, Electo E. Silva Lora, *Syngas production in downdraft biomass gasifiers and its application using internal combustion engines.* Renewable Energy, 2012. **38**(1): p. 1-9.
71. Abedin, M.R. and H.S. Das, *Electricity from rice husk: a potential way to electrify rural Bangladesh.* International Journal of Renewable Energy Research (IJRER), 2014. **4**(3): p. 604-609.
72. Bhattacharya, S.C., S.S. Hla, and H.L. Pham, *A study on a multi-stage hybrid gasifier-engine system.* Biomass & Bioenergy, 2001. **21**(6): p. 445-460.
73. Das, T.B.R.a.A., *Handbook of Biomass Downdraft Gasifier Engine Systems.* 1998.
74. Sastry, A.B.a.R.C., *Biomass Gasification Processes in Downdraft Fixed Bed.* International Journal of Chemical Engineering and Applications, 2011. **2**.
75. Hofbauer, H., et al., *Biomass CHP Plant Güssing; Vortrag Pyrolysis and Gasification Expert Meeting, Strassburg, France; 31.10. 2002.* Proceedings of Pyrolysis and Gasification ExpertMeeting, 2002.
76. Bühler, R. and P. Hasler, *Stand und Entwicklung der Vergasungstechnik.* VDI BERICHTE, 1997. **1319**: p. 81-108.
77. Sikarwar, V.S., et al., *An overview of advances in biomass gasification.* Energy & Environmental Science, 2016. **9**(10): p. 2939-2977.
78. Gomez-Barea, A. and B. Leckner, *Modeling of biomass gasification in fluidized bed.* Progress in Energy and Combustion Science, 2010. **36**(4): p. 444-509.
79. Gräbner, M., S. Ogriseck, and B. Meyer, *Numerical simulation of coal gasification at circulating fluidised bed conditions.* Fuel Processing Technology, 2007. 88(10): p. 948-958.
80. Basu, P., *Biomass gasification and pyrolysis: practical design and theory*. 2010: Academic press.
81. M. Baratieri P. Baggio, L.F., M. Grigiante, *Biomass as an energy source: Thermodynamic constraints on the performance of the conversion process.* 2008. **99**(15): p. 3831–3840.
82. Plus, A., *Aspen Technology Inc.* Cambridge, MA, USA, 2006.
83. Patra, T.K. and P.N. Sheth, *Biomass gasification models for downdraft gasifier: A state-of-the-art review.* Renewable and Sustainable Energy Reviews, 2015. 50: p. 583-593.
84. Ramzan, N., et al., *Simulation of hybrid biomass gasification using Aspen plus: A comparative performance analysis for food, municipal solid and poultry waste.* Biomass and Bioenergy, 2011. **35**(9): p. 3962-3969.
85. Phillips, J.N., *Study of the off-design performance of integrated coal gasification combined-cycle power plants*. 1986, Stanford Univ., CA (USA).
86. Xiangdong, K., et al., *Three stage equilibrium model for coal gasification in entrained flow gasifiers based on aspen plus.* Chinese Journal of Chemical Engineering, 2013. 21(1): p. 79-84.
87. Baggio, P., et al., *Experimental and modeling analysis of a batch gasification/pyrolysis reactor.* Energy Conversion and Management, 2009. **50**(6): p. 1426-1435.
88. Mansaray, K., et al., *Mathematical modeling of a fluidized bed rice husk gasifier: Part I-Model development.* Energy sources, 2000. **22**(1): p. 83-98.
89. Mathieu, P. and R. Dubuisson, *Performance analysis of a biomass gasifier.* Energy conversion and management, 2002. **43**(9): p. 1291-1299.
90. Kuo, P.-C., W. Wu, and W.-H. Chen, *Gasification performances of raw and torrefied biomass in a downdraft fixed bed gasifier using thermodynamic analysis.* Fuel, 2014. 117: p. 1231-1241.

91. Paviet, F., F. Chazarenc, and M. Tazerout, *Thermo chemical equilibrium modelling of a biomass gasifying process using ASPEN PLUS.* International Journal of chemical reactor engineering, 2009. **7**(1).
92. Joshi, R.R. and B. Kulkarni, *Simulation of biomass gasification reactor for fuel in gas turbine.* International Journal of Chemical Sciences and Applications, 2012. **3**(1): p. 232-240.
93. Chowdhury, R., P. Bhattacharya, and M. Chakravarty, *Modelling and simulation of a downdraft rice husk gasifier.* International Journal of Energy Research, 1994. 18(6): p. 581-594.
94. Tigabwa Y. Ahmed, M.M.A., Suzana Yusup, Abrar Inayat, Zakir Khan, *Mathematematical and computational approaches for design of biomass gasification for hydrogen production: A Review.* Renewable & Sustainable Energy Reviews, 2012. 16

95. E, S., *Catalytic steam gasification of biomass surrogates: a thermodynamic and kinetic approach.* Chem Biochem Eng. London, Ontario, Canada: university of Western Ontario, 2010: p. 266.
96. wang, Y.K.C.M., *Kinetic model of biomass gasification.* Solar Energy, 1993. 51(1): p. 19-25.
97. Chee, C.S., *The air gasification of wood chips in a downdraft gasifier.* 1987.
98. Senelwa, K.A., *Air gasification of woody biomass from short rotation forests: opportunities for small scale biomass-electricity systems: a thesis submitted in partial fulfilment of the requirements for the degree of Doctor of Philosophy in Agricultural Engineering at Massey University, New Zealand*. 1997, Massey University.
99. Babu, B.V. and P.N. Sheth, *Modeling and simulation of reduction zone of downdraft biomass gasifier: Effect of char reactivity factor.* Energy Conversion and Management, 2006. 47(15-16): p. 2602-2611.
100. Di Blasi, C., *Modeling wood gasification in a countercurrent fixed-bed reactor.* AIChE Journal, 2004. 50(9): p. 2306-2319.
101. Di Blasi, C. and C. Branca, *Modeling a stratified downdraft wood gasifier with primary and secondary air entry.* Fuel, 2013. 104: p. 847-860.
102. Horton, S.R., et al., *Molecular-level kinetic modeling of biomass gasification.* Energy & Fuels, 2015. 30(3): p. 1647-1661.
103. Saravanakumar, A., et al., *Numerical modelling of a fixed bed updraft long stick wood gasifier.* biomass and bioenergy, 2011. 35(10): p. 4248-4260.
104. Gordillo, E. and A. Belghit, *A downdraft high temperature steam-only solar gasifier of biomass char: a modelling study.* Biomass and bioenergy, 2011. 35(5): p. 2034-2043.
105. Inayat, A., et al., *Process modeling for parametric study on oil palm empty fruit bunch steam gasification for hydrogen production.* Fuel processing technology, 2012. 93(1): p. 26-34.
106. Smith, J.D., et al., *Validation and Application of a Kinetic Model for Downdraft Biomass Gasification Simulation.* Chemical Engineering & Technology, 2019. 42(12): p. 2505-2519.
107. S. jarungthammachote, A.D., *Equilibrium modeling of gasification : Gibbs free enegy minimization approach and its application to stouted bed and spout-fluid bed gasifiers.* 2008. 49: p. 1345 -1356.
108. WC, R., *The element potentials method for chemical equilibrium analysis : implementation in the interactive programme STANJAN*, in *Department of mechanical Engineering, Stanford University*. 1986.
109. Altafini, C.R., Mirandola A.A, *Equilbrium model of coal gasification process based on minimization of Gibbs free energy*. 1997: In: Flowers 97, Floreence, Italy.
110. Tapas, k.P., Patrik, N. S., *Biomass gasification models for downdraft gasifier: A- state- of-the- art review.* Renewable and Sustainable Energy Reviews, 2015. 50: p. 583-593.
111. Chern, S.-M.W., Walawender, WP., Fan, LT., *Equilibrium modelling of a downdraft gasifier i-overall gasifier .* Chemical Engineering Community, 1991. 108: p. 243-265.

112. Zainal, Z.A., et al., *Prediction of performance of a downdraft gasifier using equilibrium modeling for different biomass materials.* Energy Conversion and Management, 2001. 42(12): p. 1499-1515.
113. S. Jarunthammachote, A.D., *Thermodynamic equilibrium model and second law analysis of a downdraft waste gasifier.* science direct, 2007. **32**: p. 1660-1669.
114. Jayah, T.H., Aye, L., Fuller, R. J., Stewart, D. F, *Computer simulation of a downdarft gasifier for tea drying* International technology centre, 2003. **3**: p. 11.
115. Jarunthammachote, S., Dutta, A., *Equilibrium modeling of gasification : Gibbs free energy minimisation approach and its application to spouted bed and spout-fluid bed gasifiers.* Energy conversion and management, 2008. **49:** p. 1345-1356.
116. Vaezi, M., M. Passandideh Fard, and M. Moghiman. *Modeling Biomass Gasification: A New Approach to UtilizeRenewable Sources of Energy*. in *The 2008 ASME International Mechanical Engineering Congress and Exposition*. 2008.
117. Ratnadhariya, J.K. and S.A. Channiwala, *Three zone equilibrium and kinetic free modeling of biomass gasifier – a novel approach.* Renewable Energy, 2009. 34(4): p. 1050-1058.
118. Sharma, A.K., *Equilibrium and kinetic modeling of char reduction reactions in a downdraft biomass gasifier: A comparison.* Solar Energy, 2008. **82**(10): p. 918-928.
119. Antolini, D., et al., *Experimental and modeling analysis of Air and CO2 biomass gasification in a reverse lab scale downdraft gasifier.* Energy Procedia, 2019. 158: p. 1182-1187.
120. Pepiot, P., C. Dibble, and T. Foust, *Computational fluid dynamics modeling of biomass gasification and pyrolysis.* Computational modeling in lignocellulosic biofuel production, 2010: p. 273-298.
121. Janajreh, I. and M. Al Shrah, *Numerical and experimental investigation of downdraft gasification of wood chips.* Energy Conversion and Management, 2013. **65**: p. 783-792.
122. Rogel, A. and J. Aguillon, *The 2D Eulerian approach of entrained flow and temperature in a biomass stratified downdraft gasifier.* American Journal of Applied Sciences, 2006. **3**(10): p. 2068-2075.
123. Gao, J., et al., *Experiments and numerical simulation of sawdust gasification in an air cyclone gasifier.* Chemical engineering journal, 2012. **213**: p. 97-103.
124. Dogru, M., et al., *Gasification of hazelnut shells in a downdraft gasifier.* Energy, 2002. **27**(5): p. 415-427.
125. Pacelli, V. and M. Azzollini, *An artificial neural network approach for credit risk management.* Journal of Intelligent Learning Systems and Applications, 2011. **3**(02): p. 103.
126. Brown, D., T. Fuchino, and F. Maréchal, *Solid fuel decomposition modelling for the design of biomass gasification systems.* Computer Aided Chemical Engineering, 2006. **21**: p. 1661-1666.
127. Gu, J., et al., *Differences in gasification behaviors and related properties between entrained gasifier fly ash and coal char.* Energy & Fuels, 2008. **22**(6): p. 4029-4033.
128. S. jarungthammachote, A.D., *Thermodynamic equilibrium and second law analysis of a downdraft waste gasifier.* Science Direct, 2007. **32**: p. 1660 - 1669.
129. Shabbar Syed, I.J., Chauki Ghenai, *Thermodynmics Equillibrium Analysis within the Entrained Flow Gasifier Enviroment.* 2012. **4**(1): p. 47-54.
130. Perry, R.H., D. Green, and J. Maloney, *Chemical Engineers Handbook. 6th*. 1997, New York: McGraw-Hill.
131. Koroneos, C. and S. Lykidou, *Equilibrium modeling for a dwndraft biomass gasifier for cotton stalks biomass in comparison with experimental data.* Journal of Chemical Engineering and Materials Science, 2011. **2**(4): p. 61-68.
132. Gao, N., et al., *Hydrogen-rich gas production from biomass steam gasification in an updraft fixed-bed gasifier combined with a porous ceramic reformer.* International Journal of Hydrogen Energy, 2008. **33**(20): p. 5430-5438.

133. Dejtrakulwong, C. and S. Patumsawad, *Four zones modeling of the downdraft biomass gasification process: effects of moisture content and air to fuel ratio.* Energy Procedia, 2014. **52**: p. 142-149.
134. Centeno, F., et al., *Theoretical and experimental investigations of a downdraft biomass gasifier-spark ignition engine power system.* Renewable Energy, 2012. 37(1): p. 97-108.
135. Li, X., et al., *Equilibrium modeling of gasification: a free energy minimization approach and its application to a circulating fluidized bed coal gasifier.* Fuel, 2001. 80(2): p. 195-207.
136. Koukkari, P. and R. Pajarre, *Calculation of constrained equilibria by Gibbs energy minimization.* Calphad, 2006. **30**(1): p. 18-26.
137. Jarungthammachote, S. and A. Dutta, *Equilibrium modeling of gasification: Gibbs free energy minimization approach and its application to spouted bed and spout-fluid bed gasifiers.* Energy Conversion and Management, 2008. 49(6): p. 1345-1356.
138. people.clarkson.edu/~wwilcox/Design/HYSYSpropSelect.pdf. *A property methods and calculation*.
139. Proust, P. and J. Vera, *PRSV: The stryjek-vera modification of the peng-robinson equation of state. Parameters for other pure compounds of industrial interest.* The Canadian Journal of Chemical Engineering, 1989. 67(1): p. 170-173.
140. Bassyouni, M., et al., *Date palm waste gasification in downdraft gasifier and simulation using ASPEN HYSYS.* Energy conversión and management, 2014. 88: p. 693-699.
141. Žecová, M. and J. Terpák, *Mathematical Modeling of Gasification and Combustion of Biomass in Matlab.* 2010.
142. Nikoo, M.B. and N. Mahinpey, *Simulation of biomass gasification in fluidized bed reactor using ASPEN PLUS.* Biomass and Bioenergy, 2008. 32(12): p. 1245-1254.
143. Telmo, C. and J. Lousada, *Heating values of wood pellets from different species.* Biomass and bioenergy, 2011. 35(7): p. 2634-2639.
144. Rockwood, D.L., et al., *Energy product options for Eucalyptus species grown as short rotation woody crops.* International journal of molecular sciences, 2008. **9**(8): p. 1361-1378.
145. Krukanont, P. and S. Prasertsan, *Geographical distribution of biomass and potential sites of rubber wood fired power plants in Southern Thailand.* Biomass and bioenergy, 2004. **26**(1): p. 47-59.
146. Shuit, S.H., et al., *Oil palm biomass as a sustainable energy source: A Malaysian case study.* Energy, 2009. 34(9): p. 1225-1235.
147. Doherty, W., A. Reynolds, and D. Kennedy, *The effect of air preheating in a biomass CFB gasifier using ASPEN Plus simulation.* Biomass and bioenergy, 2009. **33**(9): p. 1158-1167.
148. Sulaiman, S., et al., *Feasibility study of gasification of oil palm fronds SA Sulaiman1, S. Balamohan2, MNZ Moni1, SM Atnaw3 and AO Mohamed4.*
149. Dr. Matthew J. Traum, M.S.o.E., *An Inexpensive Inverted Downdraft Biomass Gasifier for Experimental Energy-*

Thermal-Fluids Demonstrations, in *ASEE Annual Conference & Expositition*. 2013, American Society for Engineering Education: Atlanta. p. 16.
150. Bacon, D., et al., *Modelling of fluidized bed wood gasifiers*, in *Fundamentals of thermochemical biomass conversion*. 1985, Springer. p. 717-732.
151. K. Manish., P.B., Y, Singh, *Effect of Moisture Content and Equivalence Ratio on the Gasification Process for Different Biomass Fuel.* International Journal of mechanical Engineering and Technology(IJMET), 2016. **7**(6): p. 209-220.
152. Gunarathne, D., et al., *The Effect of Throat Diameter on the Performance a Downdraft Biomass Gasifier.* International Journal of Energy Engineering, 2013. **3**(3): p. 171-175.
153. Jarungthammachote, S. and A. Dutta, *Thermodynamic equilibrium model and second law analysis of a downdraft waste gasifier.* Energy, 2007. **32**(9): p. 1660-1669.
154. Kumar, A., D. Jones, and M. Hanna, *Thermochemical biomass gasification: a review of the current status of the technology.* Energies, 2009. **2**(3): p. 556-581.

155. Lv, P., et al., *An experimental study on biomass air–steam gasification in a fluidized bed.* Bioresource technology, 2004. **95**(1): p. 95-101.
156. Werther, J., et al., *Combustion of agricultural residues.* Progress in energy and combustion science, 2000. **26**(1): p. 1-27.
157. Sheth, P.N. and B. Babu, *Experimental studies on producer gas generation from wood waste in a downdraft biomass gasifier.* Bioresource Technology, 2009. 100(12): p. 3127-3133.
158. Hanping, C., et al., *Experimental investigation of biomass gasification in a fluidized bed reactor.* Energy & Fuels, 2008. **22**(5): p. 3493-3498.
159. Sun, K., *Optimization of biomass gasification reactor using Aspen Plus*. 2015, Høgskolen i Telemark.
160. Mahishi, M.R. and D. Goswami, *Thermodynamic optimization of biomass gasifier for hydrogen production.* International Journal of Hydrogen Energy, 2007. **32**(16): p. 3831-3840.
161. Turn, S., et al., *An experimental investigation of hydrogen production from biomass gasification.* International journal of hydrogen energy, 1998. **23**(8): p. 641-648.
162. Institute, E.a.R., *Application of Biomass gasifier technology for thermal application in food processing unit in India*. 2010, GNESD Energy Access Knowledge Base: India.
163. Shafizadeh, F., *Introduction to pyrolysis of biomass.* Journal of Analytical and Applied Pyrolysis, 1982. **3**(4): p. 283-305.
164. P.M. Lv, Z.H.X., J. Chang, C.Z. Wu, Y. Chen, J.X. Zhu, *An experimental study on biomass air–steam gasification.* elsevier, 2004. **95**: p. 95-101.

Appendix – MATLAB code for modelling a gasification reactor

Input file

```
function[feedstock,Ta,Tr,air,pdimd,pdimid,pthickness,kp,odimd,odimid,othickness,ko,rdimd,rdimid]=inputdata
feedstock = 'wood chips'; %Specify feedstock type, either 'wood chips' or 'wood pellets'.
%fc = 3.1; %Specify feedstock consumption in kg/hr.
%moisture = 0.1
%7.36; %Specify moisture (water) content of the feedstock as a percentage of its total consumption
Ta = 25; %Specify outside ambient temperature in degrees C.

%---------------------------------------PYROLYSIS ZONE-----------------------------------------%
pdimd = 272; %Specify depth of the pyrolysis chamber in mm.
pdimid = 206.5; %Specify inner diameter of the pyrolysis chamber in mm.
pthickness = zeros (3,1);
pthickness (1,1) = 6.3; %Specify thickness of the innermost wall of pyrolysis chamber in mm.
pthickness (2,1) = 3; %Specify thickness of the middle wall of the pyrolysis chamber in mm.
%pthickness (3,1); %Specify thickness of the outermost wall of the pyrolysis chamber in mm.
kp = zeros (3,1);
kp (1) = 54; %Specify conductivity of the innermost wall of the pyrolysis chamber in W/mK.
kp (2) = 0.05; %Specify conductivity of the middle wall of the pyrolysis chamber in W/mK.
%kp (3) = %Specify conductivity of the middle wall of the pyrolysis chamber in W/mK.
```

```
%------------------------OXIDATION ZONE---------------------------------%
air = 6.3/3600; %Specify air input mass flow rate in kg/s.
%air = 55.6/3600;
odimd = 100; %Specify depth of the oxidation chamber in mm.
odimid = 206.5; %Specify inner diameter of the oxidation chamber in mm.
thickness = zeros (3,1);
othickness (1,1) = 53; %Specify thickness of the innermost wall of oxidation chamber in mm.
othickness (2,1) = 6.3; %Specify thickness of the middle wall of the oxidation chamber in mm.
othickness (3,1) = 3; %Specify thickness of the outermost wall of the oxidation chamber in mm.
ko = zeros (3,1);
ko (1,1) = 17; %Specify conductivity of the innermost wall of the oxidation chamber in W/mK.
ko (2,1) = 54; %Specify conductivity of the middle wall of the oxidation chamber in W/mK.
ko (3,1) = 0.05; %Specify conductivity of the middle wall of the oxidation chamber in W/mK.

%--------------------------REDUCTION ZONE-------------------------------%
%rdimd = 105; %Specify depth of the reduction chamber in mm.
rdimd = 220;
rdimid = 88; %Specify inner diameter of the reduction chamber in mm.
%rdimid=100;
Tr = 950; %Specify temperature of the reduction zone. Use only for the reduced model.
end
```

Pyrolysis file

```
function[ArC,ArH,ArO,moisturefrac,mdot,mash,mchar,wH2O,npH2O,npCO,npCO2,
npH2,npCH4,npC2H2,npC]=pyro
%clear;
%clf;
[feedstock,Ta,Tr,air,pdimd,pdimid,pthickness,kp,odimd,odimid,othickness,ko,rdimd,
rdimid]=inputdata;
ArC=12.011; %molar mass of carbon
ArH=1.008;  %molar mass of hydrogen
ArO=15.999; %molar mass of oxygen
Ars= [ArC ArH ArO]';
nfracC=1; %molar fraction of carbon in feedstock. This is always 1 as mole fractions
are expressed as CHmOn
z=0;
while z==0
   if     strcmp (feedstock,'wood chips') ==1
          nfracH=1.586; %molar fraction of volatile hydrogen in wood chips.
          nfracO=0.7089; %molar fraction of volatile oxygen in wood chips.
          moisturefrac=0.0736; %moisture fraction of wood chips by mass.
          %moisturefrac=0;
          charfrac=0.173; %fixed carbon (char) fraction in wood chips by mass.
          ashfrac=0.000338;%ash fraction in wood chips by mass.
          mdot=3.1/3600; %consumption of wood chips in kg/h/3600 = kg/s.
          z=1;
elseif strcmp (feedstock,'wood pellets') ==1
         nfracH=1.615;%molar fraction of volatile hydrogen in wood pellets.
          nfracO=0.664; %molar fraction of volatile oxygen in wood pellets.
          moisturefrac=0.05; %moisture fraction of wood pellets by mass.
          charfrac=0.08; %fixed carbon (char) fraction in wood pellets by mass.
          ashfrac=0.000574;%ash fraction in wood pellets by mass.
          mdot=2.9/3600; %consumption of wood pellets in kg/h/3600 = kg/s.
          z=1;
   elseif strcmp(feedstock,'other')==1
```

```
        nfracH=1.541;%molar fraction of volatile hydrogen in other biomass.
        nfracO=0.6225;%molar fraction of volatile oxygen in other biomass.
        moisturefrac=0.0855; %moisture fraction of other biomass by mass.
        charfrac=0.08;      %fixed carbon (char) fraction in other biomass by mass.
        mdot=23.5/3600;     %consumption of other biomass in kg/h/3600 = kg/s
        z=1;
    else
    x=input('unrecognized feedstock in input data, please enter 1 for wood chips, 2 for
wood pellets, or 3 for other biomass');
        if    x==1
            feedstock='wood chips';
            break;
        elseif x==2
            feedstock='wood pellets';
            break;
        elseif x==3
            feedstock='other';
            break;
        else   break;
        end
    end
end

mash=mdot*ashfrac;              %mass of ash in feedstock, kg/s
mchar=mdot*charfrac;            %mass of fixed carbon in feedstock, kg/s
mwater=mdot*moisturefrac;       %mass of moisture in feedstock, kg/s
mvolatile=mdot-mash-mchar-mwater; %mass of volatiles in feedstock, kg/s
CbC=1000*mchar/ArC;                 %moles of fixed carbon in feedstock
wH2O=(1000*mwater)/(2*ArH+ArO);         %moles of water in feedstock moisture
volatiles_mass_ratio=[nfracC*ArC nfracH*ArH nfracO*ArO]'; %mass ratio of
volatiles [rCv rHv rOv]'
volatiles_mass_fractions=(1/sum(volatiles_mass_ratio))*volatiles_mass_ratio;
%mass fractions of volatiles [%C %H %O]'
```

```
volatiles_mdot=mvolatile*volatiles_mass_ratio; %consumption of volatiles in kg/s [mdot mdot mdotO]'
volatiles_moles = 1000*volatiles_mdot./Ars; %molar consumption of volatiles in mol/s or number of moles of each volatile [CvbC HbvH ObvO]

bvC=volatiles_moles(1,1);
bvH=volatiles_moles(2,1);
bvO=volatiles_moles(3,1);

%Products' amounts calculated from mass balance equation and assumptions:

npH2O =0.8*bvO + wH2O;
npCO   =0.2*bvO*44/(44+28);
npCO2 =0.2*bvO*28/(44+28);
npH2   =0.5*(bvH-2*0.8*bvO) *0.5;
npCH4  =0.5*(bvH-2*0.8*bvO)*26/(26+16);
npC2H2 =0.5*(bvH-2*0.8*bvO)*16/(26+16);
npC    =CbC+bvC-npCO-npCO2-npCH4-2*npC2H2;

ArN=14.007;
%Calculate moles of oxygen and nitrogen entering oxidation zone
a=((air*1000/(2*ArO+(3.76*2*ArN)))/2);
%a=air*1000/(2*ArO+(3.76*2*ArN)); %Here 1:3.71 is taken as the molar fraction between O2 and N2 in the atmosphere.
                %If we are to assume atmospheric constituents behave as ideal gases and the
                %volumetric fraction is ~78% N2 and ~21% O2 and 1% Ar (78/21 = 3.71).
                %The literature uses 3.76 instead of 3.71, assuming that the atmosphere contains
                %only N2 and O2 in a 79:21 ratio (and think why, you tool! I'm putting it back to 3.76).

npO2=a;
```

```
%Assumption 1 - calculate moles of products from total oxidation of acetylene.
if npO2 ~=0
   if npO2>(2.5*npC2H2)
      npCO2=2*npC2H2+npCO2;
      npH2O=npC2H2+npH2O;
      npO2 =npO2-2.5*npC2H2;
   else
      npCO2=0.8*npO2+npCO2;
      npH2O=0.4*npO2+npH2O;
      npO2=0;
   end
else
   npCO2=npCO2;
   npH2O=npH2O;
   npO2=0;
end
%Assumption 2 - calculate moles of products from oxidation of H2
if npO2 ~=0
   if npO2>0.5*npH2          %If there is more oxygen than required to completely
oxidize H2
      npH2O=npH2O+npH2;
      npH2=0;
      npO2 =npO2-0.5*npH2;
   else                      %If there is less oxygen than required to completely oxidize H2
      npH2O=npH2O+2*npO2;
      npH2 =npH2-2*npO2;
      npO2 =0;
   end
else
   npH2=npH2;
end

%New assumption - calculate moles of products from oxidation of CH4
if npO2 ~=0
```

```
   if npO2>2*npCH4            %If there is more oxygen than required to completely oxidise CH4
      npH2O=npH2O+2*npCH4;
      npCO2=npCO2+npCH4;
      npCH4=0;
      npO2 =npO2-2*npCH4;
   else                       %If there is less oxygen than required to completely oxidise CH4
      npH2O=npH2O+npO2;
      npCO2=npCO2+0.5*npO2;
      npCH4=npCH4-0.5*npO2;
      npO2 =0;
   end
else
   npCH4=npCH4;
end
%Assumptions 3 & 4 - Remaining oxygen (if any) is consumed in the reduction of char and
%CO2 and CO are produced in the ratio 1:3.5606
%combined formula: 4.5606C + 2.7803O2 --> 3.5606CO + CO2

if npO2 ~=0
   if npO2<(2.7803/4.5606)*npC        %If there is enough char to completely use up remaining oxygen
      npCO =(3.5606/2.7803)*0.5*npO2+npCO;
      npCO2=npCO2+(1/2.7803)*npO2;
      npC  =npC-(4.5606/2.7803)*npO2;
      npO2=0;
   else                       %If there isn't enough char to completely use up remaining oxygen
      npCO =(3.5606/4.5606)*npC+npCO;
      npCO2=npCO2+(1/4.5606)*npC;
      npC=0;
      npO2=npO2-(2.7803/4.5606)*npC;
   end
```

```
else %If there isn't any oxygen left to react with any char at all.
   npC=npC;
   npCO=npCO;
end

%Assumption 5 - amounts of CO, CO2 and H2O produced in the oxidation zone
%have been added to the amounts produced in the pyrolysis zone.

%Assumption 6 - N2 doesn't react
npN2=3.76*a;

species   =['H2O' 'CO' 'CO2' 'H2' 'CH4' 'C2H2' 'C'];
moles     =[npH2O npCO npCO2 npH2 npCH4 npC2H2 npC];
%masses    =moles.*[18 28 44 2 16 26 12]*0.001;
fractions=moles*(1/sum(moles))

figure(1)
bar(fractions);
title(['Mole fractions of gases by produced in the pyrolysis zone from ',feedstock]);
set(gca,'XTick',1:7);
set(gca,'XTickLabel',[164'H2','CH4','C2H2','C']);

end
```

Oxidation file

```
function [moles,masses,Mrs,Trc]=oxi
[feedstock,Ta,Tr,air,pdimd,pdimid,pthickness,kp,odimd,odimid,othickness,ko,rdimd,
rdimid]=inputdata;
%[npH2O npCO npCO2 npH2 npCH4 npC2H2 npC]=moles;
%[ArC,ArH,ArO,moisturefrac,mdot,mash,mchar,wH2O,npH2O,npCO,npCO2,npH2,
npCH4,npC2H2,npC]=pyro2
[ArC,ArH,ArO,moisturefrac,mdot,mash,mchar,wH2O,npH2O,npCO,npCO2,npH2,n
pCH4,npC2H2,npC]=pyro;
ArN=14.007;
```

```
%Calculate moles of oxygen and nitrogen entering oxidation zone
a=air*1000/(2*ArO+(3.76*2*ArN)); %Here 1:3.71 is taken as the molar fraction between O2 and N2 in the atmosphere.
%If we are to assume atmospheric constituents behave as ideal gases and the
%volumetric fraction is ~78% N2 and ~21% O2 nd 1% Ar (78/21 = 3.71).
%The literature uses 3.76 instead of 3.71, assuming that the atmosphere contains
%only N2 and O2 in a 79:21 ratio (and think why, you tool! I'm putting it back to 3.76).
 noO2=a;
%Assumption 1 - calculate moles of products from total oxidation of acetylene.
if noO2 ~=0
   if noO2>(2.5*npC2H2)
      noCO2=2*npC2H2+npCO2;
      noH2O=npC2H2+npH2O;
      noO2 =noO2-2.5*npC2H2;
   else
      noCO2=0.8*npO2+npCO2;
      noH2O=0.4*npO2+npH2O;
      noO2=0;
   end
else
   noCO2=npCO2;
   noH2O=npH2O;
   noO2=0;
end
%Assumption 2 - calculate moles of products from oxidation of H2
if noO2 ~=0
   if noO2>0.5*npH2          %If there is more oxygen than required to completely oxidize H2
      noH2O=noH2O+npH2;
      noH2=0;
      noO2 =noO2-0.5*npH2;
   else                      %If there is less oxygen than required to completely oxidize H2
      noH2O=noH2O+2*noO2;
      noH2 =npH2-2*noO2;
```

```
        noO2 =0;
    end
else
    noH2=npH2;
end

%New assumption - calculate moles of products from oxidation of CH4
if noO2 ~=0
    if noO2>2*npCH4             %If there is more oxygen than required to completely
oxidize CH4
        noH2O=noH2O+2*npCH4;
        noCO2=noCO2+npCH4;
        noCH4=0;
        noO2 =noO2-2*npCH4;
    else                        %If there is less oxygen than required to completely oxidize CH4
        noH2O=noH2O+noO2;
        noCO2=noCO2+0.5*noO2;
        noCH4=npCH4-0.5*noO2;
        noO2 =0;
    end
else
    noCH4=npCH4;
end
%Assumptions 3 & 4 - Remaining oxygen (if any) is consumed in the reduction of
char and
%CO2 and CO are produced in the ratio 1:3.5606
%combined formula: 4.5606C + 2.7803O2 --> 3.5606CO + CO2

if noO2 ~=0
    if noO2<(2.7803/4.5606)*npC             %If there is enough char to completely use
up remaining oxygen
        noCO = (3.5606/2.7803) *0.5*noO2+npCO;
        noCO2=noCO2+(1/2.7803)*noO2;
        noC =npC-(4.5606/2.7803) *noO2;
```

```
        noO2=0;
    else  %If there isn't enough char to completely use up remaining oxygen
        noCO =(3.5606/4.5606)*npC+npCO;
        noCO2=noCO2+(1/4.5606) *npC;
        noC=0;
        noO2=noO2-(2.7803/4.5606) *npC;
    end
else %If there isn't any oxygen left to react with any char at all.
    noC=npC;
    noCO=npCO;
end
%Assumption 5 - amounts of CO, CO2 and H2O produced in the oxidation zone
%have been added to the amounts produced in the pyrolysis zone.

%Assumption 6 - N2 doesn't react
noN2=3.76*a;
%Carbon mass balance to calculate noCH4
%noCH4=npC+npCO2+npCO+npCH4+2*npC2H2-noC-noCO2-noCO;
%Energy balance to calculate reduction zone entry temperature.

Trc                                                                    =
energybalance(Ta,Tr,pdimd,pdimid,pthickness,kp,odimd,odimid,othickness,ko,mdot,
a,wH2O,mash,mchar,noH2O,noCO,noCO2,noH2,noCH4,noN2,noC);

species     =['H2O' 'CO' 'CO2' 'H2' 'CH4' 'N2' 'C' 'O2'];
moles       =[noH2O noCO noCO2 npH2 noCH4 noN2 noC noO2];
Mrs         =[18 28 44 2 16 28 12 32];
masses      =moles.*Mrs*0.001;
fractions =moles*(1/sum(moles));
figure(2);
bar(fractions);
title(['Mole fractions of gases produced in the oxidation zone from ',feedstock]);
set(gca,'XTick',1:7);
set(gca,'XTickLabel',{'H2O','CO','CO2','H2','CH4','N2','C','O2'});
```

end

Reduction Zone file

```
clear
%'inputdata'
[feedstock,Ta,Tr,air,pdimd,pdimid,pthickness,kp,odimd,odimid,othickness,ko,rdimd,
rdimid]=inputdata;
%'pyro'
[ArC,ArH,ArO,moisturefrac,mdot,mash,mchar,wH2O,npH2O,npCO,npCO2,npH2,n
pCH4,npC2H2,npC,Mc,Mbmass]=pyro;
%'oxi'
[moles,masses,Mrs,Trc]=oxi;
%-------------------------------------------------------------------------------%
%---------------------------------- CONSTANTS ----------------------------------%
%-------------------------------------------------------------------------------%
rdimd = 220;
z=rdimd*0.001; %reaction zone depth
C=1; %Char reactivity factor's linear coefficient
b=30; %Char reactivity factor's exponential coefficient (CRF=C*exp(b*z)) if b=0,
then CRF doesn't vary with chamber depth, z. Nominal: C=1, b=28 to vary
exponentially between 0 and ~8000
%b=42;
Patm=101325; %atmospheric pressure, 101,325 Pa
R=8.314472; %Universal gas constant in J/mol.K
Ra=286.9; %specific gas constant for air, 286.9 J/Kg.K
Ta = 25;
rhoair=Patm/(Ra*(Ta+273)); %density of air at ambient temperature
Aip=(pi*0.008^2); %cross-sectional area of air inlet pipe.
air = 6.3/3600;
vair=air/(rhoair*Aip); %air velocity at air inlet pipe (that has an ID of 16mm)
rdimid = 88;
Ac=pi*(0.5*rdimid*0.001) ^2; %cross-sectional area of the reduction zone
```

```
g=[-228610 -137160 -394390 0 -50790 0]; %Gibbs functions of formation for each species
g=-1. *g;
%-----------------------------------------------------------------------------------------%
% Frequency factors, Ai (1/s), activation energies, Ei (J/mol) and reaction enthalpies, H (J/mol) %
%-----------------------------------------------------------------------------------------%
A=zeros (1,4); E=zeros (1,4);H=zeros(1,4);
%Reaction 1: C + CO2 <--> 2CO
A(1,1)=36.16;    E(1,1)=77390;  H(1,1)=-172600;

%Reaction 2: C + H2O <--> CO + H2
A (1,2) =15170; E(1,2)=121620; H(1,2)=-131400;

%Reaction 3: C + 2H2 <--> CH4
A (1,3)=0.004189; E(1,3)=19210;  H(1,3)=75000;

%Reaction 4: CH4 +H2O <--> CO + 3H2
A(1,4)=0.07301;  E(1,4)=36150;  H(1,4)=-206400;

H=-1.*H;
%-----------------------------------------------------------------------------------%
%---------------------------------- INITIAL CONDITIONS ----------------------------%
%-----------------------------------------------------------------------------------%
Po=Patm*1.005; %initial operating pressure of the reduction zone (so used by Babu & Sheth 2006)
n=moles (1,1:6)'; %moles of gaseous components exiting oxidation zone
P=(Po/sum(n)) *n; %partial pressures of gaseous components
%T=(Tr+273); %Use this expression if using reduced model
T=Trc;%Use this expression if using full model
rhogas=0.001*(Mrs(1,1:6)*P)/(R*T); %total density
v=0.001*Mrs(1,1:6)*n/(rhogas*Ac); %velocity
%v=1.175;
nc=(1/(Ac*v)) *n; %molar concentrations
```

```
f0= [Po v T [nc(1) nc(2) nc(3) nc(4) nc(5) nc(6)]];
%-------------------------------------------------------------------------%
%-------------------------------- THE INTEGRATOR ---------------------------%
%-------------------------------------------------------------------------%
%For the use of ODE45 to integrate the ODEs, the functions for pressure,
%velocity, temperature and molar concentrations are contained within
%function vector f:
%f(1)=P, f(2)=v, f(3)=T, f(4)=nx(1), f(5)=nx(2),...,f(9)=nx(6).
p=zeros (1,28);
p(1:6) =Mrs(1:6);
%p(7:12) =c(1:6);
p(13:16) =H (1:4); p(17)=Ra; p(18)=R; p(19)=Ac; p(20)=b; p(21:24)=A(1:4);
p(25:28)=E(1:4); p(29)=C;
p(30:35)=g;
%opts = odeset('RelTol',1e-3,'AbsTol',1e-3);
[Z,F]=ode45(@gradients,[0 z],f0,[],p);
[i j]=size(F);
last_concs=F(i,4:9);
last_values=(Ac*F(i,2))*last_concs; %moles of gaseous species exiting the reduction
zone
mole_fractions=(1/sum(last_values)).*last_values
%dry_mole_fractions=(1/sum(F(i,5:9)).*F(i,5:9))
dry_mole_fractions=(1/sum(last_values(1,2:6)).*last_values(1,2:6))
partial pressures=F(i,1). *mole_fractions;
cool_concs=(1/(R*293)).*partial pressures;
%mdot=Ac*v*(Mrs(1:6).*last_values);
mdot=Mrs(1:6).*last_values;
mass fractions=(1/sum(mdots))*mdots';
LHV=[0 10900 0 120100 50100 0]; %[H2O CO CO2 H2 CH4 N2]
LHVm=[0 283 0 244 801 0]';
LHVt=LHV*mass_fractions;
LHVg=cool_concs*LHVm;
fprintf('Total LHV of the gas exiting the gasifier is %f kJ/kg\n',LHVt);
```

```
fprintf('Total LHV of the gas exiting the gasifier is %f kJ/m^3\n',LHVg);
figure(3)
plot(Z,F(:,1),'.')
figure(4)
plot(Z,F(:,2),'.')
figure(5)
plot(Z,F(:,3),'.')
figure(6)
plot(Z,F(:,4),'-',Z,F(:,5),'-',Z,F(:,6),'-',Z,F(:,7),'-',Z,F(:,8),'-',Z,F(:,9),'-')
xlabel('Depth of reduction zone (m)');
ylabel('Molar concentration (mol/m3)');
title('Gas species concentration profile');
hleg1=legend('H2O','CO','CO2','H2','CH4','N2');
%figure(7)
%bar(F(i,4:9));
%title(['Molar concentrations of gases leaving the reduction zone from ',feedstock]);
%set(gca,'XTick',1:7);
%set(gca,'XTickLabel',{'H_2O','CO','CO_2','H_2','CH_4','N_2'});
%figure(8)
%bar(mass_fractions);
%title(['Final gas composition, by mass, for ',feedstock]);
%set(gca,'XTick',1:7);
%
%set(gca,'XTickLabel',{'H_2O','CO','CO_2','H_2','CH_4','N_2'});
figure(7)
bar(mole_fractions);
title(['Final wet gas composition, mole fractions, for ',feedstock]);
set(gca,'XTick',1:6);
set(gca,'XTickLabel',{'H2O','CO','CO2','H2','CH4','N2'});
figure(8)
bar(dry_mole_fractions);
title(['Final dry gas composition, mole fractions, for ',feedstock]);
set(gca,'XTick',1:5);
set(gca,'XTickLabel',{'CO','CO2','H2','CH4','N2'});
```

Energy balance file

```
function Trc = energybalance(Ta,Tr,pdimd,pdimid,pthickness,kp,odimd,odimid,othickness,ko,mdot,a,wH2O,mash,mchar,noH2O,noCO,noCO2,noH2,noCH4,noN2,noC)
%This function evaluates the temperature at exit of the oxidation zone
%and entry to the reduction zone from the energy balance equation across
%the pyrolysis and oxidation zones. It is solved by the Newton-Raphson
%method.

%The energy balance equation "energy of reactants = energy of products"
%is rearranged to take the form
%"Final temperature dependent terms - independent terms = 0"
%To satisfy the f(T)=0 condition for Newton-Rhapson iteration.
%Ambient temperature
T0=Ta+273;
%Enthalpies of formation
hfbm   = -616.6*1000; %J/kg enthalpy of formation for typical wood biomass
hflH2O = -285.83*1000; %J/mol liquid water
hfgH2O = -241.83*1000; %J/mol steam
hfCO   = -110.53*1000; %J/mol carbon monoxide
hfCO2 = -393.52*1000; %J/mol carbon dioxide
hfH2   = 0; %J/mol hydrogen
hfCH4 = -74.87*1000;%J/mol methane
hfN2   = 0;%J/mol nitrogen
hfC    = 0;%J/mol solid carbon
hfO2   = 0;%J/mol oxygen
hfx=zeros(6,1);
hfx(1,1)=hfgH2O;
hfx(2,1)=hfCO;
hfx(3,1)=hfCO2;
hfx(4,1)=hfH2;
hfx(5,1)=hfCH4;
```

```
hfx(6,1)=hfN2;

%Heat capacities for solid species (constants)
Cpwood = 2.3*1000;  %J/kg/K
Cpash  = 0.84*1000; %J/kg/K
Cpchar = 23.4;      %J/mol/K

%Specific enthalpies at room temperature (298K) from Haywood 1990 (steam
%tables)
hsO2  = 8.66*1000; %J/mol oxygen
hsN2  = 8.67*1000; %J/mol nitrogen
hsH2O = 1.886*1000; %J/mol liquid water

%Shomate equation coefficients for gaseous species, Cp = A + BT + CT^2 + DT^3 +
E/T^2 J/mol/K
A=zeros(6,1);    B=zeros(6,1);    C=zeros(6,1);   D=zeros(6,1);   E=zeros(6,1);
A(1,1)=30.092;          B(1,1)=6.832514;        C(1,1)=6.793435;     D(1,1)=-2.53448;
E(1,1)=0.082139;  %H2O
A(2,1)=25.56759;     B(2,1)=6.09613;          C(2,1)=4.054656;     D(2,1)=-2.671301;
E(2,1)=0.131021;  %CO
A(3,1)=24.99735;  B(3,1)=55.18696;   C(3,1)=-33.69137; D(3,1)=7.948387;  E(3,1)=-
0.136638; %CO2
A(4,1)=33.066178;    B(4,1)=-11.363417;    C(4,1)=11.432816;    D(4,1)=-2.772874;
E(4,1)=-0.158558; %H2
A(5,1)=-0.703029;    B(5,1)=108.4773;          C(5,1)=-42.52157;    D(5,1)=5.862788;
E(5,1)=0.678565;  %CH4
A(6,1)=26.092;          B(6,1)=8.218801;        C(6,1)=-1.976141;   D(6,1)=0.159274;
E(6,1)=0.044434;  %N2

%molar values of species at exit from oxidation zone
nx=zeros(1,7);
nx(1,1)=noH2O;
nx(1,2)=noCO;
nx(1,3)=noCO2;
```

```
nx(1,4)=noH2;
nx(1,5)=noCH4;
nx(1,6)=noN2;
nx(1,7)=noC;

%heat loss expressions
h= 25; %Surface heat transfer coefficients in W/m^2K

%n=size(kp,1)+1;
%pr=zeros(n,1);                          %
%pr(1,1)=(pdimid/2)*0.001;                %
%for m=2:n  %array of rp (cylinder radii in pyrolysis zone) values
%    pr(m,1) = pr(m-1,1) + pthickness(m-1,1)*0.001; %
%end                                     %
%par1=pr(1:n-1,1);  %array of rn values
%par2=pr(2:n,1);    %array pf rn+1 values
%pak =kp(:,1);      %array of k values
%pnzak=pak(pak~=0);  %k value array trimmed of 0 elements (to prevent division by
0)
%plr=log(par2./par1);%array of ln(rn+1/rn) values.
%pnzlr=plr(plr~=0);  %ln array trimmed of 0 elements (to prevent division by 0)

%Qp = (pdimd*0.001*2*pi)/(sum(pnzlr./pnzak)+1/(pr(n,1)*h)); %Heat transfer
temperature gradient multiplier for the pyrolysis zone

n=size(ko,1)+1;
or=zeros(n,1);   %
or(1,1)=(odimid/2)*0.001; %
for m=2:n     %array of rp (cylinder radii in oxidation zone) values
   or(m,1) = or(m-1,1) + othickness(m-1,1)*0.001; %
end                                     %

oar1=or(1:n-1,1);  %array of rn values
oar2=or(2:n,1);    %array pf rn+1 values
```

```
oak =ko(:,1);      %array of k values
onzak=oak(oak~=0);  %k value array trimmed of 0 elements (to prevent division by 0)
olr=log(oar2./oar1);%array of ln(rn+1/rn) values.
onzlr=olr(olr~=0);  %ln array trimmed of 0 elements (to prevent division by 0)

Qo = ((odimd*0.001*2*pi)/(sum(onzlr./onzak)+1/(or(n,1)*h))*6); %Heat transfer temperature gradient multiplier for the oxidation zone.
%%Newton Rhapson Scheme
syms T;
guessT=Tr+273;
%f_T=(mdot*hfbm+wH2O*hflH2O)-4737-(nx(1,1:6)*((T-T0)*A+((1/2000)*(T^2-T0^2))*B+((1/(3*(1000^2)))*(T^3-T0^3))*C+((1/(4*(1000^3)))*(T^4-T0^4))*D-((1000^2)*((1/T)-(1/T0)))*E)+nx(1,1:6)*hfx+nx(1,7)*Cpchar*(T-T0)+mash*Cpash*(T-T0));
%Use the above equation for manually fixed heat losses.
%f_T=mdot*hfbm+wH2O*hflH2O-Qo*(T-T0)-(nx(1,1:6)*((T-T0)*A+((1/2000)*(T^2-T0^2))*B+((1/(3*(1000^2)))*(T^3-T0^3))*C+((1/(4*(1000^3)))*(T^4-T0^4))*D-((1000^2)*((1/T)-(1/T0)))*E)+nx(1,1:6)*hfx+nx(1,7)*Cpchar*(T-T0)+mash*Cpash*(T-T0));
f_T=mdot*hfbm+wH2O*(hflH2O+hfgH2O)-Qo*(T-T0)-(nx(1,1:6)*((T-T0)*A+((1/2000)*(T^2-T0^2))*B+((1/(3*(1000^2)))*(T^3-T0^3))*C+((1/(4*(1000^3)))*(T^4-T0^4))*D-((1000^2)*((1/T)-(1/T0)))*E)+nx(1,1:6)*hfx+nx(1,7)*Cpchar*(T-T0)+mash*Cpash*(T-T0));
%Use the above equation for calculated heat losses.
Trc=newton_n_dim(0.0001,guessT,T,f_T); %Trc ('calculated reduction zone temperature') is the temperature at entry to the reduction zone calculated from the energy balance.
end
```

Gradients file

```
function df = gradients(z,f,p)
df=zeros(9,1);
Mrs=p(1:6);
%c=p(7:12);
```

```
H=p(13:16); Ra=p(17); R=p(18); Ac=p(19); b=p(20); A=p(21:24); E=p(25:28);
C=p(29); g=p(30:35);
%%%EVERY VARIABLE IS A ROW VECTOR, APART FROM f(1:9) AND df(1:9)
WHICH ARE
%%%COLUMNS; IF IT'S TRANSPOSED IT'S BECOME A COLUMN VECTOR.
df(1)=1183*(rhogas(Ac,Mrs,R,f(1),f(2),f(3),f(4:9))*(f(2)^2)/rhoair(Ra,f(1),f(3)))+38
8.19*f(2)-79.896; %dP/dz
df(2)=(1/(c(f(3))*f(4:9)+sum(f(4:9))*R))*(((c(f(3))*f(4:9))*sum(srates(Ac,R,b,A,E,f
(1),f(2),f(3),f(4:9),C,z,g))/sum(f(4:9)))-
((rspeeds(Ac,R,b,A,E,f(1),f(2),f(3),f(4:9),C,z,g)*H')/f(3))-
df(1)*(f(2)/f(3)+(f(2)*(c(f(3))*f(4:9))/f(1)))-
(srates(Ac,R,b,A,E,f(1),f(2),f(3),f(4:9),C,z,g)*(c(f(3)))'); %dv/dz
df(3)=(1/(f(2)*c(f(3))*f(4:9)))*(-
1*rspeeds(Ac,R,b,A,E,f(1),f(2),f(3),f(4:9),C,z,g)*H'-f(2)*df(1)-f(1)*df(2)-
(srates(Ac,R,b,A,E,f(1),f(2),f(3),f(4:9),C,z,g)*(c(f(3)))')*f(3)); %dT/dz
df(4:9)=(1/f(2))*((srates(Ac,R,b,A,E,f(1),f(2),f(3),f(4:9),C,z,g))'-(df(2)*f(4:9))); %
dnx/dz
end

%Density and velocity of gas in zone
function gas_density = rhogas(Ac,Mrs,R,P,v,T,nx)
n=Ac*v*nx; %moles of gaseous components exiting the last control volume
Pp=(P/sum(n))*n; %partial pressures of gaseous components
gas_density=0.001*(Mrs*Pp)/(R*T); %total density
end
function air_density = rhoair (Ra, P,T)
air_density=P/(Ra*T);
end
function heat_capacities =c(T) %Species heat capacities in the form Cp = A + Bt +
Ct^2 + Dt^3 + E/t^2
t=T/1000;
Cp (1,1) = 30.092   + 6.832514*t  + 6.793435*(t^2)  - 2.53448*(t^3)  + 0.082139/(t^2);
%Cp H2O
```

```
Cp(1,2)= 25.56759  + 6.09613*t  + 4.054656*(t^2)  - 2.671301*(t^3) - 0.131021/(t^2);
%Cp CO
Cp  (1,3)  =  24.99735  +  55.18696*t  -  33.69137*(t^2)  +  7.948387*(t^3)  -
0.136638/(t^2); %Cp CO2
Cp(1,4)=  33.066178  -  11.363417*t  +  11.432816*(t^2)  -  2.772874*(t^3)  -
0.158558/(t^2); %Cp H2
Cp(1,5)=  -0.703029  +  108.4773*t  -  42.52157*(t^2)  +  5.862788*(t^3)  +
0.678565/(t^2); %Cp CH4
%Cp(1,6)=  26.092  +  8.218801*t  -  1.976141*(t^2)  +  0.159274*(t^3)  +
0.044434/(t^2); %Cp N2 (298-6000K)
Cp(1,6)=  19.50583  +  19.88705*t  -  8.598535*(t^2)  +  1.369784*(t^3)  +
0.527601/(t^2); %Cp N2 (500-2000K)
heat_capacities=Cp;
end

function Rx = srates(Ac,R,b,A,E,P,v,T,nx,C,z,g)
%Equilibrium constants
%K(1,1)=10^(-8992.926/T + 9.183)*P^(2-1);    %
%K(1,2)=10^(-6999.663/T + 7.404)*P^(1+1-1);    % Equations determined according
to Filipe
%K(1,3)=10^(4330.847/T - 5.436)*P^(1-2);     %
%K(1,4)=10^(-11330.509/T + 12.840)*P^(1+3-1-1);  %

K (1,1) =(exp(-2*g(2)/(R*T) + g(3)/(R*T));                    %
K (1,2) =(exp(-g(2)/(R*T) - g(4)/(R*T) + g(1)/(R*T));          %Equations determined
according to Prokash
K (1,3) =(exp(-g(5)/(R*T) + 2*g(4)/(R*T)));                    %
K (1,4) =(exp(-g(2)/(R*T) - 3*g(4)/(R*T) + g(5)/(R*T) + g(1)/(R*T))); %
%Ki=K
%Partial pressures
n=Ac*v*nx; %moles of gaseous components exiting oxidation zone
%c=Cms (1,1:6);
%Pp=(P/sum(n)) *n %partial pressures of gaseous components
%PH2O=Pp (1);
```

```
%PCO =Pp (2);
%PCO2=Pp (3);
%PH2 =Pp (4);
%PCH4=Pp (5);

y=(1/sum(n))*n; %molar fractions of gaseous components
yH2O=y(1);
yCO =y(2);
yCO2=y(3);
yH2 =y(4);
yCH4=y(5);
%Reaction speeds according to Giltrap
%(why are reaction speeds not dependent on total molar gas concentration?)
%r(1,1)=crf(C,b,z)*A(1,1)*exp(-E(1,1)/(R*T))*(PCO2-((PCO2^2)/K(1,1)));
%Reaction 1
%r(1,2)=crf(C,b,z)*A(1,2)*exp(-E(1,2)/(R*T))*(PH2O-((PCO*PH2)/K(1,2)));
%Reaction 2
%r(1,3)=crf(C,b,z)*A(1,3)*exp(-E(1,3)/(R*T))*((PH2^2)-(PCH4/K(1,3)));
%Reaction 3
%r(1,4)=crf(C,b,z)*A(1,4)*exp(-E(1,4)/(R*T))*((PCH4*PH2O)-
((PCO*PH2^3)/K(1,4)));    %Reaction 4

%Reaction speeds according to Babu & Sheth
%(why is CRF used in reaction 4 where no char is involved?)
%r(1,1)=sum(nx)*crf(C,b,z)*A(1,1)*exp(-E(1,1)/(R*T))*(PCO2-
((PCO2^2)/K(1,1)));          %Reaction 1
%r(1,2)=sum(nx)*crf(C,b,z)*A(1,2)*exp(-E(1,2)/(R*T))*(PH2O-
((PCO*PH2)/K(1,2)));         %Reaction 2
%r(1,3)=sum(nx)*crf(C,b,z)*A(1,3)*exp(-E(1,3)/(R*T))*((PH2^2)-(PCH4/K(1,3)));
%Reaction 3
%r(1,4)=sum(nx)*crf(C,b,z)*A(1,4)*exp(-E(1,4)/(R*T))*((PCH4*PH2O)-
((PCO*PH2^3)/K(1,4))); %Reaction 4

%Reaction speeds according to Prokash
```

```
%(why is CRF used in reaction 4 where no char is involved?)
%r(1,1)=sum(nx)*crf(C,b,z)*A(1,1)*exp(-E(1,1)/(R*T))*(yCO2-((yCO^2)/K(1,1)));
%Reaction 1
%r(1,2)=sum(nx)*crf(C,b,z)*A(1,2)*exp(-E(1,2)/(R*T))*(yH2O-
((yCO*yH2)/K(1,2)));          %Reaction 2
%r(1,3)=sum(nx)*crf(C,b,z)*A(1,3)*exp(-E(1,3)/(R*T))*((yH2^2)-(yCH4/K(1,3)));
%Reaction 3
%r(1,4)=sum(nx)*crf(C,b,z)*A(1,4)*exp(-E(1,4)/(R*T))*((yCH4*yH2O)-
((yCO*yH2^3)/K(1,4))); %Reaction 4

%Reaction speeds according to Centino
r(1,1)=crf(C,b,z)*A(1,1)*exp(-E(1,1)/(R*T))*(yCO2-((yCO^2)/K(1,1)));
%Reaction 1
r(1,2)=crf(C,b,z)*A(1,2)*exp(-E(1,2)/(R*T))*(yH2O-((yCO*yH2)/K(1,2)));
%Reaction 2
r(1,3)=crf(C,b,z)*A(1,3)*exp(-E(1,3)/(R*T))*((yH2^2)-(yCH4/K(1,3)));
%Reaction 3
r(1,4)=crf(C,b,z)*A(1,4)*exp(-E(1,4)/(R*T))*((yCH4*yH2O)-
((yCO*yH2^3)/K(1,4))); %Reaction 4
%r(1,4)=A(1,4)*exp(-E(1,4)/(R*T))*((yCH4*yH2O)-((yCO*yH2^3)/K(1,4)));
%Reaction 4

%Net rates of production for each gaseous species
RN2 =  0;                          %Nitrogen
RCO2= -r(1,1);                        %Carbon dioxide
RCO =2*r(1,1)+r(1,2)          +r(1,4); %Carbon monoxide
RCH4=               r(1,3)  -r(1,4); %Methane
RH2O=       -r(1,2)          -r(1,4); %Steam
RH2=         r(1,2)-2*r(1,3)+3*r(1,4); %Hydrogen
%RT=    r1+r2  -r3+2*r4; %Total number of gas molecules

Rx=[RH2O RCO RCO2 RH2 RCH4 RN2];
end
```

```
function r = rspeeds(Ac,R,b,A,E,P,v,T,nx,C,z,g)
%Equilibrium constants
%K(1,1)=10^(-8992.926/T + 9.183)*P^(2-1);    %
%K(1,2)=10^(-6999.663/T + 7.404)*P^(1+1-1);    % Equations determined according to Filipe
%K(1,3)=10^(4330.847/T - 5.436)*P^(1-2);     %
%K(1,4)=10^(-11330.509/T + 12.840)*P^(1+3-1-1);  %

K(1,1)=(exp(-2*g(2)/(R*T) + g(3)/(R*T)));   %
K(1,2)=(exp(-g(2)/(R*T) - g(4)/(R*T) + g(1)/(R*T)) %Equations determined according to Prokash
K(1,3)=(exp(-g(5)/(R*T) + 2*g(4)/(R*T)));                    %
K(1,4)=(exp(-g(2)/(R*T) - 3*g(4)/(R*T) + g(5)/(R*T) + g(1)/(R*T))); %

%Partial pressures
n=Ac*v*nx; %moles of gaseous components exiting oxidation zone
%c=Cms(1,1:6);
%Pp=(P/sum(n))*n %partial pressures of gaseous components
%PH2O=Pp(1);
%PCO =Pp(2);
%PCO2=Pp(3);
%PH2 =Pp(4);
%PCH4=Pp(5);

y=(1/sum(n))*n; %molar fractions of gaseous components
yH2O=y(1);
yCO =y(2);
yCO2=y(3);
yH2 =y(4);
yCH4=y(5);
%Reaction speeds according to Giltrap
%(why are reaction speeds not dependent on total molar gas concentration?)
%r(1,1)=crf(C,b,z)*A(1,1)*exp(-E(1,1)/(R*T))*(PCO2-((PCO^2)/K(1,1)));
%Reaction 1
```

```
%r(1,2)=crf(C,b,z)*A(1,2)*exp(-E(1,2)/(R*T))*(PH2O-((PCO*PH2)/K(1,2)));
%Reaction 2
%r(1,3)=crf(C,b,z)*A(1,3)*exp(-E(1,3)/(R*T))*((PH2^2)-(PCH4/K(1,3)));
%Reaction 3
%r(1,4)=crf(C,b,z)*A(1,4)*exp(-E(1,4)/(R*T))*((PCH4*PH2O)-
((PCO*PH2^3)/K(1,4)));    %Reaction 4

%Reaction speeds according to Babu & Sheth
%(why is CRF used in reaction 4 where no char is involved?)
%r(1,1)=sum(nx)*crf(C,b,z)*A(1,1)*exp(-E(1,1)/(R*T))*(PCO2-((PCO^2)/K(1,1)));
%Reaction 1
%r(1,2)=sum(nx)*crf(C,b,z)*A(1,2)*exp(-E(1,2)/(R*T))*(PH2O-
((PCO*PH2)/K(1,2)));          %Reaction 2
%r(1,3)=sum(nx)*crf(C,b,z)*A(1,3)*exp(-E(1,3)/(R*T))*((PH2^2)-(PCH4/K(1,3)));
%Reaction 3
%r(1,4)=sum(nx)*crf(C,b,z)*A(1,4)*exp(-E(1,4)/(R*T))*((PCH4*PH2O)-
((PCO*PH2^3)/K(1,4))); %Reaction 4

%Reaction speeds according to Prokash
%(why is CRF used in reaction 4 where no char is involved?)
%r(1,1)=sum(nx)*crf(C,b,z)*A(1,1)*exp(-E(1,1)/(R*T))*(yCO2-((yCO^2)/K(1,1)));
%Reaction 1
%r(1,2)=sum(nx)*crf(C,b,z)*A(1,2)*exp(-E(1,2)/(R*T))*(yH2O-
((yCO*yH2)/K(1,2)));          %Reaction 2
%r(1,3)=sum(nx)*crf(C,b,z)*A(1,3)*exp(-E(1,3)/(R*T))*((yH2^2)-(yCH4/K(1,3)));
%Reaction 3
%r(1,4)=sum(nx)*crf(C,b,z)*A(1,4)*exp(-E(1,4)/(R*T))*((yCH4*yH2O)-
((yCO*yH2^3)/K(1,4))); %Reaction 4

%Reaction speeds according to Centino
r(1,1)=crf(C,b,z)*A(1,1)*exp(-E(1,1)/(R*T))*(yCO2-((yCO^2)/K(1,1)));
%Reaction 1
r(1,2)=crf(C,b,z)*A(1,2)*exp(-E(1,2)/(R*T))*(yH2O-((yCO*yH2)/K(1,2)));
%Reaction 2
```

```
r(1,3)=crf(C,b,z)*A(1,3)*exp(-E(1,3)/(R*T))*((yH2^2)-(yCH4/K(1,3)));
%Reaction 3
r(1,4)=crf(C,b,z)*A(1,4)*exp(-E(1,4)/(R*T))*((yCH4*yH2O)-
((yCO*yH2^3)/K(1,4))); %Reaction 4
%r(1,4)=A(1,4)*exp(-E(1,4)/(R*T))*((yCH4*yH2O)-((yCO*yH2^3)/K(1,4)));
%Reaction 4
%ri=r
%ri=r
end
function CRF =crf(C,b,z) %Exponential CRF function
%Char reactivity factor
CRF=C*exp(b*z);
end
%function CRF =crf(C,b,z) %Linear CRF function
%Char reactivity factor
%CRF=C*b*z;
%end
```